Department of Forest Products Technology

Interfacial forces in nanocellulose based composite materials

Anna Maria Olszewska

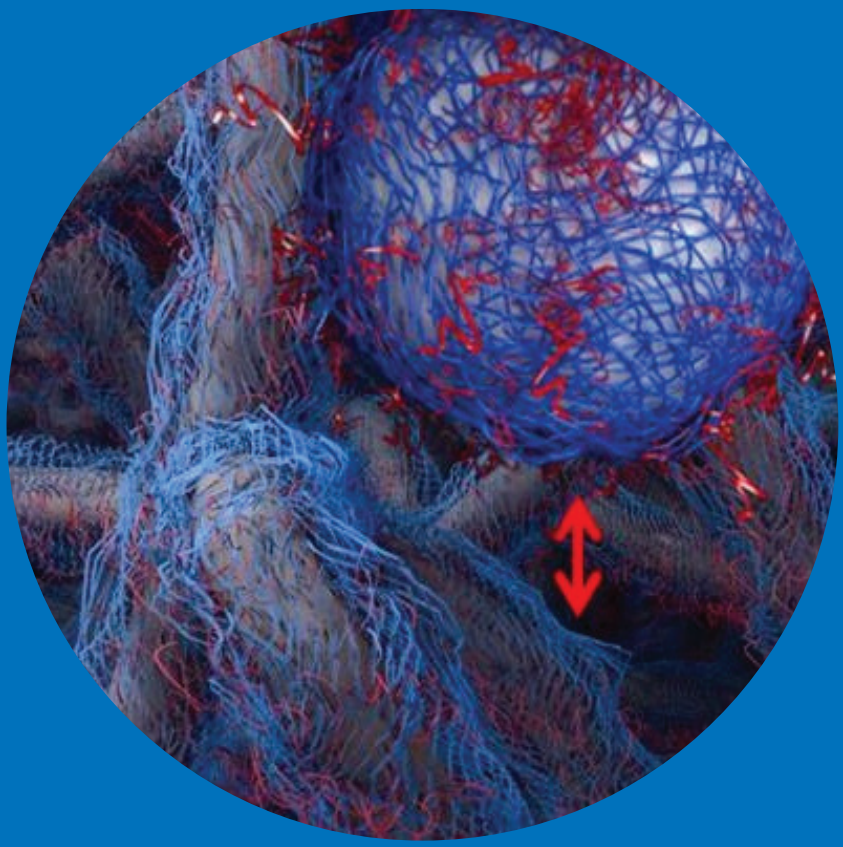

Aalto University

DOCTORAL DISSERTATIONS

Aalto University publication series
DOCTORAL DISSERTATIONS 151/2013

Interfacial forces in nanocellulose based composite materials

Anna Maria Olszewska

A doctoral dissertation completed for the degree of Doctor of Science Technology to be presented, with due permission of the School of Chemical Technology and debate in Auditorium Puu 2 at the Aalto University School of Chemical Technology (Espoo, Finland) on the 18th of October 2013 at 12 noon.

Aalto University
Aalto University School of Chemical Technology
Department of Forest Products Technology

Supervising professor
Professor Janne Laine

Thesis advisor
Professor Monika Österberg

Preliminary examiners
Professor Kristiina Oksman, Luleå University of Technology, Luleå Sweden
Professor Jouko Peltonen, Åbo Akademi, Turku, Finland

Opponent
Professor Emeritus Derek Gray, McGill University, Canada

Aalto University publication series
DOCTORAL DISSERTATIONS 151/2013

ISBN 978-952-60-5352-3
ISBN 978-952-60-5353-0 (pdf)
ISSN-L 1799-4934
ISSN 1799-4934 (printed)
ISSN 1799-4942 (pdf)
http://urn.fi/URN:ISBN:978-952-60-5353-0

Unigrafia Oy
Helsinki 2013

Finland

441 697
Printed matter

Author
Anna Maria Olszewska

Name of the doctoral dissertation
Interfacial forces in nanocellulose based composite materials

Publisher School of Chemical Technology

Unit Department of Forest Products Technology

Series Aalto University publication series DOCTORAL DISSERTATIONS 151/2013

Field of research Forest Products Technology

Manuscript submitted 10 May 2013 **Date of the defence** 18 October 2013

Permission to publish granted (date) 20 August 2013 **Language** English

☐ **Monograph** ☒ **Article dissertation (summary + original articles)**

Abstract

In this work, fundamental interactions in nanocellulose systems and their utility in fabricating novel and advanced cellulose-based materials was studied. More specifically two major aims were investigated. The first concentrates on cationic NFC and its morphology, its fundamental behavior with relation to charge and solvent, and its interactions with other nanocellulose particles. In the second, the approach focuses on the interfacial interaction between NFC and polymers (polysaccharides) to assess the importance of their mutual interplay on the mechanical performance of the nanocomposite films. Atomic force microscopy (AFM) in different imaging conditions (liquid and air, and different force detection modes) and the quartz crystal microbalance with dissipation (QCM-D), and tensile tests were combined to carry out this research.

The dimensions of cationic (cat) NFC were determined through AFM imaging. Individual nanofribils were found to be smaller in liquid than in air, which pointed at the importance of characterizing nanocellulosic material *in situ*, before drying. The influence of electrolyte concentration and pH on the swelling of cat NFC films was studied using the QCM-D technique. Cationically modified fibrils were amphoteric in nature; therefore, the swelling of the film was associated with pH conditions. Films with higher water content were observed at lower pH. Cationic NFC incorporated with anionic CNCs was also examined in terms of layer build-up. The significance of a dense and well-constructed first layer for successful multilayers formation was shown. Layer-by-layer (LbL) films were further measured by applying the colloidal probe AFM technique which pointed to the importance of charge and the interpenetration of the layers in the behavior of the films. Interfacial forces between NFC and the polysaccharide or polymer were studied by applying colloidal probe AFM and QCM-D. The importance of the aqueous lubrication of CMC-g-PEG between the NFC segments for the stability and film formation were assessed by studying lateral responces between the interacting particles. The adsorption of CMC-g-PEG markedly increased stability, repulsions and the lubrication in liquid. The reduction of the friction coefficient compared to the bare NFC film was observed both in liquid and in air. This lubricating effect was evaluated in terms of the mechanical properties of films composed of NFC/CMC-g-PEG. An NFC based nanocomposite with a high fraction of reinforcement was prepared by ionic complexation of anionically charged NFC and cationic block copolymers micelles. This prevented macroscopic phase separation and gave rise to composites with an alternating nanoscale hard /soft architecture. Due to the nanoscopic control over fracture, energy dissipation a significantly larger strain and toughness was achieved.

Keywords nanocellulose, surface force, biocomposites, AFM

ISBN (printed) 978-952-60-5352-3 **ISBN (pdf)** 978-952-60-5353-0

ISSN-L 1799-4934 **ISSN (printed)** 1799-4934 **ISSN (pdf)** 1799-4942

Location of publisher Helsinki **Location of printing** Helsinki **Year** 2013

Pages 183 **urn** http://urn.fi/URN:ISBN:978-952-60-5353-0

PREFACE

This study was carried out at the Department of Forest Products Technology, Aalto University School of Chemical Technology during the years 2009-2013. The work was performed within "Designcell" and "Naseva"- projects founded by European WoodWisdom-Net research program, and National Agency for Technology and Innovation (TEKES). All the funding, the research and industrial parties of these projects are gratefully acknowledged for their contribution.

I am extremely grateful to Professor Janne Laine for giving me this great opportunity to join his group and conduct a very interesting research under his supervision. Not only he offered me a job, but also gave me a lot of freedom and exceptional environment to develop my scientific interest towards biomaterials. I always felt your support Janne, it was very important for me. Kiitos Paljon!

I am indebted to Professor Monika Österberg (my thesis advisor) for her massive amount of work and inexhaustible patience towards me and my late and constant emails, questions, suggestions, and ideas. Her enormous help with manuscript preparation and stimulating discussions were substantial. Without you Monika, I would not be able to graduate.

I want to thank all of my co-authors for their valuable contributions. Special thanks to prof. Olli Ikkala and prof. Mark Rutland. The time I spent working in your groups, is unforgettable and had supported my development in many aspects. Thank you both for the inspiring discussion and the opportunity to work with you and your excellent teams (most importantly Andreas, Miao, and Niklas). Mark, thank you for wonderful time I spent both in Sweden and in Australia. You are not only a great professor but also an admirable and very good person, I am glad we met.

My sincere thanks go to Dr. Eero Kontturi, who never said NO to my repeated "Can I ask you a question?" Eero, I hope you know how much it meant to me that I could always count on you, and that you devoted a lot of time to talk with me about cellulose.

Dr. Juan José Valle-Delgado and Mr. Miika, thank you both for your patience, hard work and involvement in our last article. JJ, your knowledge about force measurements, your goodness and tolerance towards my constant questions are considerable- thank you.

I would like to also thank prof. Orlando Rojas, prof. Herbert Sixta, prof. Tom Linström and prof. Ilkka Kilpeläinen for they credence in me and encouragement they gave me to practice research.

Prof. Kristiina Oksman and prof. Jouko Peltonen are thanked for time their spent on reviewing this thesis and for their valuable comments which helped to improve it.

It is difficult to put in words my enormous gratitude that I feel for all my present and former colleagues from the department. The working atmosphere you had created here is distinct! I would like to thank all of the members of our department; especially Paula, Tiina, Laura, Karoliina, Leena-Sisko, Elli, Trang, Delphine, Katri, Raili, Iina, Timbe, Jani, Jean, Petri, Carlos- thank you for your goodness, help and the opportunity to conduct many significant discussions, thank you for fun we had together. My thanks go also to the laboratory technicians, whose work was very important: Maria, Anu, Aila, Rita and Risu- thank you, without your help and maintaining the laboratories, it would be very difficult to finalize the project. I also want to thank Ari, Timo, Iina, Pena and Sirje for their help in practical matters. Special thanks for Hannes and Niko, you both are very special to me in many aspects; I will be missing your creativity towards building new equipment and "funny" jokes. Joe- I want to thank you for reading my manuscripts and thesis which undeniably

required from you a lot of patience and tolerance to spelling mistakes. Dr. Misha, thank you for your help with issues related to thesis preparation, but most importantly I want to thank you for your presence at work - almost every weekend, which made me feel less alone.

Special M club (Mao, Micheal, Mindas, Miro, Michi, Marcelo), I would like to thank you for all the great nights out we had, and funny coffee breaks. Mao- I am very grateful for your help and support you gave me during difficult times. My lovely AAA club (Alina, Arcot, Alexey) thank you all for friendship and support I got from you. Alina, you are like my little sister, thank you for all the great time we had together, Saturday movie nights and trips to Stockmann. Arcot- you are an excellent office mate ☺, thank you for "allowing me" to assimilate your office, but most essentially I want to thank you for your friendship, support and believing in me. I will be missing you! Alexey and Mindas- you are my boys in Finland. You helped me a lot with all the everyday life issues (which required to have a man around), thank you both for always being here for me! Working with all of you "Puu people", was an indescribable experience. I not only learned a lot about cellulose and science in general, but also could work and study in the most helpful and friendly environment one can ask for.

There are some people with whom I spent most of my international conferences and symposia. Sole, Emily, Ilari, Tekla, Eero, Pan, Nori, Ali, I want to thank you for sharing with me all those unforgettable moments. Here I want to also acknowledge Prof. Maija Tenkanen who is a brain and motor of Bioregs and PolyRefNorth. I extremely appreciate the fact that I could always count on their support.

I was very lucky to spend two months of my PhD studies in Sweden at KTH (Department of Chemistry, Surface and Corrosion Science) were I met excellent people like Elenora, Shadi, Josefine, Olya, Dariush, Majid, Niklas, Per, Simon, Troy, and many others to whom I am very thankful. Your warm reception, sharing the coffee breaks and all the scientific and non-scientific talks were very important to me. Special thanks to Esben, Niklas and Ruben for they help and great suggestion how to force AFM to obedience. I am extremely grateful to Zahra, who took extremely good care of me during my staying there, and who became a lifelong friend!

I am particularly grateful to Mari, Paula, Annika, Annastiina, Pirkko, King A, Jari, Tom, Tuomas, Hannu, Ilkka, and many other colleges from Helsinki Yliopsito (where I started my adventure in Finland) for their help, friendship and tolerance to my very "extreme" linguistic skills at that time. Your endless support was very important for a rooky person like me, in the land of snow and short days. I am grateful to Mari- without your help I will not be here today. I also met there tree excellent Finnish girls Paula, Annika and Annastiina, whose friendship can withstand the time and distance.

My dear-almost-neighbors from Tapiola with whom I share mutual love to G&T: Kirsi and Ben, I want to thank you for your help and mental support.

Very special thanks to Mikko Kanerva, whose friendship and care are extremely important to me. I am grateful for our bike trips, long discussions about life, and for the fact that that I could always count on your genuine help and advices, and that you could stick with me for such a long time despite my changing moods☺. I will never forget you!!!

My polish friends who shared my adventure in Finland: Asia and Grzesiu, Basia and Michał, Ania and Kuba, Edyta, Szymon, Magda (special thanks for your hospitality in Pohjois Tapiola) and of course Paulina- I want to deeply thank you for keeping the Polish sprit here far from home. Paula- we had many good times here, and many excellent trips together, which will always stay in my mind. Thank you for your help, and support you gave me during very difficult moments I occasionally had in Finland, I will never forget that.

Finally, I want to thank people in Poland who are always there for me, despite the time and distance. My high school friends Karolina and Sylwia- I want to thank you for your long-lasting friendship. Karolina, who I hope one day, will become my sister- in- law- I want to thank you for your support and help. I admire your excellent taste in Mokobelle ☺.

I want to immeasurably thank my parents and my brother, who always believed in me and gave me freedom to choose my way of life.

Mamo i Tato bardzo Wam dziekuje za wszystko co dla mnie zrobiliscie i ze zawsze moglam na Was liczyc!

Special thanks to my husband-to-be Maciej, who improved this thesis with his excellent artistic skills; but most importantly whose love and patience helped me to go through that difficult process which is finalizing the thesis. Thank you for your understanding, and excellent food you cooked to cheer me up. I am extremely glad I met you!

Berlin, September 18th, 2013

Anna Olszewska

LIST OF PUBLICATIONS

This thesis is mainly based on the results presented in five publications which are referred as Roman numbers in the text. Some additional data related to the work are also discussed.

Paper I Olszewska A., Eronen P., Johansson L-S., Malho J-M., Ankerfors M., Lindstöm T.; Ruokolainen J.; Laine J., Österberg M. *(2011)* The behaviour of cationic NanoFibrillar Cellulose in aqueous media. *Cellulose*, 18, 1213-1226.

Paper II Olszewska A., Kontturi E., Laine J., Österberg M. (2013) All-cellulose multilayers: long nanofirbils assembled with short nanocrystals. *Cellulose,* 20, 1777-1789.

Paper III Wang M., Olszewska A., Walther A., Malho J-M., Schacher F. H., Ruokolainen J., Ankerfors M., Laine J., Berglund L. A., Österberg M., Ikkala O. (2011) Colloidal Ionic Assembly between Anionic Natvie Cellulose Nanofibrils and Cationic Bloc Copolymer Micelles into Biomimetic Naoncomposites. *Biomacromolecules*, 12, 2074-2081.

Paper IV Olszewska A., Junka K., Nordgren N., Laine J., Rutland M., Österberg M. (2013) Non-ionic assembly of nanofibrillated cellulose and polyethylene grafted carboxymethylcellulose and the effect of aqueous lubrication in polysaccharide-based nanocomposite formation. *Soft Matter*, 9, 7448-7457.

Paper V Olszewska A., Valle Delgado J.J., Nikinmaa M., Laine J. Österberg M. (2013) Direct measurements of non-ionic attraction and nanoscaled lubrication in biomimetic composites from nanofibrillated cellulose and modified carboxymethylated cellulose (accepted Nanoscale DOI: 10.1039/C3NR03091A)

Author's contribution to the appended joint publications:

I, II, IV, Anna Olszewska was responsible for the experimental design, performed the main part of the experimental work and analyzed the results. She wrote the manuscripts with the co-authors (corresponding author)

III Anna Olszewska was responsible for the experimental design with the co-authors performed the QCM-D, AFM and DLS experimental work, also she took an active part in the discussion of results and analysis and she wrote the corresponding part of the manuscript.

V Anna Olszewska was responsible for experimental design and part of the experimental performance which she shared with coauthors. She wrote the manuscript with help of co-authors (corresponding author)

Additional publications

Paper VI Green G.W.; Olszewska A.; Österberg M.; Zhu H.; Horn R.; Mimicking the cartilage lubrication System, (2013) submitted to Biomacromolecules

LIST OF MAIN ABBREVIATIONS

AFM	atomic force microscopy
Cat NFC	cationic nanofibrillar cellulose
CD	charge density
CMC	carboxymethylated cellulose
CMC-g-PEG	carboxymethylated cellulose graft polyethylene glycol
CNC	crystalline cellulose
COF	co-efficient of friction
CPM	colloidal probe microscopy
Cryo-TEM	cryogenic transmission electron microscopy
BCP	block copolymer
DLVO	Derjaguin, Landeau, Verway and Overbeek
DP	degree of polymerization
EPAC	2,3-epoxy-propyltrimethylammonium chloride
LbL	layer-by-layer
MFC	microfibrillated cellulose
NFC	nanofibrillated cellulose
PB-*b*-PDMAEMAq	poly(1,2 butadiene)-*block*-poly(dimethylaminoethyl methacrylate) block copolymer
PEG	polyethylenglycol
PEI	polyethylenimine
RH	relative humidity
QCM-D	quartz crystal microbalance with dissipation
TEMPO	2,2,6,6-tetramethylpiperidine-1-oxyl radical

TABLE OF CONTENTS

1. INTRODUCTION AND OBJECTIVE OF THE STUDY

Technology based on renewable materials can help support the enormous requirements of growing population in a sustainable fashion. Cellulose, which is the most abundant renewable material on our planet, is thus an appropriate choice to guide humanity towards a truly ecofriendly existence. This natural polymer represents about third of plant tissues and can regenerate though photosynthesis. Moreover, some sea animals called tunicates, several species of algae, some bacteria and fungi can also produce cellulose. A wealth of applications running from textile and paper to the fields of biotechnology and medicine depend on cellulose. The year 1977 witnessed the pioneering work of researchers at Rayonier in New Jersey, who succeeded in producing nanocellulose gel for the first time by defibrillating pulp fibers. The gel produced initially by Rayonier researchers and later by Turbak and coworkers (1983) was named microfibrillated cellulose (MFC) and was found to consist of micro- and nanometer scale fibrils. Since 1983 there has been a rapid growth in the magnitude of scientific articles and patents related to this topic. A number of reviews articles dealing with nanocellulose have been published in last years (Habibi et al. 2010, Siró, Plackett 2010, Eichhorn et al. 2010, Moon et al. 2011, Klemm et al. 2011). In the article of Durán *et al.* (2012) the authors illustrated the actual impact of nanocellulose based materials in different areas based on patent databases. The recent review on nanocellulose patent trends published by Charreau *et al.* (2013) revised the increase with the patent applications on cellulose whiskers, microfibrillated cellulose, and bacterial cellulose (Fig. 1).

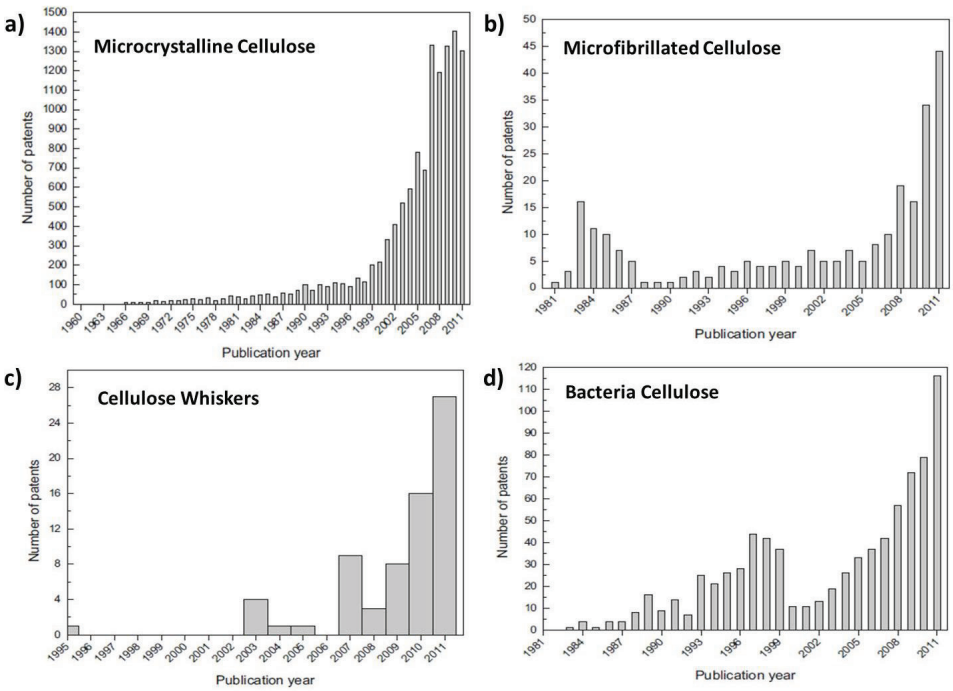

Figure 1. Evolution of the annual number of patents on a) microcrystalline cellulose, b) microfibrillated cellulose. c) cellulose whiskers and d) bacteria cellulose. Figures adopted from Carreau *et al.* (Charreau, Forest & Vazguez 2013)

Extraction of nano-scale cellulosic elements from lignocellulosic fibers is one of the most studied topics in the cellulose literature today. Many applications, such as reinforcement of composite materials, tissue engineering scaffolds, filtration media, thickening agents, rheology modifiers, adsorbent, and paper reinforcement deploy nanocellulose. However, before nanocellulose can be suitably applied for the above mentioned uses, the inherent properties of that material need to be studied. By applying surface sensitive techniques and with the aid of well-defined cellulose model films, information on cellulose molecular level properties could be obtained. The behavior of cellulose surfaces in different media as well as their interaction with different chemicals also can be described. It is of great importance to understand and study their interfacial properties in order to make nanocellulose suitable for current and future applications. The degree of dispersion of fibers in the polymer matrix as well as the nature and extent of cellulose-polymer adhesion interactions, are crucial information which affects the mechanical performance of composite materials. Thus, understanding the role of interfacial forces in nanocellulose-polymer composite systems is essential.

The objective of this work was to explore how nanocellulose can be use as a reinforcing part in biocomposite materials. Motivation to use nanocellulose as a stiffening agent in composite came from its excellent and well reported mechanical properties. Moreover the sustainability and not interfering with the food chains makes cellulose promising material to be used in high end applications. Main focus in this thesis work was to study interfacial forces between nanocellulose and different polymers to assess their importance in nano-scale phenomena so essential for the composite formation and its function. Nanofibrillated cellulose (NFC) and crystalline nanocellulose (CNC) were the most studied cellulosic substrates in this thesis work. Many prominent techniques were combined to find the most feasible ways to characterize these nano-sized cellulosic materials and their interactions. Surface sensitive techniques such as The Quartz Crystal Microbalance with Dissipation (QCM-D), Atomic Force Microscopy (AFM) and Colloidal Probe Microscopy (CPM) were extensively applied. These techniques were used to evaluate the interactions of NFC with water, different polymers and other nanocellulosic materials to gain knowledge of the interfacial forces in those systems. All studies were performed in aqueous phase, and this ensured the preservation of the fine nano-or microfibillar structure of the cellulose fibrils. But water would also be the best choice of solvent to perform the environmentally friendly cellulose modification and produce cellulose based material on an industrial scale.

The fundamental properties of nanofibrillated cellulose such as its interactions with water and different electrolyte were studied in **Paper I**. In this article extended characterization of cationized NFC has been presented including the analysis of the size distribution of the fibrils, swelling properties and its interactions with water. The amphoteric nature of the cationic NFC fibrils was observed and the importance of that finding was further analyzed in **Paper II**, where the interactions between cationically charged nanofibrillated cellulose and anionically charged cellulose whiskers (CNCs) in all-cellulose multilayers were studied. A fundamental understanding of the interactions between the short rod like cellulose whiskers and the long, flexible cationic nanofibrills could be used in designing all-cellulosic coatings, or composite materials of desired properties.

A major part the work was devoted to examine of NFC in composite materials, and it was studied in **Paper III-V**. In **Paper III** a new, simple and versatile concept to complex native nanofibrillated cellulose with a block copolymer via electrostatic interactions was presented. Significantly larger strain and toughness could be achieved due to the now possible nanoscopic control over fracture energy dissipation and the interfibrillar lubrication between the NFC domains by using low T_g block copolymer. The importance of lubrication between nanocellulose fibrils in composite formation was further studied in **Paper IV**. The concept was based on NFC surface modification via nonionic interactions. The strong affinity of polysaccharides towards cellulosic material, known to originate from the similarity in backbone structure, was utilized in this paper. The effect of carboxymethyl cellulose grafted with polyethylene glycol (CMC-*g*-PEG) on the surface of NFC films on friction forces was evaluated using colloidal probe microscopy. The adsorbed CMC-*g*-PEG markedly reduced the

friction by 88% compared to bare NFC films. Such a reduction in friction between the colloidal level fibrils improved the formation of the composite films. Further investigation including the dry state friction forces and mechanical properties of such constructed films were studied in **Paper V**.

Understanding the fundamental interactions between the nano-sized cellulose fibrils is of great importance not only for the sake of gaining basic knowledge but also for better utilization of this new material in novel applications.

2. BACKGROUND

This chapter will focus on the background information related to morphology and structure of cellulose at molecular level. It will also deliver a summary of the available literature related to surface forces, multilayer films and composite materials employing nanocellulose.

2.1. Cellulose fibers

Cellulose is one of the most important natural polymers and can be considered as a key source of sustainable materials on an industrial scale. In plants and trees cellulose acts as a structural reinforcing agent, whose main function is to provide mechanical strength. Cellulose has been used for millennia from being a basic energy and textile source, ranging to building material, and paper. Recently, cellulose has been utilized in biotechnology and has gained significant interest in medical implementations. The growing importance of bio-based materials have drawn public interest into incorporating renewable resources such as polysaccharides in areas where synthetic fibers and petroleum based polymer were used before. One of the big markets for cellulose is concentrated on novel composite materials, utilizing the natural good mechanical properties of cellulose fibers.

For the aforementioned reasons it is of great importance to understand the structure of cellulose and also how it interacts with other materials when introdued to different environmental conditions. By acquiring knowledge of the chemical nature of the cellulose molecules in addition to its structure and morphology in the solid state, the chemical and physical properties of cellulose can be understood (Krässig 1996)

2.1.1. Structure of cellulose at molecular level

Cellulose is a linear and fairly rigid homopolymer consisting of D-anhydroglucopyranose units (AGU), which are linked together by β-(1→4) glycosidic bonds formed between C-1 and C-4 of adjacent glucose moieties (Klemm et al. 2005), Fig. 2. The repeating unit is cellobiose, with estimated length of 1.03 nm consisting of two AGUs (Fengel, Wegener 1989, Sjöström 1993). In the solid state, AGU units are rotated by 180° with respect to each other due to the constraints of β-linkage (Haworth 1932). Each of the AGU units has three hydroxyl (OH) groups at the C2, C3 and C6 positions. Terminal groups at the either end of the cellulose molecules, as illustrated on Fig. 2, are quite different in nature from each other.

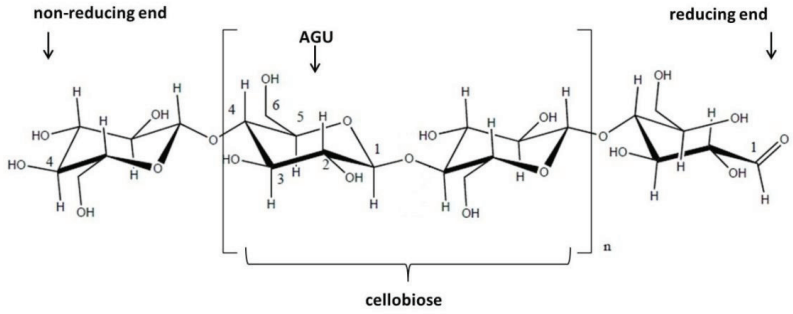

Figure 2. Molecular structure of cellulose with repeating cellobiose units showing reducing (right) and non-reducing (left) end-groups

One end contains an alcoholic OH group at C4, while on the other end C1 is part of an aldehyde group with reducing activity. The chain length of the cellulose polymer varies depending on the cellulose source (Krässig 1996) where native cellulose has a degree of polymerization (*DP*) between 5000 - 15 000 (Klemm et al. 2005). The *DP* value, however is greatly dependent on the method of isolation. The cellulose used in practice has an average *DP* of between 800-3000 (Krässig 1996). Cellulose is insoluble in water when the DP is over 6 (Nehls et al. 1994). The reactivity and chemical character of cellulose is determined by reactivity of the primary and two secondary OH groups in the AGU (Klemm et al. 1998). Those hydroxyl groups are responsible for forming both intra- and intermolecular hydrogen (H)-bonding network in native cellulose. Intramolecular H-bonds can form between suitably positioned OH groups within the same molecule and are located between C2-OH and C6-OH groups and between C3-OH and endocyclic oxygen (Figs. 2a and b). H-bonds can also be formed between two neighboring cellulose chains which interact via their C3-OH and C6-OH groups (Fig. 2c). Those interactions are called intermolecular H-bonds.

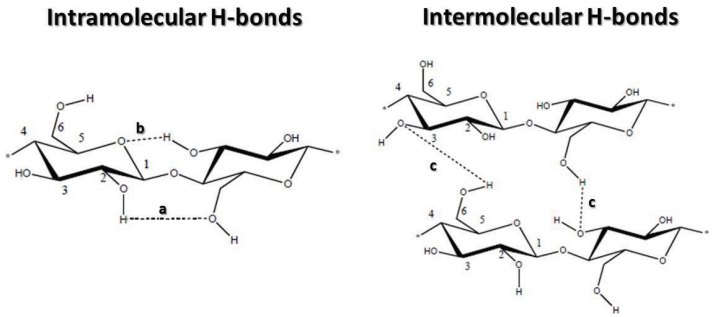

Figure 3. Cellulose structure showing intramolecular hydrogen bonding between C2-OH and C6-OH (a) and C3-OH with endocyclic oxygen (b); and the intermolecular hydrogen bonding between C3-OH and C6-OH (c).

The H-bonds are responsible for cellulose structure and characteristic rigidity via co-crystallization of multiple chains into parallel structures forming elementary fibrils, which are further organized into microfibrils (Fengel, Wegener 1989, Kontturi et al. 2006, Gandini 2011, Moon et al. 2011). The structure of cellulose is responsible for its insolubility in water and common organic solvents. However, the fundamental reason behind this has been debated. One hypothesis states that the main reason of cellulose almost non-dissolving properties lies in the fact that the hydroxyl groups are responsible for the extensive hydrogen bonding network which suppresses the solubility (Klemm et al. 1998). Recently, Lindman (2010) asserts that the solubility (or insolubility) characteristics of cellulose are based upon amphiphilic and hydrophobic molecular interactions, which have been extensively discussed by many authors (Glasser et al. 2012). Also Johansson and coworkers (Johansson et al. 2011) showed important evidence that the reactivity of the surface hydroxyl groups governs the behavior of cellulose in different media.

Recently ILs (ionic liquids) emerged as a convenient solvent for cellulose. These new solvents are salts composed of a large organic cation and an inorganic or organic anion. ILs show many interesting properties such as high thermal stability, very low vapour pressure, low melting point, and non-flammability. Study by Swatloski et al. (2002) can be seen as a foundation in the dissolution of cellulose by ILs. In his work he demonstrated that cellulose can be dissolved at high concentrations even as high as 25% (w/w) by using an imidazolium-based ILs. It is suggested that the major contributor for the solubility of cellulose in ILs are anions which are strong hydrogen bond acceptors and as such can allows rapid and efficient dissolution by breaking the hydrogen bond network of cellulose. For more extensive information regarding dissolution of cellulose in ILs reader is referred to recent review by Wang *et al.* (2012).

2.1.2. Structure of cellulose microfibrils

The supramolecular model of cellulose is based on the organization of cellulose chains. Parallel synthesis of cellulose in the biosynthesis of wood or other non-wood plants leads to noncovalent association between multiple chains, which results in substructures termed microfibrils. Wood microfibrils consists of elementary fibrils which start formation from the terminal enzyme complexes (TC) that takes shape of a six-lobed “rosette” (Mueller, Brown 1980), where β-D-glucose chains are held together via van der Waals forces. Those microfibrils are micrometers long and few nanometers thick (Xu et al. 2007). They contain both ordered and disordered components (Wickholm et al. 1998, Atalla, Vanderhart 1999, Vietor et al. 2002) but their structure and exact size is still under debate. A schematic representation of wood microfibril structure is presented on Fig. 4.

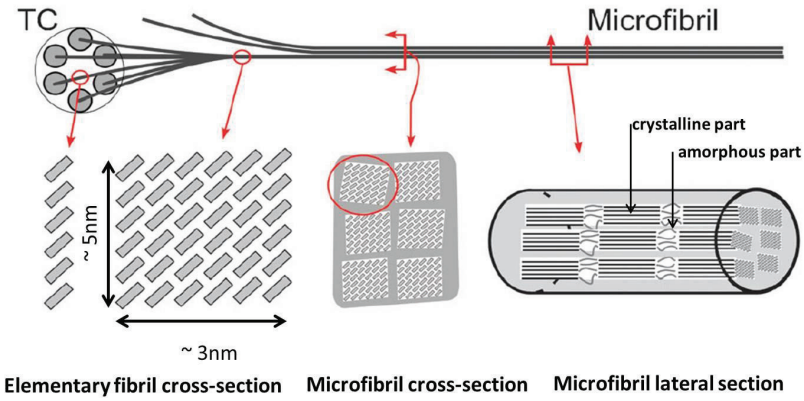

Figure 4. Schematic formation of cellulose microfibrils in wood (adopted from (Moon et al. 2011). TC (terminal enzyme complexs).

There are several polymorphs of crystalline cellulose (I, II, III, IV). Each has been extensively studied (O'Sullivan 1997). Cellulose I is the crystalline cellulose which is naturally produced by trees, plants, tunicates, algae and bacteria. Depending on the source of cellulose, native cellulose (cellulose I) has been found to exhibit two different parallel crystalline structures (Cellulose Iα and Iβ) (Atalla, Vanderhart 1984). Cellulose Iα (triclinic structure) is the dominant crystalline structure for native bacterial and Valonia cellulose, whereas cellulose Iβ (monoclinic structure) dominates in the higher plants such as wood and cotton. Structure of Cellulose I is thermodynamically metastable and can be converted to either cellulose II or III. Cellulose II has been the most stable structure of technical relevance and can be produced by two processes: regeneration (solubilization and recrystallization) and mercerization (aqueous sodium hydroxide treatments) (Klemm 2005). Cellulose III can be formed from Cellulose I or II through liquid ammonia treatments, and subsequent thermal treatments can then be used to form Cellulose IV.

The crystalline regions of cellulose are interspersed with less ordered paracrystalline or amorphous areas (Fig. 4). Those amorphous areas were shown to be distributed on the surface (Larsson et al. 1997) as well as along the cellulose microfibrils (Nishiyama et al. 2003). Depending on the source, the degree of crystallinity in native cellulose is typically 50-70% (Hermans, Weidinger 1949), but can also be over 94% (Hon 1994).

Variability amongst the dimensions of microfibrils also depends on the cellulose source. A number of plants such as ramie (Frey-Wyssling 1954), spruce wood (Fengel 1970, Jakob et al. 1995), flax fiber (Mueller et al. 1998) and pulp fiber (Duchesne et al. 2001) have been characterized in terms of the size of their microfibirils. Experimental techniques such as small angle neutron scattering (SANS), wide angle X-ray scattering (WAXS), and solid state ^{13}C NMR (Newman 1999, Andersson et al. 2003, Newman 2004, Peura et al. 2008), have been

successfully used to characterize the dimensions of the supramolecular structure of cellulose. It is important to notice that the characterization of the structure of microfibrils is particularly challenging since the extraction of individual fibrils is difficult, the methods used for sample preparation can alter the native size of the fibrils (e.g. staining the samples for TEM experiments) or the presence of other polysaccharides, particularly glucomannas, may be closely enough associated with the cellulose microfibrils to be considered part of their structure (Akerholm, Salmen 2001, Altaner et al. 2006). There is also strong evidence that microfibrils tend to assemble into aggregates in the region of 10-20 nm across (Donaldson 2007).

Theoretically, the cellulose crystallite cross section could be as small as 1.5 x 2 nm^2 (six group chains) to a maximum of 3 x 5 nm^2 (36 cellulose chains) (Jakob et al. 1995, Newman 1999, Ding, Himmel 2006). The values are calculated on the basis of the model cellulose Iβ crystal structure where it is assumed that microfibrils are approximately circular in cross section and each chain occupies 0.317 nm^2 (Nishiyama et al. 2002). A study carried by Ding and Himmel (2006) investigated the cellulose structure within the developing maize primary plant cell wall by using AFM. They revealed elementary fibril dimensions which have a rectangular cross section of 3 x 5 nm. Based on that finding they proposed 36 cellulose chains model. They proposed that the elementary fibrils are heterogeneous structures containing a crystalline core and layers of subcrystalline/paracrystalline sheaths. The crystalline core displays an Iβ structure. The 36 cellulose chains model is currently frequently suggested (Endler, Persson 2011). Yet, the evidence on which it is based on are indirect (Herth 1983). Recently, Fernandes *et al.* (2011) thoughtfully investigated the nanostructure of cellulose microfibrils in spruce wood, and they proposed the 24 cellulose chains model, where microfibrils are possibly twisted and with substantial disorder increasing towards the surfaces. Furthermore, they concluded that the number of chains in one microfibril is fixed and corresponds to the number of synthesized chains by one terminal complex (Ding, Himmel 2006, Niimura et al. 2010). They proposed that each lobe of the terminal complex would synthesize four chains rather than six as has been assumed. As a consequence the terminal complex, as it travels through the cell membrane, would have to rotate leaving microfibrils twisted behind it (Somerville 2006). Both these models are still widely discussed.

The morphological shape can be attributed to the action of the terminal complexes which forms fibrils during the biosynthesis. Depending on the sepsis, different arrangements of terminal complexes have been observed (Brown 1996) which, as a consequence, generates different geometries for cellulose crystals. Based on the TEM observation by Revol (1982) the cross section of cellulose crystallites from Valonia is square. In contrast the crystalline cellulose from tunicate analyzed by TEM (Sassi, Chanzy 1995) and SANS was found to be rectangular in cross section shape (Terech et al. 1999).

2.1.3. Chemistry of macroscopic cellulose fibers in wood

Most of the cellulose in wood (between 80 and 85% of the total cellulose matter in wood) is presented in the middle layer (S2 layer) of the cell wall. The S2 layer is the thickest layer representing about 80% of the total cell wall thickness (Fengel, Stoll 1973). Its main function is mechanical reinforcement and the layer is considered as the main load-bearing element in wood fibers. Cellulose in wood is closely associated with polysaccharides (Fig. 5a).

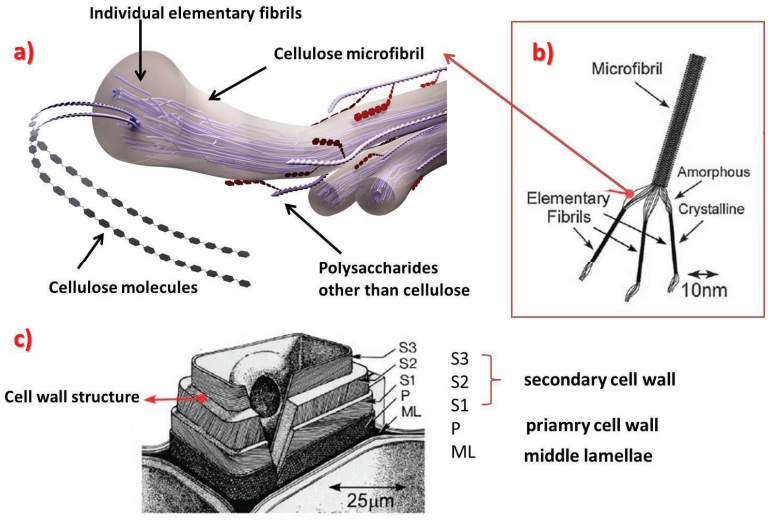

Figure 5. A schematic representation of hierarchical structure of wood tissue (c) and microfibril (b) (adopted from (Postek et al. 2011) and schematic representation of cellulose microfibrils with closely associated polysaccharides other than cellulose (a) (adopted from Purves 1994 et al Life: The Science of Biology, 4th Edition) Courtesy of Maciej Elert

The composition and relative amount of hemicelluloses in the cell wall depends on the wood species. The main hemicellulose in hardwood is xylan, more specifically an O-acetyl-4-Omethylglucurono-ß-D-xylan (15 - 30% in wood) and glucomannan 1-4-linked-ß-D-glucopyranoses and ß-D-mannopyranoses (about 2 - 5% in wood). The main softwood hemicelluloses are galactoglucomannan (about 20% in wood) and arabino-4-O-methylglucuronoxylan (5-10% in wood) (Fengel, Wegener 1989, Sjöström 1993). Hemicelluloses are associated with cellulose microfibrils via hydrogen bonding and with other cell wall constituents via covalent linkage (Sun et al. 2004). Hemicelluloses contribute to the strength formation of cell wall in association with cellulose microfibrils. Other function of hemicelluloses is to bring flexibility to the structural assembly of cell wall components. The presence of hemicelluloses also inhibits the coalescence of cellulose microfibrils which

improve the fibrillation of cellulose into nanosized fibrills. The influence of hemicellulose on the size of nanofibrils produced is in more detail described in the next section.

Cell walls are also surrounded by lignin, which is mainly located in Middle Lamella (ML) in the cell wall structure (Fig. 5c). To liberate the cellulose fibers from other cell wall constituents, the pulping process is used. The main propose of chemical pulping is to selectively remove lignin. However, due to lignin-carbohydrate complexes (LCC) and poor selectivity it is never fully achieved. After pulping bleaching is applied as follow up treatment which helps to remove lignin, but also hemicelluloses and cellulose are partly depolymerized. All these treatments can strongly affect the properties and composition of the cellulose fibers produced.

2.2. Isolation of nanostructured cellulose materials

Cellulose can be extracted from a broad range of plants and animals, giving a wide range of different cellulose particles. The diversity depends on few main factors, one of which is the biosynthesis of cellulose microfibrils. As it was discussed in the previous section, the size and shape of microfibrils depends strongly on the source of material. Another very important factor is the extraction process of the cellulose fibrils from the plant sources, which can strongly, affects the properties and dimensions of the produced nano-scale fibrils. In this thesis the most used nanocellulose particles were nanofibrillated cellulose (NFC) produced by disintegration of different wood pulp sources and nanocrystalline cellulose (CNC) produce by acid hydrolysis of cotton. It is worth mentioning that cellulose can also be formed by Acetobacter xylinum or see animals. Bacterial cellulose (BC) is a gel-like very homogeneous material and consists of long and individual cellulose fibrils. BC, in contrast to nanofibrils disintegrated from wood fibers, does not contain lignin, pectin and hemicelluloses. Because of it high purity and biocompatibility BC has been shown to be an interesting biomedical material, and has been used in several biomedical applications such as wound dressings and scaffolds for tissue engineering of cartilage and blood vessels (Klemm 2001).

2.2.1. Fiber modification prior to disintegration vs. the size of the nanofibrils obtained

The diameter distribution of nanofibrils is strongly influenced by the manufacturing process and the nature of the cellulose source. Isolation of cellulose fibrils occurs in two stages. The first stage is purification of the source material. This involves a complete or partial removal of matrix material (hemicelluloses and lignin). The second step consists of separation of “purified” cellulose materials (some hemicellulose can still be closely associated to cellulose) into small micro- or nano-sized components. The size of fibrils depends on the raw material from which the fibrils are liberated. Depending on the cellulose source the degree of polymerization, morphology and nanofiber aspect ratio may vary (Siró, Plackett 2010). Various cellulosic materials including hardwood and softwood industrial pulps (Stelte, Sanadi 2009, Spence et al. 2010, Zimmermann et al. 2010,

Xhanari et al. 2011) have been compared as potential raw material for the cellulosic nanomaterials. Also cellulose fibrils from non-wood plants can act as a raw material for production of nanocellulose (Dufresene et al. 1997, Zuluaga et al. 2007). The presence of non-cellulosic polysaccharides correlates with a smaller nanofibrils aggregation size, which was reported by various authors (Hult et al. 2000, 2001, 2003, Zhang, Tong 2007, Zhang et al. 2008, Iwamoto 2008). This suggests that hemicellulose limits the association between cellulose nanofirbers (Iwamoto 2008).

The first attempts to produce microfibrils from wood pulp were taken already in 1980's (Turbak et al. 1983). The new material obtained by disintegration of microscopic fibers through a homogenization process was named by Turbak, microfibrillated cellulose (MFC). MFC consisted of microfibrils which were 25-100 nm in width. The original process was never commercialized because of its high energy use (30000 kWh/ton) and problems with clogging in the homogenizers. The principle of the method is to pass a dilute cellulose pulp water suspension through a mechanical homogenizer in which high a pressure drop facilitates fibrillation. Later the method was improved by many research groups by combining high pressure homogenization with extensive shearing and impact force (Nakagaito, Yano 2004, Lindström et al. 2007, Iwamoto et al. 2005). An alternative method to produce MFC and NFC by mechanical means is frictional grinding, introduced by Abe (2007). The mechanical treatments to disintegrate the cellulose fibers into nano-scale dimensions are still considered as too challenging to scale up for industrial production. Therefore, the need for producing cellulose nanofibrils in large amounts leads to a search for alternatives, one of which is to apply different pre-treatments prior to fibrillation which could reduce energy consumption. Pre-treatment methods include enzymatic disintegration by endoglucanase (Pääkkö et al. 2007), selective oxidation with 2,2,6,6-tetramethyl-piperidinyl-1-oxyl (TEMPO) radical as catalyst (Saito et al. 2007) or introduction of charge to fibers via carboxymethylation (CM) (Wågberg et al. 2008, Eyeholzer et al. 2010). The introduction of charged groups into the pulp fibers has long been known to enhance delamination of the fiber walls (Walecka 1956). When these anionic groups are in sodium salt the pulp formed is more swollen, and as such has lower cell-wall cohesion. When the charge density of pulp fibers increases, the charge repulsion leads to a drastic decrease in fiber–fiber friction. This leads to drop in tendency to flocculate among fibers consequently decreasing clogging in the homogenizer (Horvath, Lindström 2007). Hence, these pretreatments combined with mechanical disintegration of fibers before homogenization became a fairly obvious approach to reduce the energy consumption and a good way to produce more uniform and smaller size nanofibrils. More detailed information about currently available methods for the disintegration of pulp fibers to MFC or NFC can be found in a recent review by Klemm (2011).

The width of smallest fibrils produced with enzymatic pre-treatments is typically between 5-10 nm and a length of over 1 µm, for unmodified NFC (Pääkkö et al. 2007). The size distribution of fibrils in those materials is very broad (a highly polydisperse material with larger aggregates), and the size of the fibrils strongly depends

on how many homogenization passes were implemented. When charge is introduced by carboxymethylation (Wågberg et al. 2008, Eyeholzer et al. 2010), TEMPO-oxidation (Saito et al. 2007) or recently also cationization **Paper I, II** (Aulin et al. 2010, Ho et al. 2011, Pei et al. 2013) the individual fibrils produced are much smaller with a width in the range of 2.0 - 4.5 nm. Furthermore, the polydispersity of those materials also decreases. The differing charge density of pulps can lead to differences in the size of the nanofibrils. For instance, Lindström and co-workers (Wågberg et al. 2008) reported fibrillar widths ranging from 5–15 nm for an MFC with a negative charge density of 0.5 meq/g. Isogai and co-workers (Saito et al. 2006, Saito et al. 2007), on the other hand reported uniform microfibrils with widths of 3–5 nm for TEMPO-oxidized cellulose with a negative charge density of 1.5 meq/g. Cationic modification of pulp before disintegration leads to even smaller fibrils, which are on average 1.6 – 2.1 nm in width, and 1.3 – 2.0 µm in length (Pei et al. 2013). Even smaller sizes for the width of the cationic NFC have been reported, as low as 0.8-1.2 nm for the smallest non- aggregated fibrils when imaged in the liquid state (**Paper I**).

Depending on the pretreatment, nanofibrils appear to have two hierarchical levels—one with the fibril width in the range of 15–20 nm and another smaller 2–5 nm. The latter corresponds to the elementary fibril, which results from extrusion from the cellulose-synthesizing complex (rosette complex) during biosynthesis. The higher dimensions result from the aggregation of microfibrils after biosynthesis (Bardage et al. 2004). Figure 6 presents AFM images of model films made by spin coating on silica crystal: carboxymethylated NFC (a, b) and unmodified NFC (c, d).

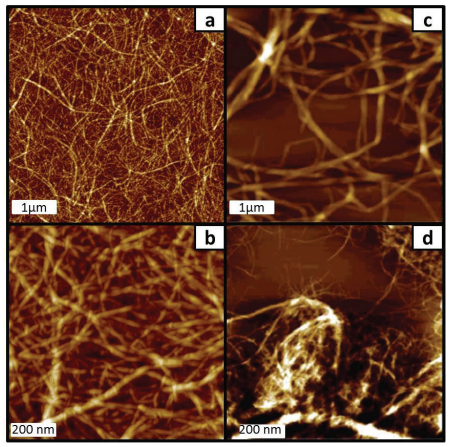

Figure 6. Examples of cellulose fibril grades: AFM height image of carboxymethylated NFC (a, b) adopted from (Ahola et al. 2008b) and unmodified NFC (c, d) adopted from (Pääkkö et al. 2007). The size of the fibrils is 4-5 nm (a, b) and 5-10 nm (c, d)

2.2.2. Crystalline nanocellulose CNC

Crystalline nanocelluloses (CNCs), also commonly known as nanowhiskers, consist of rod-like cellulose crystals with widths of 5–10 nm and with lengths between 100 nm and several micrometers (Eichhorn et al. 2010). The first report of cellulose crystals produced in solution is dated in early 60´s (Ranby, Noe 1961). The first production of nanowhiskers by acid hydrolysis was reported almost 30 years later by prof. Gray´s group (Revol et al. 1992). The most popular process for isolation of CNCs from cellulose fibers is based on acid hydrolysis (Edgar, Gray 2003). By applying acid treatment the disordered or paracrystalline regions of cellulose are preferentially hydrolyzed, whereas crystalline regions have a higher resistance to acid attack and remains intact (Ruiz et al. 2000, Angles, Dufresne 2001). As a result of the acid treatment rod-like nanocrystals are produced. The morphology and crystallinity of CNCs obtained by acid hydrolysis is similar to the original cellulose fibers from which they are produced (Roman, Winter 2004, Garcia de Rodriguez et al. 2006, Elazzouzi-Hafraoui et al. 2008, Habibi et al. 2008). The acid hydrolysis leads to rapid decrease in the cellulose degree of polymerization (DP) to the so called level-off DP (LODP) (Nishiyama et al. 2003). The value of the LOPD was shown to be dependent on the cellulose fibers origin with typical values of 250 for cotton (Battista 1950), and from 140-200 for bleached wood pulp (Battista et al. 1956). After hydrolysis homogeneous crystallites are generated and their presence have been confirmed by different spectroscopic methods such as X-ray crystal diffraction (Schurz, John 1975), electron microscopy (Schurz, John 1975), small angle X-ray diffraction (Yachi et al. 1983) and neutron diffraction analysis (Nishiyama et al. 2003). Depending on the cellulose fiber source, different geometrical dimensions of CNCs can be produced. The reported widths for CNCs are usually approximately a few nanometers, but the length can vary from tens of nanometers to several micrometers. CNCs from cotton, for instance, are 5 – 10 nm in width and 100 – 300 nm in length. However, tunicates and sea animals produce larger crystals, ca. 10 – 20 nm in width and 500 – 2000 nm in length (Angles, Dufresne 2001). CNCs from wood are considerably smaller, where the width is found to be between 3 – 5 nm and the length between 100 – 200 nm (Araki et al. 1999, Araki et al. 1998, Beck-Candanedo et al. 2005). The aspect ratio of CNCs spans a broad range and can vary between 10 to 30 for cotton and even 70 for tunicate. For more examples of the length and width of CNCs from various sources can be found in the recent review article by Habibi et al. (2010).

The dimensions of CNC particles also depend on the duration of the hydrolysis, whereby a longer reaction time produces shorter crystals (Dong et al. 1996, Beck-Candanedo et al. 2005, Elazzouzi-Hafraoui et al. 2008). Specific hydrolysis and separation protocols have been developed for each of the various sources of cellulose fibers, e.g. cotton (Dong et al.1998, Araki et al. 2000), bleached softwood (Araki et al. 1999), hardwood (Beck-Candanedo et al. 2005), microcrystalline cellulose (Bondeson et al. 2006, Capadona et al. 2009) and bacterial cellulose (Araki, Kuga 2001, Grunnert, Winter 2002, Hirai et al. 2009). For the preparation of CNCs sulfuric and

hydrochloric acids are the most extensively used. However other acids have also been reported for the purpose (Okano et al. 1999, Ono et al. 1999, Filppolnen 2009). If CNCs are produced by hydrochloric acid (Araki et al. 1998) their ability to disperse is limited and they tend to flocculate in the water suspension. However, when sulfuric acid is used, negative sulfate esters group on the surface of crystals to promote dispersibility of the CNCs in water (Revol et al. 1992).

It is important to note that the diameter of the cellulose fibrils and the proportion of crystalline material are key information in understanding the mechanical performance of cellulose (Kong et al. 2008, Salmen, Bergstrom 2009, Zabler et al. 2010). They are indispensable input in theoretical calculations of the strength of different man- made fibers, wood and also cellulose-based nanocomposite materials (Xu, Liu 2004, Momeni, Yassar 2009).

2.3. Interfacial forces in nanocellulose systems

The interaction forces acting between colloidal particles in suspensions or between thin surfaces play an important part in determining the properties of a variety of materials as well as the behavior of a range of industrial processes. Since NFC often possesses substantial anionic charge originating from pulping operation or from the close association of hemicelluloses, a many interactions between nanofibrils can be electrostatic in origin. The adsorption and interaction between NFC and polyelectrolyte, non-charged polymers or polysaccharides can also be studied by applying the colloidal force technique to understand more deeply the interfacial forces between those colloidal objects. Below a brief theoretical review of the colloidal forces between particles and surfaces, with special emphasis on cellulosic systems, is presented. The chapter encompasses van der Waals forces, electrical double layer forces, hydration forces, hydrophobic, hydrodynamic forces, bridging forces and steric forces.

2.3.1. DLVO Forces

In the case of charged surfaces in a liquid medium, the classical theory developed independently by Derjaguin & Landeua (1941) and Verwey & Overbeek (1948), known as DLVO theory, is often used to describe the combined interaction forces arising from van der Waals attraction and electrostatic repulsion of similarly charged particles. The theory can describe many phenomena related to colloidal stability.

Van der Waals forces (*vdW*) arise from the fluctuations of the electron clouds of the atoms (polarization) creating permanent or temporary dipoles. Those forces are rather weak and short ranged between atoms or molecules. To calculate van der Waals force between two macroscopic surfaces, the Hamaker-method can be used (Hamaker 1937), in which the energy of all atoms in one body is summed with all the atoms in the other

Eq. (2.1). In this way we obtain a simple expression for the van der Waals forces which for a sphere/surface (used in this thesis) takes the form:

$$\frac{F}{R} = -\frac{A}{6x^2} \qquad \text{Eq. 2.1}$$

Where R is the radius of the sphere, A is the material dependent Hamaker constant and x is the normalized separation. The assumption of pairwise additivity doesn't take into account the effect of the neighboring atoms on the interactions of pair of atoms, which makes it difficult to include the effect of the medium in which the pair of atoms is interacting. Lifshitz theory (Lifshitz 1956) can be used to calculate the Hamaker constant, which takes into account both the surrounding medium and neighboring atoms. The Hamaker constant can be roughly defined as a material property that represents the strength of van der Waals interactions between macroscopic bodies. The Hamaker constant (A) is given by:

$$A = \pi^2 C \rho_1 \rho_2 \qquad 2.2$$

where ρ_1 and ρ_2 are the number of atoms per unit volume in interacting bodies and C is the coefficient in the particle-particle pair interactions. The Hamaker constant can be calculated in various ways: through the surface tension (γ) of materials, or from the thermodynamic properties of liquids (Heimenz, Rajagopalan 1997). The van der Waals interactions between identical bodies in a medium are always attractive as it is seen also in cellulose-cellulose system studied in this thesis.

Bergström *et al.* (Bergström et al. 1999) calculated the Hamaker constant of cellulose from spectroscopic ellipsometric measurements on regenerated cellulose films deposited using the Langmuir-Blodgett technique. They showed that cellulose has relatively low Hamaker constant in air (58×10^{-21}J) and in water (8×10^{-21}J). Notley *et al.* (2004b), however reported a lower Hamaker constant value for two cellulose surface immersed in water (3.5×10^{-21}J). They suggested that the cellulose surfaces can be considered to be swollen in the aqueous condition, and as such, the effective cellulose content in the outer surface layer may be reduced by significant amount of water, leading to a significantly lower Hamaker constant as measured using surface force techniques.

The other contribution to the DLVO theory are *electrostatic double layer forces*. They are present between charged surfaces in liquid (Israelachvili 1991). The charge on the surface can originate via several different mechanisms such as desorption of lattice ions, dissociation of surface groups or adsorption of charged species. In the presence of an electrolyte the surface charge is balanced by oppositely charged counterions leading to system electroneutrality. The region near the surface of increased counterion concentration is called the electrical double layer. Ions close to the charged surface are strongly bound to the surface form the immobile, so-called Stern layer. The region adjacent to the Stern layer is called the diffuse layer and contains loosely associated ions that

are relatively mobile. The diffuse layer neutralizes the charge of the surface. The Poisson-Boltzmann (PB) Eq. (2.3) describes the ion distribution in the diffuse double-layer as a function of the separation from the surface, *x*, and it assumes ions as point charges which are non-interacting. By integrating the PB equation twice, the surface potential ψ, the electric field and the counterion density at any point of separation from the surface can be calculated.

$$\frac{d^2\psi(x)}{dx^2} = -\frac{e}{\varepsilon\varepsilon_0}\sum z_i\, n_{i\infty} exp\left(-\frac{z_i e\psi(z)}{kT}\right) \qquad 2.3$$

where $\psi(x)$ is the electrostatic potential at distance x from the surface, z_i is the valency of the counterion, e is the elementary charge, $n_{i\infty}$ is the number density of the ions in the bulk solution, ε_0 is the permittivity of vacuum, ε is dielectric constant of water, k is the Bolzmann constant and T is the temperature. The solutions to the Eq. 2.3 are obtained by approximation using algorithms (Ninham, Parsegian 1971) assuming either constant charge or constant surface potential and give the lower and upper limits of the interactions, respectively.

When two surfaces present similar charge, they sense repulsive force while approaching each other. The repulsion rises from the overlap of electrical double layers of the similar particles. The thickness of the electrical double layer can be estimated by calculating the Debye length (k^{-1}), which indicates the distance from the surface where the distribution of ions in the solution is affected by the presence of a charged surface. The Debye length decreases when the electrolyte concentration increases, Eq. (2.4).

$$k^{-1} = \sqrt{\frac{\varepsilon\varepsilon_0 kT}{\sum_i e^2 Z_i^2 n_i}} \qquad 2.4$$

In general, particle dispersion is stable when the particle-particle interactions are repulsive. An increase in electrolyte concentration or the valence of the counterion always decreases the stability of a colloidal suspension, and the system tends to coagulate. On the other hand, by increasing the surface charge density the stability of the particles is improved. DLVO theory predicts that electrostatic double-layer forces dominate at large separation, while the van der Waals component dominates at shorter separation. In the complementary system we can have attraction between particles caused by the attractive electrostatic interactions of oppositely charged particles.

2.3.2. Non-DLVO Forces

In many systems, like in nanocellulosic systems, it is not enough to consider only van der Waals forces and electrostatic double layer forces for the total surface force interactions. Forces exist outside the DLVO theory, like an additional repulsive component which originates from organization of the solvent or water molecules around the particles and is known as the *hydration force*. These forces are short-range structural repulsive forces, which initiate from the energy required for the dehydration of the interacting surfaces containing adsorbed

hydrated cations (Israelachvili, Pashley 1984, Argyris et al. 2011). On hydrophilic materials this force increases as the electrolyte concentration increases and is opposite to the electrostatic double layer behavior (Israelachvili, Wennerström 1996). However, hydration forces are usually not observed in cellulose systems due to the roughness and porosity of the cellulose surfaces, which induce steric forces in proximity of the surface. *Steric forces* are repulsive forces and they are mostly observed in systems where large polymeric molecules are present. When an adsorbed polymer has loops and tails extending from the surface, the mingling and overlapping of the stretched chains coming from the opposite surface can lead to loss of the entropy (due to steric hindrance of the chains) and loss of enthalpy (due to reduced solvent-polymer contacts) which results in repulsive forces. The steric force depends on the grafting density of the polymer, the surface affinity, polymer structure and solvent conditions. When the polymer is charged, double layer forces can also contribute to these interactions, and then the force is often referred to as electrosteric force (Poptoshev, Claesson 2002). At low surface coverage of polymer, *bridging* is possible. This phenomenon is observed when a polymer from one surface attaches to the second surface forming a bridge between both surfaces (La Mer, Healy 1963, Almog, Klein 1985, Ji et al. 1991). The mechanism responsible for bridging to occur is based on enthalpy gains from the decrease of polymer-solution contact. When the surfaces are separated, bridging keeps them together. This adhesion can be relatively long ranged (Rand et al. 1979, Biggs 1995) and can be also present in cellulose systems (Eronen et al. 2012). Another, non-DLVO contribution to the surface forces are *hydrophobic forces*. Those forces are long-ranged attractive forces between hydrophobic substances in water. They are mostly studied in surfactant systems (Yoon, Ravishankar 1996). They are caused by the hydrophobic substance interrupting the structure of the water medium. The orientation of water molecules in contact with hydrophobic molecules is entropically unfavorable and therefore such hydrophobic molecules attract each other, since by coming together the entropically unflavored bonded water is ejected into the bulk, reducing the total free energy of the system. *Hydrodynamic forces* are forces resulting from viscous dissipation (Chan, Horn 1985, Claesson et al. 2001, Butt et al. 2005), which are present in the dynamic systems, when solvent molecules (water when aqueous system is studied) drains from the gap between two approaching surfaces. Those forces only affect the dynamics of the solution, not the equilibrium distribution.

2.3.3. Interactions in cellulose systems

Direct force measurement methods, especially the surface force apparatus (SFA) and atomic force microscopy (AFM) have been widely used to study surfaces forces (Hartley 1999, Hodges 2002, Butt et al. 2007, Claesson et al. 2005). SFA was the first surface sensitive technique applied to measure interfacial forces in cellulose systems (Neuman et al. 1993). Studying direct surface force measurements between cellulose surfaces have revealed interesting details of the interactions of cellulose at molecular level. The surface forces between two cellulose surfaces depend on the type of the cellulose studied. When the cellulose possess slightly anionic

charge (originated either from closely associated hemicellulsoes, or from the modification of pulp) the forces are mostly repulsive with two distinguishable force regions, steric and electrosteric (double layer forces) (Holmberg et al. 1997a, Rutland et al. 1997, Holmberg et al. 1997b, Carambassis, Rutland 1999, Poptoshev et al. 2000, Paananen et al. 2004, Notley et al. 2005, Stiernstedt et al. 2006a, Stiernstedt et al. 2006b). The attractive van der Waals force component in the cellulose system could be also detected at low pH (Notley et al. 2004b). Under these solution conditions, any remaining carboxyl groups within the cellulose surfaces are protonated, thus the repulsive component due to the overlap of electrical double layers is eliminated allowing observation of the attraction. Also the reduced swelling of the cellulose at lower pH is beneficial and leads to lowering the steric repulsion in the system, enabling observation of vdW contribution. The forces observed at short separation are usually deviate from DLVO theory predictions, and have been attributed to steric (or electrosteric) forces but also could be a consequence of the deformation of the soft cellulose substrates used (Rutland et al. 1997, Zauscher, Klingenberg 2000b, Stiernstedt et al. 2006b). In the intermediate separation regions the forces observed for cellulose can be fitted to DLVO-predictions relatively well, and the most common interpretation of their origin is assigned to electrostatic repulsions. The detected surface force between the surfaces is usually located somewhere between two boundary conditions as presented in Fig. 7 where force curves obtained between two cellulose spheres in presence of electrolyte is fitted to DLVO theory.

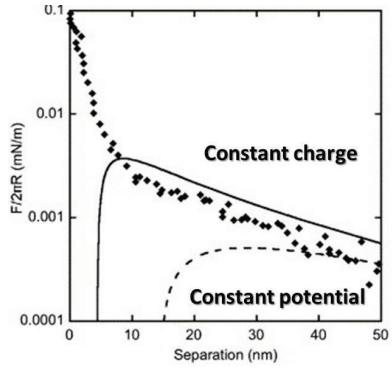

Figure 7. Normalized force profiles between a cellulose sphere and another cellulose sphere immersed in 0.1 mM NaCl solution. The lines are fits to DLVO theory where the Debye length was calculated to be 30 nm and Hamaker constant 8 x 10^{21}J. The solid line represents the constant charge boundary conditions and the dashed line the boundary of constant potential. Figure adopted from (Stiernstedt et al. 2006a)

The short range repulsive forces between cellulose systems are consequence of low, slightly negative charge present on cellulose surfaces, and when the pH is increased, the repulsion between cellulose surfaces increases as well (Carambassis, Rutland 1999, Österberg, Claesson 2000, Notley et al. 2004b, Notley, Eriksson,Wågberg 2005, Eriksson et al. 2006). The increase in repulsion force observed in the cellulose system at elevated pH comes from dissociated carboxylic groups, which is the origin of the surface charge in cellulose. Also steric

repulsion increases due to the more extended conformation of swollen charged cellulose polymer and adds to the repulsive force contribution at larger separations (Zauscher, Klingenberg 2000b, Poptoshev et al. 2000).

Hydrophobic forces could also be present in the cellulose system. Cellulose is known to be amphiphilic in nature (Lindman et al. 2010, Johansson et al. 2011, Medronho et al. 2012).The conclusion has been drawn from the structure of cellulose crystals (Nishiyama et al. 2002) and it was demonstrated that the chain of glucose rings can have sides of very different polarity (Lindman et al. 2010, Glasser et al. 2012). The hydrophobic sides would have a large tendency to attract each other in an aqueous environment, which would contribute to low solubility and could be visible as long range attractive hydrophobic forces. However so far there was no reports revealing an attractive hydrophobic force component in cellulose systems studied by the AFM technique. In previous studies of the surface forces between cellulose surfaces in aqueous conditions (Carambassis, Rutland 1999, Österberg, Claesson 2000, Notley et al. 2006, Ahola et al. 2008c), steric interaction and electrostatic repulsion have often been measured precluding the observation of attractive hydrophobic forces.

Within the last decade cellulose based nanomaterials have gained considerable interest. When NFC/MFC or CNC became easily available and the construction of ultrathin films from that substrate was developed (Kontturi et al. 2003, Kontturi et al. 2006, Ahola et al. 2008b), the possibility to study interfacial forces in nanocellulose systems was a natural consequence. The forces between an NFC ultrathin film and a regenerated cellulose colloidal sphere using CPM were studied as a function of charge and pH (Ahola et al. 2008b). The unmodified NFC used as low charged cellulose surface in that study was the first attempt to use cellulose I in surface force experiments. Even though the substrate studied by that group still had closely associated hemicelluloses, it was by far the closest model for a cellulose fiber, which in nature also contains accompanying polysaccharides. They observed that by increasing the charge of the NFC, the range and the magnitude of the repulsive forces also increased, which was similar to the system where the ultrathin film from carboxymethylated cellulose was studied (Notley et al. 2006, Notley 2008). The interfacial behavior of CNC films also show monotonically repulsive forces, which were assigned to the contribution of electrostatic double-layer interactions (Notley et al. 2006, Stiernstedt et al. 2006a) originating from the presence of sulphate groups. In general the higher the charge on the nanofibrils the more stable the suspension of fibrils in water and more repulsive interactions are expected and detected with CPM. Also the higher charge on the surface of nanofibrils leads to a more swollen network of fibrils (when studied in an aqueous environment) and in consequence, a higher extension of fibrils and more steric repulsion are detected when measured with CPM.

2.3.4. Effect of polymers/polysaccharides adsorption on cellulose interactions

Depending on the polymer properties, steric repulsion or attractive bridging can be observed between cellulose surfaces. When oppositely charged polymers (polyelectolyte) is incorporated in the cellulose system

via adsorption, the charge density (*CD*) and molecular weight (M_w) of the polymer play important role in the adsorbed polymer conformation. When a higher *CD* polymer is used, a more compact attachment and more rigid layer is formed, which results in a smaller increase in detected repulsive steric forces. The opposite behavior is observed for the system with a lower *CD* polymer. When a high M_w and low charged polymer adsorbs on the surface, the adsorbed layer is thicker and due to entropic reasons, long range repulsion is observed. But the repulsion in such system can also be a consequence of the steric hindrance induced by the loop and tail conformation of the polymer. Such behavior has been observed between two colloidal cellulose spheres in presence of cationic polyelectrolyte solution (Salmi et al. 2007b). When polyelectrolytes are use in cellulose systems, attraction is typically observed at the charge neutralization point (Holmberg et al. 1997b, Zauscher, Klingenberg 2000b, Poptoshev, Claesson 2002, Salmi et al. 2007a).

A few investigations have also been devoted to the analysis of the direct forces in systems where one surface has been constructed from nanofibrillated cellulose (Ahola et al. 2008b, Salmi et al. 2007a). The adsorption of polysaccharides such as xyloglucan (XG) (Stiernstedt et al. 2006a) or chitosan (Nordgren et al. 2009a) changes the interactions between cellulose surfaces, by increasing the range and the magnitude of repulsive forces. The explanation lies in the formation of loops and tails of the adsorbed polysaccharides that extend out from the surfaces and contribute via steric hindrance to the repulsion forces. Beside the studies regarding surfaces force interaction, the adsorption studies of structurally different hemicelluloses on nanofibraillar cellulose were studied by Eronen (2011a).

2.3.5. Cellulose multilayer systems

Multilayer films can be fabricated by layer-by-layer assembly (LbL) which is a unique and facile method for fabricating composite films with nanometer precision. This robust technique can be easily applied to form smooth films with controlled chemistry. It was first introduced by Iler (Iler 1966), brought back ca. 30 years after of discovery by Decher (1992, 1997) and quickly after that, become widely applied. The technique has been reviewed on several occasions, outlining the concepts behind, and the potential of, LbL technology (Lvov, Decher 1994, Decher 1997, Bertrand et al. 2000). Self-assembled systems obtained from the LbL technique are used for a wide range of applications, such as: sensors (Decher 1997, Jean et al. 2008b), antireflective coatings (Podsiadlo et al. 2007), drug delivery systems (Zhai et al. 2004), antifouling agents, and functional coatings (Decher, Schlenoff 2003).

The principle of the technique is based on sequential adsorption of two or more components, which are alternately deposited by solution-dipping, spraying or spin-coating with successive rinsing steps between each layer. Usually electrostatic attractive interactions dominate between alternate layers. The LbL technique has been applied to systems which include multiply-charged polyelectrolytes and nanoparticles such as nanotubes

and quantum dots, clays and proteins (Decher, Schlenoff 2003). Also, polysaccharide multilayer fabrications become an active field of research (Boddohi, Kipper 2010). While numerous works have focused on multilayers with, e.g., hyaluronin, chitosan, or heparin (Boddohi, Kipper 2010) various polysaccharide-based multilayers have still received relatively little attention.

Recently, the multilayer build-up and layer properties of nanocellulose systems, both NFC (Aulin et al. 2010, Eronen et al. 2012) and CNC (Cranston, Gray 2006, Cranston, Gray 2008, Jean et al. 2008a, Jean et al. 2009, Cranston et al. 2010) combined with cationic polyelectrolytes were studied. Podsiadlo *et al*. (Podsiadlo et al. 2005) were the first to report the preparation of CNC-based multilayers with poly (diallyldimethylammonium chloride, poly-DADMAC) using LbL assembly, where they observed uniform coverage and a densely packed CNC surface by applying AFM and SEM analyses. The formation of a well-ordered alignment from anisotropic CNC suspensions and the smoothening effect of flexible poly(allylamine hydrochloride), (PAH) macromolecules was reported by Jean *et al*.(2008a). Layer-by-layer orientated self-assembled multilayer films containing CNCs and PAH were also prepared by Cranston and Gray (2006, 2008, and 2010).

The build-up of LbL films and the structure of the adsorbed polyelectrolyte have also been studied with the help of the surface force measurements technique (Blomberg et al. 2004, Blomberg et al. 2006). This has provided a good starting point for experiments where nanocellulose particles, such as CNCs, were incorporated in the multilayer build up (Rojas et al. 1998, Plunkett et al. 2003, Notley et al. 2004a). The interactions between polyelectrolyte multilayers containing CNCs and PAH were found to be more complicated than those that would be displayed by the monolayers alone. It has also been shown that under special solution conditions the underlying layer was able to extend and migrate from the LbL film and affect the surface forces (Cranston et al. 2010). The effect of NFC negative charge and the properties of a cationic counterpart in relation to LbL formation was studied recently by Eronen *et al.* (2012). They found that non-electrostatic interactions had a determining role in multilayer formation between cationic and anionic NFC particles. Cationically modified NFC has also been used to prepare self-organized LbL films with anionic NFC (Aulin et al. 2010) and with CNCs (**Paper II**).

2.3.6. Friction Forces and Wear

Friction occurs when two surfaces move laterally with respect to each other. The classic rules of sliding friction were discovered by Leonardo da Vinci (1452–1519) but remained in his notebooks unpublished. Rediscovery was accomplished almost 200 years later by Guillaume Amontons (1699). Amontons presented the nature of friction in terms of surface irregularities and the force required to raise the weight pressing the surfaces together. In his law he stated that the friction force is linearly dependent on the applied load.

$$F_f = \mu L \qquad 2.5$$

where F_f is the friction force, μ is the friction coefficient and L is the applied load. According to Amonton's law friction is independent of the contact area. However, it has been later proven that for rough surfaces the true contact area is dependent on the load, whereas the apparent contact area is constant. F. Phillip Bowden and David Tabor (Bowden, Tabor 1950) showed that at a microscopic level, the actual area of contact between surfaces is a very small fraction of the apparent area. As the normal force increases, more asperities come into contact and the average area of each asperity contact grows. Thus, the frictional force was shown to be dependent on the true contact area.

More studies on friction phenomena observed that friction is also dependent on the adhesion. The adhesion present between studding surfaces adds to the effective load increasing the friction force.

$$F_f = \mu\,(L_{adh} + L) \tag{2.6}$$

where the L_{adh} is adhesion. The adhesive contribution is mostly observed between hydrophilic surfaces studying in the dry state when humidity is present. The adhesion between the surfaces can come from water condensation between the colloidal probe and surface. This phenomenon was observed for the cellulose system by Feiler *et al.* (2005), where the force of two cellulose colloidal probes where measured the in dry state under various humidities. Roughness decreases adhesion so it becomes less significant compared to the load and for rough surfaces (which have a low adhesion) Eq. 2.6 can be reduced to Eq. 2.5. Even though the roughness of surface can decrease the adhesion and therefore the friction force, it has been shown to increase the friction coefficient (Plunkett et al. 2003, Gao et al. 2004, Feiler et al. 2005).

When the normal force applied to the probing sample exceeds the critical value, which depends both on the tip geometry and the material under investigation, the surface topography is permanently modified. When such a permanent change is observed we talk about wear of the material. Wear is related to interactions between surfaces and more specifically the removal and deformation of material on a surface as a result of mechanical action of the opposite surface (Rambowicz 1995). Some commonly referred to wear mechanisms (or processes) include: *abrasive wear* –occurs when a hard rough surface slides across a softer surface; *fatigue wear* – failure of the material due to repeated stressing from hard irregularities on the counter surface; and *adhesive wear* – loss of material during frictional contact by transfer and adhesion to the opposite surface.

The development of the atomic force microscope has enabled scientists to study friction (Perry et al. 1995, Heim et al. 1999, Feiler et al. 2000, Butt et al. 2005) and wear (Bhushan et al. 1995) at the molecular scale. Those two phenomena are closely related. Appearance of scratches and deformation of the surface as a result of wear mechanism can alter the roughness and induce changes to the friction forces as reported by Kopta (2000).

So far only a few studies have dealt with nanotribological response of cellulose. Stiernstedt *et al.* (2006b) studied different cellulose model surfaces and their interaction with an amorphous cellulose sphere. Also the effect of xyloglucan (Stiernstedt et al. 2006a) and chitosan (Nordgren et al. 2009b) the adsorption and lubrication properties in aqueous polysaccharide solutions (Stokes et al. 2011) have also been studied. The coefficient of friction (COF, μ) measured in liquid, between two cellulose surfaces was reported to vary between 0.6 and 1. When different roughness levels are taken in consideration (Zauscher, Klingenberg 2000c, Zauscher, Klingenberg 2000a, Theander et al. 2005, Stiernstedt et al. 2006b), these values are relatively constant and similar. Upon increasing the applied load, friction force becomes more constant which could be caused by flattening the asperities (Zauscher, Klingenberg 2000a). An adsorbed polymer layer on cellulose affects the frictional forces also between two cellulose surfaces like in case of normal forces (described in section *Chapter 2.3.2*). Generally, an addition of polymer lowers the COF but the added polymer concentration and properties such as charge affects the forces in different ways. At low polymer concentration the friction force increases with applied load, while at higher polymer concentration the friction force is no longer linear with applied load. These changes have been reported to be associated to the monolayer formation by (Zauscher, Klingenberg 2000a). The effect of xyloglucan (Österberg et al. 2001, Stiernstedt et al. 2006a) and chitosan adsorption (Nordgren et al. 2009a) on the friction response between cellulose colloidal spheres showed that overall friction force reduced upon adsorption of polymer while adhesion increased.

Many studies have adapted the concept of interfacial shear stress to study the solid state interactions between a nano-reinforcement and a soft phase, namely the matrix, of the composite material (Lachman, Wagner 2010, Lachman et al. 2012). Force transfer between the two distinct components can take place through intermolecular bonds and also via frictional phenomena (Lachman, Wagner 2010, Lachman et al. 2012). Thus, even though microscopic friction studies are not always easy to conduct and apply, they could be of potential importance of understating the interactions between composite phases from the fundamental point of view.

2.3.7. Lubrication

When friction is reduced between two solid surfaces we talk about lubrication. Lubrication can be divided into different regimes depending on the thickness of the fluid film present between the surfaces studied. Also what is important to note is that the fluid film viscosity, the load that is carried by the two surfaces and the speed that the two surfaces move relative to each other determine the thickness of the fluid film. This, in turn determines the lubrication regimes, which are the following:

Hydrodynamic or elastic lubrication – when two surfaces are separated by a fluid film;

Mixed lubrication – when two surfaces are partly separated and partly in contact;

Boundary lubrication – where two surfaces are mostly in contact even though a fluid is present (It should be note that through this work friction was measured mostly at the boundary lubrication conditions).

How the viscosity of the fluid, velocity and the applied load affect the friction losses and how they correspond to the different regime is shown on the Stribeck curve (Fig. 8).

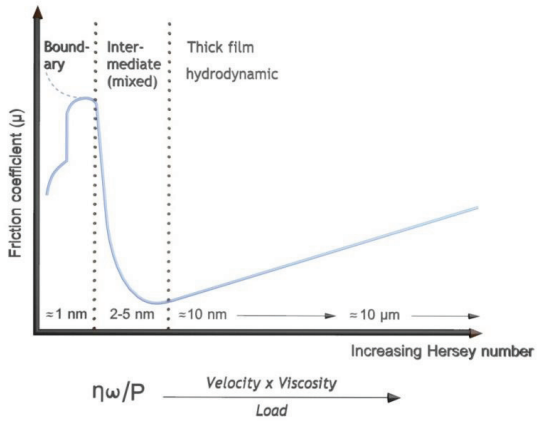

Figure 8. The Stribeck curve exemplifying the variation of friction force as a function of Hersey number (adopted from Bhushan "Nanotribology and nanomechanics II" third edition 2011)

The Stribeck Curve is a plot of the friction as it relates to viscosity, speed and load. On the vertical axis is the friction coefficient. The horizontal axis shows a parameter that combines the other variables: the Hersey number, where η is the fluid viscosity, ω is the relative speed of the surfaces and P is the load on the interface per unit bearing area. The combination of low speed, low viscosity and high load will produce boundary lubrication, which is characterized by little fluid in the interface and large surface contact. It can be clearly seen from the Stribeck curve, that this combination results in very a high friction coefficient. As the speed and viscosity increase, or the load decreases, the surfaces will begin to separate, and a fluid film begins to form. Even though the fluid film layer can still be very thin, it can already support more of the load. This moves us on the curve to the mixed lubrication regime and is seen on the Stribeck curve as a sharp drop in friction coefficient. This drop in friction is a result of decreasing surface contact and more fluid lubrication. When the speed or viscosity increases until there is no more surface contact (surfaces will continue to separate away from each other), the friction coefficient will reach its minimum (hydrodynamic lubrication regime). As can be seen from the Fig. 8, in which hydrodynamic region the curve shows an increase in friction coefficient with increasing Hersey number. This is due to the friction produced by the fluid. In the situation when a higher speed is applied (which results in thicker fluid layer) the fluid friction increases on the moving surface. Higher viscosity, which

also increases the fluid film thickness, also increases the friction between the fluid layer and the surface. Thus there is general trend in the Stribeck curve with increasing friction force in the hydrodynamic region.

Boundary lubricants are especially important in lubricating the tribological contacts where asperity-asperity contact is dominant, which is a condition of high load and/or low speed. The main mechanism of boundary lubricant is based upon modification of the shear strength of surface interfaces rather than formation of a fluid layer, which could bear the load between two surfaces. For this reason, the continued presence of lubricant is critical. Aqueous lubrication is particularly important in biomedical applications (Lee et al. 2007, Kanika et al. 2009) and food and pharmaceutical industries (Lee et al. 2006).

In this thesis we address the lubrication properties of polyethylene glycol grafted carboxymethyl cellulose on nanofibrillated cellulose substrate in liquid (**Paper IV**) and in air (**Paper V**) to extend the knowledge about the nanotribiology of cellulose.

2.4. Nanofibrillated cellulose reinforced composites

2.4.1. The excellent mechanical properties of nanocellulose

The elastic modulus of cellulose crystals was first determined in 1936 by Meyer and Lotmar (1936) using a theoretical model. They obtained a value of 120 GPa which was later confirmed by experiment (Nishino et al. 1995). Sakurada (1962) reported a value of 138 GPa for crystal modulus of cellulose, which was determined using X-ray diffraction. This experimental approach paved the way for many more measurements exploiting X-ray diffraction (Matsuo et al. 1990, Nishino et al. 1995) but also theoretical studies were conducted to determine the elastic modulus of crystal in crystalline cellulose (Tashiro, Kobayashi 1991, Sturcova et al. 2005, Eichhorn, Davies 2006). Atomic force microscopy was also used to assess the stiffnes of cellulose crystals obtained from tunicate which were TEMPO oxidized or acid hydrolyzed, and they were 145 GPa and 150 GPa respectively (Iwamoto et al. 2009). AFM was also used to estimate the strength of bacterial cellulose (Guhados et al. 2005) and wood-driven CNCs (Lahiji et al. 2010). Raman spectroscopy technique was also utilized to measure the elastic modulus of native cellulose crystals from tunicate and cotton with values of 143 GPa (Sturcova et al. 2005) and 105 GPa (Rusli, Eichhorn 2008), respectively. Recently, Saito et al. (2013) used a statistical approach to estimate the stiffness of single cellulose nanofibrils prepared by TEMPO-meditated oxidation, it had a mean strength value of 1.6 – 3 GPa, and for crystalline tunicate cellulose fibrils 3 – 6 GPa.

By comparing the value of the crystalline modulus of cellulose with other commonly known materials (Table 1) the value found for cellulose is quite large especially if the density of materials is considered (specific modulus). As can be seen from the Table 1, by comparing the specific modulus of crystalline cellulose to

commonly use engineering materials, the low density of cellulose makes it especially interesting. When the specific moduli are taken into consideration, the value of common macroscopic fibers (with its density 1.5 Mg/m^3 to be assumed) suppresses those of glass and other engineering materials. For more information reader is referred to review by Eichhorn (2010).

Table 1. Moduli of engineering materials compared to cellulose (table adopted from (Eichhorn et al. 2010))

Material	Modulus (GPa)	Density (Mg/m^3)	Specific modulus (GPa m^3/Mg)	Reference
Aluminium	69	2.7	26	(Ashby, Jones 1989)
Steel	200	7.8	26	(Ashby, Jones 1989)
Glass	69	2.5	28	(Ashby, Jones 1989)
Crystalline cellulose	138	1.5	93	(Sekurada, Nukushina & Ito 1962)

Due to the intrinsic high performance, nano-sized cellulose whiskers are predicted to enhance the stress transfer and to increase the composite moduli more than 3-fold, when compared to composites made of traditional microsized fillers. However, such an effect can only be possible for filler fibers with high aspect ratio. Filaments with an aspect ratio lower than 10 would not bring any major benefit to composite mechanical performance compared with conventional micron size fillers. Fibrils with an aspect ratio: higher than 50 enable efficient reinforcement (Eichhorn et al. 2010). Usually cellulose whiskers have a low aspect ratio with typical values of 10 to 30, with the exception of tunicate where the aspect ratio is 70 (Siqueira et al. 2010).

Higher aspect ratios are found for nanofibrillated cellulose, with values of 3 – 5 nm in fibrils thickness and over 1µm length. In contrast to CNC, the NFC whether cast (Dufresene et al. 1997, Andresen et al. 2006, Saito et al. 2006, Andresen et al. 2007) or vacuum filtered (Iwamoto et al. 2005, Nakagaito, Yano 2005, Henriksson, Berglund 2007, Henriksson et al. 2008, Seydibeyoglu, Oksman 2008), can relatively easily form an entangled network with interfibrillar hydrogen bonds. The mechanical properties of films made from NFC depend on the NFC source and the method used for film preparation. In general filtration in contrast to casting, resulted in films with higher modulus and tensile strength. A comprehensive collection on film formation of NFC from different sources and with various preparation procedures can be found in a recent review by Siró (2010).

In fact the high stiffness reported for crystalline cellulose is hardly achieved in reality for NFC films (sometimes called nanopaper) (Henriksson et al. 2008). Henriksson *et al.* (2008) studied the mechanical performance of MFC films prepared in different solvents and also with varying the DP values of cellulose. The

porosity of films also varied depending on the solvent used. Interestingly, they noticed that higher molar mass (higher DP) containing nanofibrils formed a nanopaper structure of much higher toughness than previously reported for microfibrillated cellulose from wood (Taniguchi, Okamura 1998, Yano, Nakahara 2004, Henriksson, Berglund 2007) or bacterial cellulose (Nakagaito et al. 2005a). Most of the literature indicates Young's modulus values of 6-12 GPa of nanopaper films made from cellulose fibrils and tensile strength values around 100-150 MPa (Bruce 2005, Zimmermann 2004, 2005). In the report by Henriksson *et al.* (2008) the film prepared from carboxymethylated NFC with a porosity of 28% and high molar mass was characterized with a high Young's modulus (13.2 GPa) and high tensile strength (214 MPa). The nanopaper sample also showed very high toughness, with a high value for work of fracture, W_A = 15 MJ/m^3 (associated to 10 % strain-to-failure). These values decreased significantly with increased porosity.

Recently nanopaper also was prepared from cationically modified fibrils (Pei et al. 2013). The film demonstrated excellent mechanical properties, with a high tensile strength *ca.* 200 MPa, Young's modulus of *ca.* 10 GPa and a high stain-to-failure (*ca.* 5%).

Typically NFC films are brittle material with strain-to-failure values in the range of 6-9 % (Nakagaito, Yano 2008a, 2008b, Syverud, Stenius 2009, Saito et al. 2009). Despite the brittleness the singularly attractive properties like high Young's modulus and high strength mark nanofibrillated cellulose a promising agent for reinforcement of high-performance materials.

2.4.2. Nanocellulose reinforced composite materials

The study of cellulosic nanofibres as a reinforcing phase in nanocomposites started 18 years ago when Fevier *et al.* reported for the first time the reinforcing effect of CNCs extracted from tunicate (Fevier et al. 1995a, 1995b). During the last few decades nanocellulose reinforced composites became a subject of cellulose research and many review articles have emerged covering that subject (Azizi Samir et al. 2005, Siró, Plackett 2010, Eichhorn et al. 2010, Klemm et al. 2011, Moon et al. 2011, Duran et al. 2012). In essence, the one of the major reasons to utilize cellulose nanoparticles in composites is the high stiffness of the cellulose crystals. A high aspect ratio especially of the long nanofibrils is desirable as this enables a critical length for stress transfer from the matrix to the reinforcing phase. When the reinforcing effect of cellulose whiskers was compared to the effect of NFC in poly (styrene-co-butyl acrylate) latex (Azizi Samir et al. 2004), it was shown that even though both nancellulose particles led to an increase in tensile modulus and tensile strength the significantly higher values where observed for NFC. The higher mechanical performance of the composite where the reinforcement was associated with longer fillers could be due to the entanglement between the fibrils in NFC network, and better stress transfer from the matrix.

A number of research groups explored nanocellulose composites with thermoset resins (Nakagaito, Yano 2004, 2005b), poly(vinyl alcohol) (Millon, Wan 2006), amylopectin (Svagan et al. 2007), poly(ethylene oxide) (Brown, Laborie 2007), or poly(lactide) (Okubo et al. 2009). Very often, however, they focused on rather small amounts of reinforcements without self-assemblies and alignments. Interestingly, most of the polymers used for composite applications are so far either water-soluble or post-filtrated into NFC fiber sheets. This exemplifies a main obstacle for a broader applicability of NFC, which is the poor compatibility in non-aqueous dispersions and the often insufficient interaction with commonplace plastics. The aggregation of nanofibrillated cellulose in blends of hydrophobic polymers is a considerable problem (Wu et al. 2007). The cellulose surface can be functionalized for better control of the hydrophilic nature of the cellulose molecules. Acetylation, and silylation reactions, polymer grafting or polyelectrolyte adsorption are a few of the ways to modify nanocellulose to improve stability in dispersions or to impart special properties to fibrils. Chemical modification of NFC (Lin et al. 2011, Bulota et al. 2012) to work in a non-aquatic solvent to enhance mixing with polymers in composite preparation may, however, lead to disruption of the hydrogen bonds between and inside the fibrils, which consequently can lead to lower strength fibrils and leading to a deterioration in the mechanical performance of the composite material.

So far the most common way of preparing composite materials is to use a low fraction of reinforcing agent mixed with a large domain of soft and usually hydrophobic polymer (Okubo et al. 2009, Wu et al. 2007). Such construction of composite may first lead to aggregation because of the immiscibility of those two components, which later results in a badly dispersed film with fibrils agglomerating through hydrogen bonding. It is even more pronounced at higher reinforcing fibril loading. When composites are made in approach above the mechanical properties evolved in a typically predictable and systematic fashion as a function of the ratio of the components. With decreasing amount of NFC, the stiffness and strength decreases, but the strain-to-failure of the materials increases (mostly because of the use of rubbery polymer as a matrix material) (Bulota et al. 2011). The challenge in constructing nanocellulose based composite materials is to maintain the stiffness and strength of NFC, while increasing the strain-to-failure. This undoubtedly requires synergy between the stiffness, strength and toughness in the material, and requests for new concepts toward biomimetic materials. The importance of uniform mixing different components in the composite film also has to be considered. The concept will be discussed in the following section.

2.4.3. Biomimetic approach

In nature, the hierarchical structure of biological nanocomposites has synergistically evolved to achieve the desired mechanical properties and complex biological functions. Molecular mechanisms which involve the interaction at different levels of the hierarchy govern composite deformation behavior (Manias 2007). A control of the nanoscale hard/soft architecture and lubrication at the same time represents a promising approach

(Nakagaito, Yano 2004, Munch et al. 2008, Bonderer et al. 2008, Walther et al. 2010). Typically stiff and strong materials like NFC suffer from reduced toughness. These materials lack the available deformation mechanism that would allow crack deflection, and in consequence, avoid catastrophic failure when the material is under stress (Fratzl, Weinkamer 2007).

In order to improve toughness Nature has used a range of different mechanisms to dissipate energy at the crack tip. One of the examples can be nacre, where the layers of platelets of calcium carbonate are glued together by a protein matrix (Pokroy et al. 2009). Interestingly only a tiny amount of soft organic phase is sufficient to increase the toughness of an inherently brittle mineral by factors of more than 1000 (Li et al. 2004). Also the presence of a large number of interfaces between the hard reinforcing fillers in composite force cracks to be deflected as they propagate through the structure. Similarly the existence of an extensive interface network can allow for crack bridging and plate pullout, which, in consequence increases energy dissipation (Menig et al. 2000). The occurrence of nanoasperities (Wang et al. 2001) and mineral bridges (Song et al. 2003) between and on the surface of the reinforcing platelets can as well give rise to strengthening interactions between the fillers (Yao et al. 2009). When they fracture they consume energy improving toughness. Likewise sacrificial bonds in the organic soft domain layers (Smith et al. 1999) can reduce brittleness. The uniform dispersion of filler elements, the unique interplay between the components interfaces, and hierarchical structure are critical to reinforcement and need to be well designed in nanocomposites (Wanasekara, Korley 2013).

The first indication that such a natural design method could also provide success in nanocellulose was demonstrated by the in situ coating of biotechnologically produced bacterial cellulose (BC) with hydroxyethylcellulose (HEC) that was added to the culture medium of the organisms (Zhou et al. 2009). Therein, the biologically grown BC with HEC coating displayed better mechanical properties than pure BC or a post-prepared blend of HEC and BC. This example shows that a well-defined soft compartmentalized shell can provide substantial synergies. Still, the main challenge in designing superior materials is to construct composites with high fractions of reinforcements that are hierarchically ordered into the hard/soft mesostructure. Most importantly the new pathways are needed which would allow the synergetic properties beyond the common rule of mixtures. The most elegant tactic is based on self-assembly of the components, which allows overcoming the laborious multistep reaction or sequential depositions. In **Paper III** we developed such a concept based on hard/soft biomimetic ordered composites by ionic complexation of two oppositely charged colloidal objects. Stiff and strong anionically modified cellulose nanofibrils, which accounted for majority of the composite phase, self-assembled with positively charged soft block copolymer micelles. Such complexations led to improvements of the mesoscale order and as consequence, better mechanical performance of material was achieved. In **Paper IV, V** we continued with the approach, but instead of ionic complexation, non-ionic interactions were driving

forces for assembling reinforcing NFC hard domains with polysaccharides that were modified with soft low T_g polymers.

3. EXPERIMENTAL

The main cellulosic and polymeric materials used in the work are described in section 3.1. The methods which were employed for characterization and the brief theory behind them are presented in the section 3.2. More detailed information of materials and methods can be found in **Papers I-V**.

3.1. Materials

3.1.1. Cellulose nanofibrils and cellulose whiskers

The nanofibrillar materials used in this study were supplied from two different research institutes. The nanofibrillated cellulosic materials used in **Papers I, and III** were disintegrated from bleached softwood sulphite pulp by using a high-pressure fluidizer (Microfluidizer M-110EH, Microfluidics Corp.; Newton, MA) at Innventia, Stockholm Sweden. Two different types of nanofibrillar materials were provided, highly anionic and highly cationic. The hemicellulose content (mainly xylan and glucomannan) of the reference pulp was 4.5%. The anionically charged nanofibrils were prepared by the carboxymethylation pre-treatment reaction of the pulp fibres before disintegration in the high-pressure fluidizer as described elsewhere (Wågberg et al. 2008) and where used in **Paper III**. The pre-treatment resulted in an increased amount of anionic carboxyl groups on the fibrils. The charge density was determined via polyelectrolyte titration to be 0.58 meq/g. The cationically charged nanofibrillated cellulose used in **Paper I** was prepared via covalent modification with 2,3-epoxy-propyltrimethylammonium chloride (EPAC) (Aulin et al. 2010). The charge density of the pulp was determined by polyelectrolyte titration and was found to be 0.35 meq/g. The zeta-potential of cationic NFC varied slightly at different pHs, due to the presence of carboxylic groups, as in detail discussed in **Paper I.** The modified pulps were further disintegrated using a high-pressure fluidizer. The nanofibrillated cellulose content was 1.87% and 1.55% for the anionic and the cationic NFC gels respectively.

The other set of cellulosic samples were prepared in the Finnish Centre for Nanocellulosic Technologies from industrial, never-dried kraft pulps obtained from Finnish pulp mills. Unmodified hardwood (birch) pulp was used as a raw material for the NFC substrates in the **Papers II, IV and V**. The pulp was washed to the sodium form according to (Swerin et al. 1990) to control both the counter ion type and ionic strength. The hemicellulose composition in the pulp was 25% xylan and 1 % mannose. The washed pulp was disintegrated through a high-pressure fluidizer (Microfluidics, M-110Y, Microfluidics Int. Co., Newton MA) after 5 and 20 passes. No chemical or enzymatic pretreatment was used prior to disintegration. The charge density of the pulp used was 0.065 meq/g and the zeta-potential of the corresponding NFC gel was -3 mV (Eronen et al. 2012). In **Paper II** the cationically charged nanofibrillated cellulose was used. The fibrils were also produced in the

Finnish Centre for Nanocellulosic Technologies from the same never-dried kraft pulp, which was then cationized via covalent modification with 2,3-epoxy-propyltrimethylammonium chloride (EPAC) (Aulin et al. 2010) before disintegration. The charge of the pulp was determined by polyelectrolyte titration, and was found to be 1.4 meq/g. The fibrils were obtained via disintegration of the washed pulp in friction grinding (Masuko Sangyo Co Ltd, Japan). More detailed information describing the fibrillation procedures can be found elsewhere (Taipale et al. 2010). The cationic NFC samples were characterized by measuring the dry matter content gravimetrically (2% w/w) and determining the zeta-potential values from electrophoretic mobility measurements (Coulter Delas 440SX, Coulter Corporation, Miami, FL) of dilute suspensions. The mobility of the supernatant was determined at a constant electrolyte concentration (1mM) and it was found to be pH dependnt +41.1mV and +35.5 mV for low (pH 4.5) and high (pH 8.3) pHs respectively.

The cellulose whiskers (CNC) were prepared by sulfuric acid hydrolysis from Whatman 541 ashless filter paper as described by Edgar and Gray (Edgar, Gray 2003)

3.1.2. Polymer and polysaccharides additives

Poly(1,2-butadien)-*b*-poly(2-dimethylaminoethyl methacrylate) (PB-*b*-PDMAEMA) was prepared by anionic polymerization in THF with molecular weight M_n = 35 200 g/mol with M_w/M_n = 1.06 with 80 wt % of PB and 20 wt % of PDMAEMA blocks, and was used as a soft component in composite preparation in **Paper III**. The PB-b-PDAMAEMA quaternization and preparation of block copolymer micelles in water is described in details in **Paper III**. The hydrodynamic radius of the micelles was determined by dynamic light scattering (DLS) technique (Malvern Zetasizer NanoZS) in a solution at a concentration of 0.2 g/L in Tris buffer (1 mM, pH 8.3) and was found to be 65 nm.

The analytical grade carboxymethyl cellulose (CMC) used in **Paper IV and V** (Na-CMC, 250 000 g/mol, DS 0.7, Sigma Aldrich) was dialyzed and freeze-dried prior to use. The charge density of dialyzed CMC was determined to be 3.6 mmol/g by direct polyelectrolyte titration. Methoxy polyethylene glycol amine (OMe-PEG-amine; 2 kDa;) was purchased from Fluka. The synthesis of methoxy polyethylene glycol (OMe-PEG)-grafted carboxymethyl cellulose (CMC-PEG) is described in **Paper IV**.

3.2. Methods

3.2.1. Ultrathin film preparation

Cellulose ultrathin films from nanocellulose (NFC and CNC) were used in **Paper I-V**. Following the method introduce by Ahola *et al.* (2008b) the NFC water dispersion was spin coated on the substrate or adsorbed in situ from diluted suspension in the QCM chamber. PEI was used as a cationic anchoring substrate when model films

from either CNCs or anionic NFC were prepared. When cationic NFC was used no polymer was needed. The substrates used for ultrathin films were: silica wafer **Paper I**, mica **Paper I, II, IV, V**, and QCM-D crystals **Paper I, II, III, IV**.

3.2.2. AFM- imaging

The topography and morphological changes on the NFC and CNC-films were characterized by using the AFM imaging technique. The method was developed by Binnig, Quate and Gerber in 1986 (Binnig et al. 1986). Since then AFM has become one of the most successful instruments in surface science and has been the subject of many review articles as a surface characterization method for deformable materials (Hansma et al. 1997, Magonov 2000). The method is rather inexpensive and gives fast and high precision information. The basic principles of AFM are illustrated in the Figure 9.

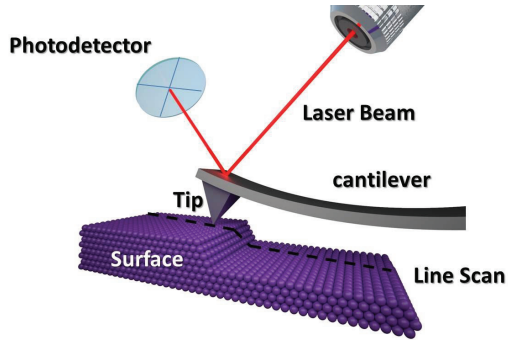

Figure 9. The basic principles of AFM imaging. (Courtesy of Maciej Elert)

The typical AFM can operated in two modes; contact mode where the tip is in contact with the surface and in so called non-contact mode where the tip oscillating at its resonance frequency close to the surface. Tapping mode (intermittent contact) is also possible where the tip touches the samples only briefly during the oscillation cycle. Contact mode was the only available mode on the first AFM in 1986, however since the tip is in constant contact with the sample, biological specimen were difficult to image because they are often weakly bound to the surface and, soft; they therefore, could be damaged easily. Only a year later non-contact mode was introduced (Martin et al. 1987). Developed in an effort to more accurately image soft biological samples, in non-contact mode the cantilever oscillates close to its resonant frequency at a small distance (1-10 nm) above the surface. Long-range attractive forces induce changes in the amplitude, frequency and phase of the cantilever and maintain a constant distance during scanning. Because the forces on the sample are much lower than in contact mode, even the softest samples can be imaged without damage.

Imaging of the topography or morphology of the surface is done by monitoring the movement of a sharp tip attached to the cantilever which interacts with the studied surfaces. The changes of the interactions due to the surfaces structures lead to a bending of the cantilever (in contact mode) or a change in amplitude (A) of the oscillating cantilever in (tapping mode). The deflection is measured using a laser spot reflected from the top surface of the cantilever into an array of photodiodes. In tapping mode (which was used for imaging in this thesis work both in air (**Paper II-IV**) and in liquid (**Paper I**)), the intensity (energy) of the oscillation is controlled by the oscillation amplitude. The damping ratio controls the tip-sample energy dissipation. The lower the damping ratio the "harder" is the force applied to the sample during the brief contact. The advantages of tapping mode is the elimination of a large part of the shearing forces (observed in contact mode), which as a consequence causes less damage to the sample surface, even with stiffer probes. Different components of the sample which could exhibit different adhesive and mechanical properties can be shown in phase contrast (Zhong et al. 1993, Magonov et al. 1997) and therefore, by applying tapping mode AFM, even compositional analysis can be possible. For good phase contrast, larger tip forces are advantageous, while minimization of force reduces the contact area and facilitates high-resolution imaging.

When tapping mode is used in liquid, as it was a case in **Paper I**, the resonance frequency is so small in comparison to air due to the additional mass (liquid coupled with the cantilever) and also additional damping due to the viscosity of the liquid around. The presence of liquid reduces the cantilever vibration amplitude significantly and shifts the cantilever resonances to smaller values. Reduction of the resonance frequency in liquid is highly related to the additional mass and shortening the separation because of the squeezed water damping between the studied surfaces. In air the tip amplitude versus separation has a constant value before contacting the sample, and after contact is reduced linearly, but in liquid just in large separations there is a saturation value and before going into contact the amplitude reduces nonlinearly by reduction of the separation, which is again related to the squeezed water damping which is related to the separation between the surface and the tip. Korayem *et al.* (2011) performed simulation and modeling to address the issues discussed above. They results were in good agreement with the experimental data reported by Putman (1994) and Rankl (2004). In **Paper I** we adjusted the response frequency of the tip (between 7 – 11 Hz) and soft silicon cantilever were used to ensure the high sensitivity measurements.

The AFM technique has also been widely applied in cellulose and cellulosic nanomaterial research. (Gustafsson et al. 2002, Koljonen et al. 2003, Pääkkö et al. 2007, Kontturi et al. 2006, Ahola et al. 2008b, Ahola et al. 2008a) In this work a Nanoscope IIIa Multimode scanning probe microscope from Digital Instruments Inc., Santa Barbara, CA, USA was used. Details for the settings and the cantilever used can be found in the attached articles (**Papers I-V**)

3.2.3. Colloidal probe microscopy (CPM)

The AFM instrument was also used for direct force measurements by applying the colloidal probe microscopy (CPM-technique) (Ducker et al. 1991, Butt 1991). Colloidal Probe Microscopy requires a tip of known shape (preferably a sphere) to be mounted cleanly on a consistently reproducible cantilever. These probes are known as "Colloidal Probes" and are used to study colloidal interactions between two surfaces and to quantify the interactive properties. Since the exact size and shape of the sharp tips used for imaging is unknown, a spherical, colloidal particle is attached to a tipless cantilever to have control over the radius of the particle(s) interacting. In this thesis a cellulose colloidal sphere was used; more detalied information about the sphere and cantiliver used can be found in **Paper II, IV** and **V**. Using an accurate piezo driven scanner, the surface and the probe are brougth into contact. The AFM is operated in the contact mode and usually in liquid (to lower the adhesive contribution, cappliary condensate and effect of the dirt to the force. The forces between the colloidal sphere and the surface is detected from the deflection of the cantiliver (Δz), while scanner is moving sample toward or away from the probe as shown schematically on Figure 10. As the sample surface approaches the colloidal probe, depending on the nature of the interactions, the canteliver can bend upwards (repulsion) or downwards (attraction). Repulsion, denoted as a positive force in force curves (2a), bends the canteliver upwards, however attraction, negative force (2b), bend the tip downwards. The deflection is converted into the surface force using Hooke's law, where the information of the spring constant (k) of the cantiliver is required (Eq. 3.1).

$$F = k\Delta z \qquad 3.1$$

Both approaching and retraction curves are reported. The force which is observed on the retrace ais force which ise needed to separate the surface from the probe and is called pull-off forces. From the pull-off force the adhesion energy can be calculated.

The raw data (cantilever deflection vs. piezo movement) has to be converted into force curves (force vs. separation) Fig. 10c.

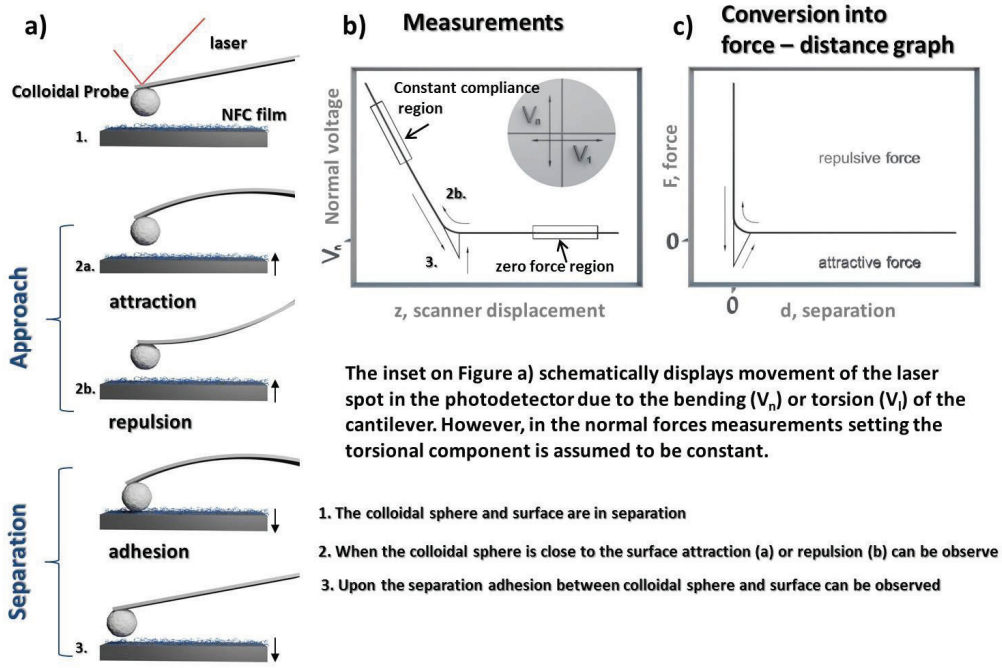

Figure 10. Illustration of a) principle of probe movement; b) raw data where cantilever deflection (normal photodetector response, V_n) is measured as a function of the piezo-scanner displacement in the z-direction; and c) conversion into force-separation curve obtained by transformation of the raw data (b) using known parameters V_n, α_0 (deflection sensitivity calculated from the slope of constant compliance) and k_v (the normal spring constant). Courtesy of Maciej Elert and Tiina Nypelö.

The constant compliance region (contact point at zero separation) is used to convert the piezo movement into distance units. The sensitivity α_0 value is determined from the slope of the linear region of the compliance region where the deflection is only caused by scanner movement (the probe is in "hard" contact with the surface). The resulting force curve ideally looks like the one presented in the Fig. 10c, however in a situation where the samples are soft and easily deformable (such as cellulose samples or adsorbed thick polymer layers), the calculations are not straightforward.

In the work where cellulose colloidal probe and soft and swollen NFC or CNC substrate was used the sensitivity value was determined by using a mica substrate before the experiment was conducted. Also, the spring constant was determined prior to attachment of the cellulose sphere by the thermal noise calibration method (Hutter, Bechhoefer 1993, Sader et al. 1999). To facilitate comparison to other studies the forces were normalized to the radius of the interacting cellulose sphere. The results from **Paper II-IV** were fitted to DLVO

theory based on the algorithm for the boundary conditions of constant surface potential and for constant surface charge using a non-linearized Poisson Boltzmann equation. The Debye length was constant depending on the ionic strength of the solution used. The Hamaker constant of cellulose was determined by ellipsometry (Bergström et al. 1999). The hydrodynamic forces were not included in the interpretations, but all measurements were conducted to minimize their influence by using a fairly low approach velocity of the cellulose probe, typically around 2 µm/s (Stiernstedt et al. 2006b). For a more detailed description of basic theory behind this technique, the reader is referred to (Butt et al. 2005, Ralston et al. 2005, Butt et al. 2007)

3.2.4. CPM friction measurements

Friction measurements were performed by using AFM in the CPM configuration with the PicoForce scanner. Also here, the cellulose colloidal sphere glued to the tipless cantilever acted as an opposing surface for probing the interactions. Friction is measured by scanning the sample surface in contact mode perpendicular to cantilever. By gradually increasing the applied load, friction loops (Fig. 11) can be plotted as a function of lateral movement, which is detected from the twisting of the AFM cantilever.

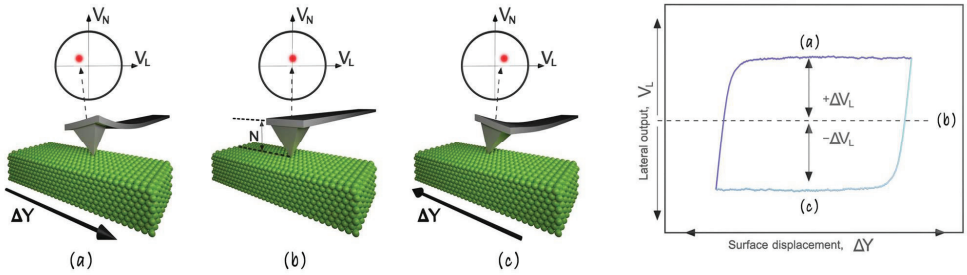

Figure 11. Illustration of the principle of probe movement during lateral force measurements. Courtesy of Maciej Elert (adopted from Reitsma et. al. 2008)

Friction ramping experiments (friction loops) were executed by, first increasing the deflection set point stepwise from no applied load up to a desired maximum applied load, and then decreasing it again stepwise until the probe was detached from the surface. The friction was determined at each load both on loading and unloading. Before and after friction ramping normal forces were measured to assess the stability of the detector signal and investigate the integrity of the sample after friction measurements. Figure 11 shows typical Lateral Force friction data, where scanning in one direction (a) and then the other (c) produces hysteresis, called a friction loop. Torsional deflection in the cantilever is caused by the frictional force at the interface acting though the lever arm *N*. The half-width of the hysteresis loop, ΔV_L is proportional to the sliding resistance force due to friction. From that the friction force can be calculated $F_{Friction}$. Additional parameters needed to calculate the friction forces are:

lateral photodetector sensitivity (δ); torsional spring constant (k_Φ); and effective height of the probe (h_{eff}), which is the diameter of the colloidal sphere plus half the thickness of the cantilever (Eq. 3.2).

$$F_{Friction} = \frac{\Delta V_{Friction}}{2} \frac{k_\emptyset}{\delta} \frac{1}{h_{eff}} \quad 3.2$$

Friction plotted as a function of the applied load enables extraction of friction coefficient (μ) from the slope of the fitted line (Fig.12) The applied load is calculated from the deflection set point (from the normal deflection sensitivity and the normal spring constant)

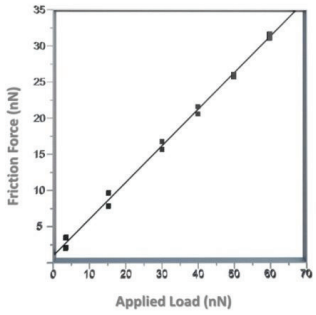

Figure 12. The calculated friction force plotted as a function of the applied load. The slope of the linear fit defines the friction coefficient, μ.

In this thesis the friction both air and in liquid was studied and they are described in more details in **Paper IV-V**. The calibration of the lateral spring constant was done according to the thermal vibration method described by Pettersson (2007).

3.2.5. Quartz crystal microbalance with dissipation (QCM-D)

QCM-D was used as the main technique to characterize the adsorbed amount of PB-*b*-PDNAENAq, CMC and CMC-*g*-PEG onto cellulose surface in **Paper III** and **IV.** This technique was also applied to study the interactions of cationic NFC with water and with anionic CNC in multilayer build up (**Paper I-II**). The method is very popular in surface science since it is a fast and reliable technique which can be applied to almost any thin film. Moreover, the technique allows monitoring, at the same time, both mass adsorption on solid surfaces, as well as information on the viscoelastic properties of the adsorbed layer. The operational principles are described in more detail by Rodahl *et al.* (1995). A schematic representation can be found in Fig. 13.

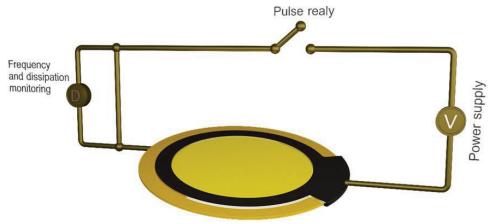

Figure 13. QCM-D schematic. Courtesy of Maciej Elert

In QCM-D the main precept is that the quartz crystal sensor oscillates at its resonance frequency and upon adsorption/or desorption of an analyte on/from the surface the frequency of the crystal changes, indicating the increase in the adsorbed mass on the sensor surface (frequency decrease) or lost of mass from the surface (frequency increase). It is important to note that this technique measures the analyte mass adsorption/desorption with the solvent coupled used in the study. In this thesis work water was used as the solvent.

The adsorbed mass per unit surface (Δm) is proportional to the decrease in the resonance frequency according to the Sauerbrey equation (Eq. 3.3.) (Sauerbrey 1959, Höök et al. 1998)

$$\Delta m = -\frac{C\Delta f}{n} \qquad 3.3$$

where C is the device sensitivity constant (17.7 ng Hz^{-1} cm^{-1}) and n is the overtone number. This equation is valid for thin and rigid films (adsorbed mass cannot be higher than the mass of the crystal).

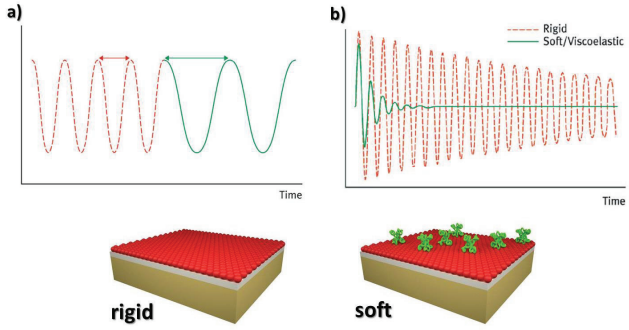

Figure 14. The viscoelastic properties of soft and rigid layers diagram (a) illustrates how the frequency of oscillating QCM sensor changes with addition of a molecular layer, diagram (b) illustrates the difference in dissipation signal generated by addition of rigid (red) and soft (green) molecular layer on the QCM sensor. (Idea adopted from Q-Sence). Courtesy of Maciej Elert

The viscoelastic properties of the adsorbed layer in QCM-D are analyzed by observing the dissipation changes (ΔD). The dissipation is measured by cutting the driving voltage of the crystal, and recording the decay of the amplitude as a function of time (Fig. 14b). The dissipation factor is defined as

$$D = \frac{E_{lost}}{2\pi E_{stored}} \quad 3.4$$

where E_{lost} is the dissipated energy and E_{stored} is the total energy stored in the oscillator.

For viscoelastic layers, a model which takes the properties of the adsorbed layer into account need to be used. The Johannsman model (Johannsmann et al. 1992) utilizes the frequency changes of multiple overtones and their variation for calculating the adsorbed mass. It is suitable to apply for swollen gel like films.

$$\hat{m} = m^0 \left(1 + \hat{J}(f) \frac{\rho f^2 d^2}{3}\right) \quad 3.5$$

Where $\hat{m}$ is the equivalent mass, ρ is the density of the fluid, d is the thickness of the film and $\hat{J}(f)$the complex shear assumed independent of the frequency and mass m^0 is the sensed mass. The latter is obtained from the intercept of plot of the equivalent mass as the function of frequency squared (Naderi, Claesson 2006)

The QCM-D experiments were carried out using a QCM-D E4 instrument (Q-Sense AB, Sweden). A constant fluid flow of 0.1 ml/min through the measurement chamber was used. Before an adsorption experiment the baseline was stabilized by driving a buffer solution through the chamber. The changes in dissipation and frequency are then followed as a function of time. The details of the experiments are presented in experimental section of **Paper I-IV**.

3.2.6. Tensile testing

The tensile test, also known as tension test, is probably the most fundamental type of mechanical test which can be performed on a material. Tensile tests are simple, relatively inexpensive, and fully standardized. By pulling the specimen in a controlled manner it is possible to quickly determine the mechanical properties of the material. As the material is being pulled, the strength of the sample along with how much it will elongate can be measured. The most common testing machine used in tensile testing has two crossheads; one is adjusted for the length of the specimen while the other is driven to apply tension to the test specimen. Alignment of the test specimen in the testing machine is critical, especially for brittle materials, because even a small offset could exert a bending force on the specimen which, in consequence could cause premature fracture.

Tensile tests produce a stress-strain diagram, which is used to determine the tensile modulus. A schematic representation can be found in Figure 15.

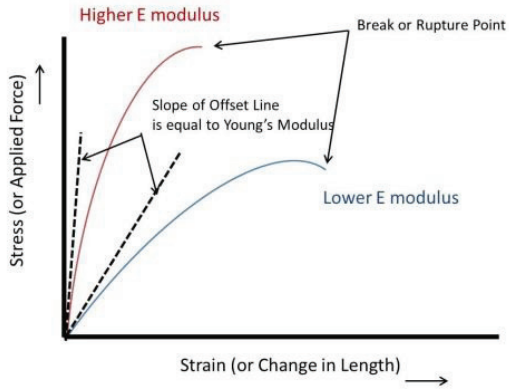

Figure 15. Stress-strain curve for brittle materials

The relationship between stress and strain (Fig. 15) is known as the Stress-Strain curve. It is unique for each material and is found by recording the amount of deformation (strain) at distinct intervals of tensile or compressive loading (stress). One datum which can be retrieved from that curve is the Modulus of Elasticity (*Young's Modulus* (*E*)). It is also known as the tensile modulus and it is a measure of the stiffness of an elastic material. It can be experimentally determined from the slope of a stress-strain curve over the uniaxial strain in the range of stress for which Hooke's law holds (Eq.)

$$E = \frac{\sigma}{\varepsilon} = \frac{F/A_0}{\Delta L/L_0} \qquad 3.5$$

where σ is a tensile stress and ε is tensile strain. F is the quasi-static force during testing, A_0 is the area through which the force is applied, ΔL is the amount by which the length of the object changes and L_0 is the original length of the object. Figure 16 shows the changes in the material when a load is applied.

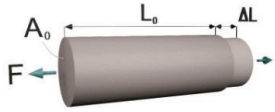

Figure 16. Deformation of the material under applied load.

In this thesis work two tensile testers were used; the mini tensile tester, 200N compression and horizontal bending stage from DEBEN (**Paper III**) and the Instron 4204 universal tensile testing machine (**Paper V**). All measurements were carried out at room temperature with humidity a of 30 – 60% (**Paper III**) or around 40 – 50 % (**Paper V**)

3.2.7. Composite film preparation

NFC/PB-b-PDMAEMAq composites were prepared by removing the water using vacuum filtration with 1.2 µm Millipore filter membranes. The specimen had dimensions of 2 cm × 2 mm × 70 - 200 µm in **Paper III**. At least 5 specimens were tested for each sample. A nominal strain rate of 0.5 mm/min was used. The composite films in **Paper V** were prepared by pressurized filtration. 150 ml of NFC/CMC-g-PEG water suspension (99/1 w/w NFC/CMC-g-PEG) was filtered through a Sefar Nitex polyamine monofilament open mesh fabric with 10 µm pore size at 2.5 bar pressure. Using this technique ~66 µm thick (dry thickness) and 78 cm^2 large films that were dry enough to handle were prepared. The films were wet pressed for 4 minutes whereupon they were further pressed in a Carver Laboratory press (Fred S. Carver Inc., New Jersey, USA) at about 100 ºC and 1800 – 2700 Pa for 2h. The hot press is presented in Figure 17.

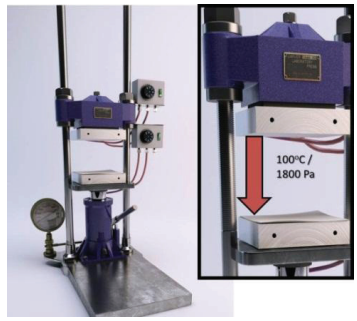

Figure 17. Photograph of the hot press used in the final step of the film preparation. Conditions used were 100˚C and 1800 – 2700 Pa. Courtesy of Maciej Elert

Before testing mechanical properties, the film samples were conditioned for seven days in standard atmosphere at 23 °C and 40 - 50 % relative humidity. Film specimens of 5.30 mm width were cut from NFC film sheets with a pair of scissors. The specimens (~50 mm × 5.30 mm) were secured to rectangular paper strips from both ends using a cyano acrylate super glue (Loctite). Specimens shape and dimensions are presented in Fig. 18. **(Paper V)**

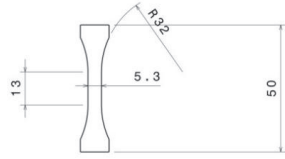

Figure 18. Dog-bone shape specimen used in the tensile test measurments. The width of each specimen was between 5.3-5.5 mm the length 50 mm. Courtesy of Mikka Kanerva.

In **Paper V** the tensile tests were carried out on the Instron 4204 universal tensile testing machine with the Bluehill 2 program. The gauge length, full-scale load and crosshead speed were 30 mm, 100 N, and 0.5 mm min^{-1}, respectively. At least five specimens were measured from each sample in order to average over the heterogeneity of the films. The thickness of the samples were measured before the experiments and were between 0.055-0.06 mm for NFC and 0.062-0.064 mm for NFC/CMC-g-PEG. (**Paper V**).

3.2.8. Additional techniques

Cryogenic Transmission Electron Microscopy (cryo-TEM): To assess the dimensions of the cationic NFC fibrils and to compare the AFM liquid images of the same sample with complementary technique, cryo-TEM was used (**Paper I).** Cryo-TEM was also applied in **Paper III** to characterize the morphology of the composite materials and to visualize the block copolymer micelles presented in the film after drying. The JEOL HEM-9200FSC TEM operating at liquid nitrogen temperature was used. Detailed information can be found in experimental section in **Paper I** and **III**.

Raman spectroscopy: The chemical composition of cationic NFC was analyzed using a Confocal Raman Spectrometer (WITec alpha 300R, WITec GmbH, Ulm, Germany) of ambient room temperature. More detailed information can be found in **Paper I**.

Scanning electron microscopy (SEM): To characterize the morphology and determine the cross section thickness of NFC/PB-b-PDMAEMAq composite films, the SEM technique was applied (**Paper III)**. In this work JEOL JSM-7500 FA field-emission scanning electron microscope was used. A thin Pt/Au layer was sputtered onto the specimens before imaging.

X-ray Photoelectron Spectroscopy (XPS): The surface composition of thin films and surface chemical composition of cationic cellulose nanofibrils (**Paper I**) and the nitrogen content from the amine group were determined using XPS. For further details of the interpretation of the XPS data see (Beamson, Briggs 1992) In this work, an AXIS 165, Kratos Analytical, Shimadzu Group, Japan) with monochromatic A1 K (alpha) radiation at 100 W was used.

4. RESULTS AND DISCUSSION

The most important findings of this work are summarized in the following chapters. More detailed information can be found in **Papers I-V**.

4.1 Nanocellulose substrate preparation, morphology and interactions with water

In order to successfully utilize nanocellulose in high-tech novel applications, the inherent properties of the material have to be studied. Recently, different types of anionic nanofibrils have been elucidated by several methods. For example, the rheological behavior of native cellulose I nano-and microfibrils has been studied extensively over past few years (Pääkkö et al. 2008, Agoda-Tandjawa et al. 2010, Iotti et al. 2011, Karppinen et al. 2011). Also, with the help of well-defined cellulose ultrathin films (Kontturi et al. 2006, Ahola et al. 2008b), probing of interfacial interactions between different nanocellulose grades namely CNCs (Cranston, Gray & Rutland 2010) and different anionic charged NFC (Ahola et al. 2008b, Eronen et al. 2011b, Eronen et al. 2012), has become possible. In **Papers I**, **and II** a new type of nanofibrillated cellulose (cationic NFC) was studied. The ultrathin cationic NFC films were prepared in **Paper I** and they were examined in terms of fibril morphology, interactions with water and with other cellulosic particles in **Paper II**.

4.1.1 Characterization of ultrathin cellulose films prepared from cationic NFC

Both cationic and anionic NFC can form stable aqueous dispersions, which enables their use in the spin coating technique for film preparation. Applying ultrasound treatment combined with ultracentrifugation has been shown to be an effective procedure for dispersing the entangled cationic/or anionic nanofibrils and removing the remaining fibril aggregates (Ahola et al. 2008b). Three different types of nanocellulose were used in this thesis: cationic NFC, anionic NFC and anionic cellulose nanocrystals (CNCs). This chapter concentrates essentially on extensive characterisation of cationic NFC, as these nanocellulose particles are rather new and have not been studied in terms of fibrils size and composition before.

Cationic NFC was characterized in respect to its size by applying microscopic techniques and in terms of chemical composition by applying XPS and Raman Spectroscopy.

Microscopic techniques

Fig. 19 summarizes the size characterization of cationic NFC fibrils by using AFM in water and air. To obtain a detailed picture of the fibril dimensions, both average width distribution determined by image analysis (Fig. 19c and h) as well as high-resolution inspection of the height of individual fibrils (Fig. 19b and g) was performed. In summary, the observed fibril width was very small, on average 4 nm and even around 1 nm for the finest fibrils observed in water, showing that the cationization pre-treatment is very efficient in liberating the fibrils; the fibril dimensions suggest that non-aggregated microfibrils are obtained. (**Paper I**). It was found that the fibril width in aqueous media is smaller compared to the same fibrils after drying. Fig. 19a presents an AFM height image of never dried cationic NFC fibrils adsorbed on mica. The fibril size estimated from the height of the fibrils directly attached to mica was found to be between 0.8-1.2 nm for the smallest non-aggregated fibrils. To ensure that the observed thin dimensions are not artifacts the height of a fibril which was aligned on top of another fibril was also measured (see magnification in Fig. 18 d and height profile Fig. 19e).

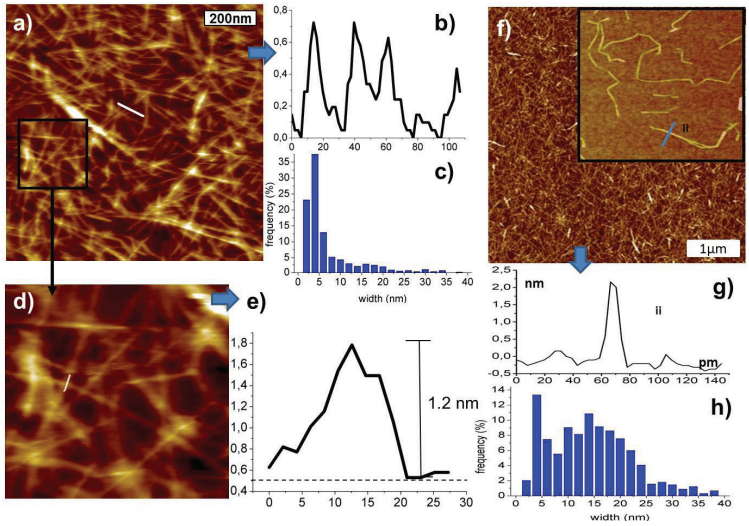

Figure 19. AFM height image of never dried cationic nanofibrils adsorbed on mica from an aqueous dispersion, imaged in water (a). From the line scans it is observed that the height of the fibrils in water is around 0.8 - 1.2 nm (b). Size distribution analysis data (c) for never dried NFC imaged in liquid, are also presented. Black square (d) shows magnification from the Fig. a) and the height of the fibril aligned on top of another fibril (e). The AFM height image of the same sample imaged in air after drying is presented in (f). A representative height profile for dried fibrils is presented in (g) and the average width based on imaged analysis for dried samples in (h). The scan size for both the never dried and dried film was 1 µm ×1 µm. The z-scale in the height images is 5 nm (a) and 8 nm (f) for images in water and in air respectively.

The size distribution was also quantified using image analysis form the AFM image of cationic NFC in liquid. 74 % of the fibrils were 6 nm or less in width, the most frequent width being 4 nm (Fig. 19c). As it was already extensively discuss in *Chapter 2.2.1*, the theoretical cellulose crystallite cross section could be from 1.5 x 2 nm^2 to a maximum of 3 x 5 nm^2. But also the pre-treatment method could alter the diameter of the fibrils. It is very probable that during chemical modification such as cationization partial dissolution could occurs leading to smaller fibrils.

Interestingly the height of fibrils increases upon drying. Fig. 19f shows the AFM image of the same cationic NFC film adsorbed on mica after drying. The size of fibrils estimated from height profile was in the range of 2 - 3 nm. The dimensions observed here correlate with the dimensions of elementary cellulose fibrils from Norway Spruce 2.5±0.2 nm, obtained using TEM, Small-angle X-ray Scattering and wide-angle X-ray scattering (Jakob et al. 1995). The increase in the size of fibrils during the transition from wet to dry could be caused by aggregation, clustering of the fibrils as a consequence of the high density of hydroxyl groups on the surface of the fibrils (Zimmermann et al. 2004). However, aggregation of the already adsorbed fibrils that further would be perfectly aligned so that the fibrils appear thicker seems unlikely.

The dimensions of NFC obtained by AFM imaging in air correlated well with the cryo-TEM images (Fig. 20). Micrometres long cationic nanofibrils with a slight distribution of the diameter 2.6 – 3 nm were observed in the TEM micrographs. The image analysis for the dried samples (from AFM data) shows a wide distribution of the fibril width (Fig. 19g). It is clearly seen that the size of the fibrils has increased after drying the sample.

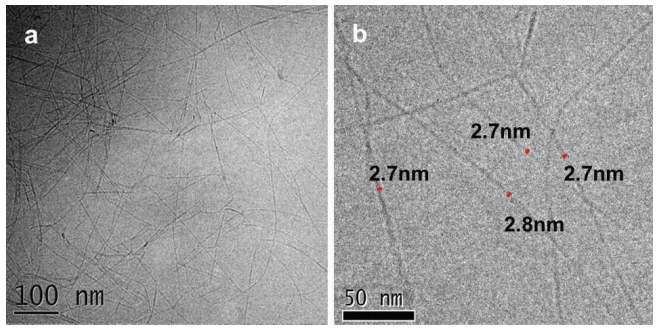

Figure 20. Cryo-TEM of frozen 0.9 g/l NFC aqua solution after the cationization and homogenization processes showing a fibrillated network of nanoscale fibrils (a) and individual fibrils (b)

We can only speculate on the reason behind the discrepancy between fibril dimensions of never dried fibrils in aqueous media and those after drying. Since chemically modified NFC has not previously been characterized by AFM imaging in the wet state this phenomenon has not been observed before. One model (Ding, Himmel 2006) proposes that the elementary fibril is a heterogeneous structure containing a crystalline core and layers of

sub crystalline/paracrystalline sheaths. It is possible that for the cationic fibrils, a disordered outer layer on the fibril is present in the wet stage but reorganizes on the fibril core during drying. Previously a similar reorganization of cellulose molecules was shown to be possible in case of fully dissolved cellulose (Aulin et al. 2009). We speculate that due to chemical modification the surface layer of the fibrils is partly dissolved, creating a core shell type structure of the fibril. The inner part of the fibril is largely unaffected by the modification and remains highly crystalline and rigid. However, the outer layer in aqueous media is diffuse and partly dissolved. This diffuse outer layer is supposedly not detectable by the AFM tip. Subsequently that leads to the false observation that the fibrils are smaller than the elementary fibril. The tip scans only the rigid core of the fibril. However, when dried, the disordered layer can organize and possibly recrystallize on the core of the fibrils, and the fibrils appear thicker. Prior to cryo-TEM analysis the fibrils are frozen in the non-aggregated and swollen state. However, in contrast to aqueous state AFM the diffuse layer is detected with cryo-TEM. The dimensions observed using cryo-TEM are closer to the dimensions observed in air using AFM.

For better comparison with previous literature data the cellulose nanofibril films were spin coated on silica substrates and further characterized in air with respect to surface morphology, roughness and thickness. Fig. 21 shows a fibrillar network structure, which has an average rms roughness of 0.97 nm. The roughness was determined from 25μm^2 areas. Previously Ahola *et al.* (2008b) have examined films from anionic nanocellulose, where the rms roughness of highly charge; carboxymethylated cellulose and low charged unmodified anionic nanocellulose films were 2 nm and 4 nm, respectively. Hence, it seems that the small thickness of cationic fibrils lead to a lower RMS roughness of the film.

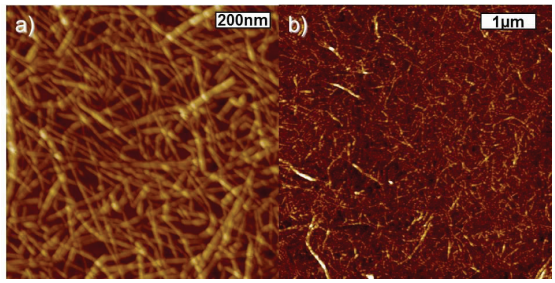

Figure 21. AFM height image of monolayer cationic NFC model film spin-coated on silica substrate image in air. The scan size is 1 µm × 1 µm (a) and 5 µm × 5 µm (b). No anchoring substance was used.

Furthermore, the very fine thickness of the cationic NFC and the good affinity of the fibrils for silica surfaces facilitate the formation of a very smooth film. The average thickness of cationic NFC films was 2 nm and 5 nm for a monolayer and nine spin coated layers, respectively. The cationic NFC films were thinner than the anionic films characterized previously, 6 nm and 4 nm for low and high charge fibrils respectively (Ahola et

al. 2008b). According to the AFM images the cationic nanofibrils form a homogeneous network fully covering the substrate. Several 25µm^2 areas were measured, and no open spots were detected.

Until now microfibrils have mostly been studied in dry state. Here we present a new method to assess the size of never-dried cellulosic fibrils by applying AFM imaging in liquid. It is clear that natural materials change their properties in the presence or absence of water.

Chemical composition of cationic NFC

XPS was used to characterize the chemical composition of the cationic nanofibril films. For moredetailed information on the experiments the reader is referred to **Paper I** or experimental section *Chapter 3.2.7.* The cationic nanofibrils were prepared by the aquatic reaction of pulp with N-(2,3 epoxypropyl) thrimethylammonium chloride dissolved in the presence of a base. More detailed information regarding the preparation procedure can be found in the article by Aulin *et al.* (2010). Fig. 22 depicts the nitrogen data obtained from XPS trace measurements, which are of interest, since they indicate the degree of amine group substitution. The degree of cellulose substitution was calculated to be 0.06 for cationic films spin coated on silica (the value is calculated from the ratio N/Cellulose). Furthermore, the charge corrected binding energy for the nitrogen N 1s peak was 403 eV, which is in good agreement with the published reference value for $^{+}N(CH_3)_3$ (Beamson, Briggs 1992).

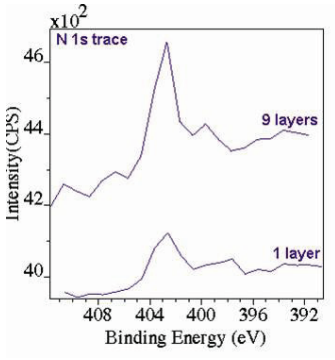

Figure 22. Low resolution XPS spectrum of nitrogen N 1s.

Raman spectroscopy

The cationization of the fibrils was also verified by using Raman spectroscopy. The Raman spectra measured from the dried cationized and anionic carboxymethylated free-standing films are shown in Fig. 23. The carboxymethylated fibrils were prepared according to the procedure describe elsewhere (Wågberg et al. 2008) and were used here for comparison. The characteristic Raman bands for the cellulose I structure can be identified

from both spectra, indicated with stars in Fig. 23. From the cationized cellulose the substituted trimethyl ammonium group can be observed. Distinct new bands at positions 761 and 3030 cm^{-1} are caused by symmetric stretching of the $(CH_3)_3$-N^+ and CH_3 antisymmetric stretching, respectively (Phillips et al. 1999, Pigorsch 2009).

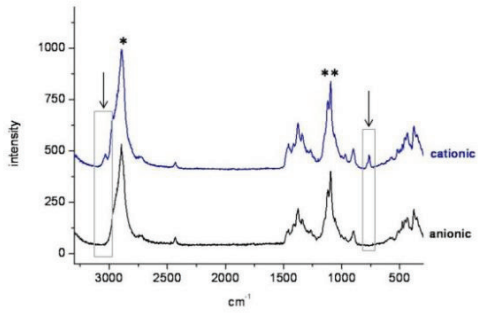

Figure 23. Raman spectra of carboxymethylated and cationic NFC. The arrows indicate the new bands emerging from cationic modification.

4.1.2 The amphoteric nature of cationic NFC

Cationic nanofibrils were positively charged in the whole pH range studied (3-11). The cationic charge was determined for modified fibers before fibrillation and it was 0.35 meq/g. The fibrils also possess a small anionic charge of 28 µeq/g, which mainly originates from the residual hemicellulose in the pulp but also a small contribution comes from cellulose oxidation during the pulping operation. The quaternized amine is positively charged at all pH values. However, the carboxyl groups which are the anionic contribution to the net charge, start to deprotonate at pH above 3.5. As a consequence the net charge of cationic NFC was also pH dependent, which was confirmed by electrophoretic mobility measurements (Fig. 24).

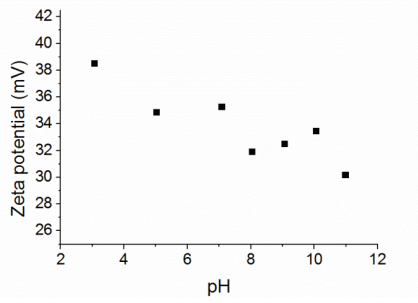

Figure 24. The zeta potential of the cationic NFC dispersion as a function of pH.

4.1.3. Effect of pH on water binding capacity of cationic NFC

The QCM-D technique was used to monitor the water binding capacity of cationic NFC at different pH values. The interactions of different cellulose model surfaces with water have been studied before by Aulin et al. (2009). They studied both anionic NFC, unmodified NFC, cellulose nanocrystals and regenerated cellulose model films. In this thesis the water binding capacity of cationic NFC with respect to pH was studied to complete the understanding of NFC interactions with water. Results are presented in Fig. 25. First air was passed through the QCM-D chamber and when the baseline was stable at (t) = 5 min, a 1 mM buffer solution was added. The frequency change upon addition of the buffer for cationic NFC films at pH 8 and 4.5 was -460 Hz and -550 Hz, respectively. Most of the water uptake took place in this initial phase immediately after introducing the aqueous buffer solution. The cellulose surface continued to swell slowly at pH 4.5 while almost no further change was detectable at pH 8.

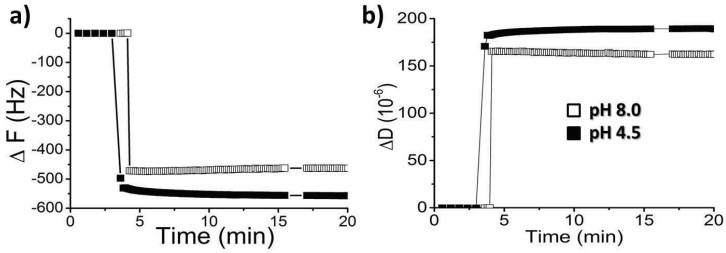

Figure 25. QCM-D data (3rd overtone) showing the swelling of cellulose model films upon exposure to 1mM $NaHCO_3$ buffer solution. Change in (a) frequency and (b) dissipation as the films swell.

There are two main reasons for the extensive swelling of the nanofibrillated cellulose film - first, the high amount of accessible hydroxyl groups in the open network of nanofibrils, and second, the charged groups in cationic NFC. The schematic representation of cationic fibrils interactions with water is presented in Scheme 1.

Scheme 1. Schematic representation of cationic NFC film interactions with buffers pH 8.0 and pH 4.5 is presented. The red and blue spheres represent the cationic and anionic charges on NFC fibrils respectively

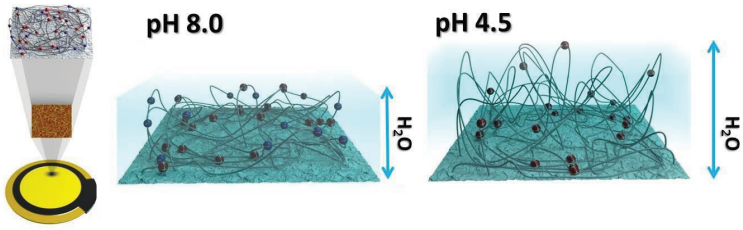

Due to the charged groups NFC behaves like a polyelectrolyte gel. The higher the charge of the NFC, the more water the film binds. At a high pH-value (pH 8.0) where the carboxyl groups are deprotonated, they will lower the net cationic charge in the nanofibrillar gel and hence, water uptake will be lowered.

The Johannsmann equestion (Eq. 3.5) was used to calculate the mass of water adsorbed in the film at both studied pHs. The dry mass of the film was estimated by using the thickness (2 nm) and area (0,785cm^2) of the film and assuming that the density of cellulose is 1.592 g/cm^3 (Sugiyama et al. 1991, Mwaikambo, Ansell 1996). For all measured films the dry mass of cellulose was 3.183 mg/m^2. The swelling percentage (mass of water/dry mass of the film) was also calculated. The results are summarized in Table 2.

Table 2. Johannsman mass of adsorbed water, and swelling percentage of cationic cellulose nanofibrils films at different pH and electrolyte concentrations

pH	Dry mass of cellulose (mg/m^2)	Adsorbed mass of water (mg/m^2)	Swelling (%)
4.5	3.18	9.7	303
8.0		4.4	137

The amount of water at both pH-values exceeds the amount of dry mass of cellulose, suggesting a highly swollen cellulose network. The measured water uptake value was found to be 4.4 mg/m^2 for cationic NFC film at pH 8.0 and can be compared to the previously reported value for unmodified low charged NFC film (4.6 mg/m^2) (Aulin et al. 2009). However, due to the lower dry mass of the cationic NFC film, compared to that studied by Aulin (2009), the swelling percentage observed here is much higher, 137 %. At a lower pH the water uptake was higher, 9.7 mg/m^2 for the same cationic film. This can be explained by the higher net positive charge of the fibrils at lower pH. The water uptake is higher when the network is more charged, and consequently the swelling percentage for film at pH 4.5 is very high, 303%. Moreover, the difference between the electrostatic swelling behaviour at the two studied pHs may be understood in terms of electrostatic cross-linking. It is possible that at higher pH (pH 8) when the carboxyl groups are dissociated they can cross link with cationic groups which would lead to reduce the number of interactions with water at elevated pH.

4.1.4 Effect of electrolyte concentration on swelling of cationic NFC

The effect of electrolyte concentration on the swelling of the cationic cellulose nanofibril film was also studied at pH 8 and 4.5, Fig. 26. The swelling of the cellulosic fibril network, as already mentioned can be

compared to the swelling of polyelectrolyte gels (Fält et al. 2003, Ahola et al. 2008b). Hence, it is controlled by the charge density of cellulose, the ionic strength of the surrounding medium, the type of counter ions, and the degree of cross-linking (Fleer et al. 1993). Figure 26 presents how the cationic NFC film responds to changes in the electrolyte concentration at both studied pHs.

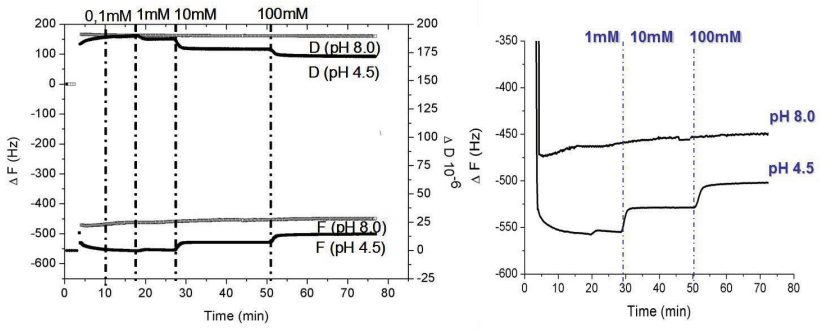

Figure 26. QCM-D data (3rd overtone) showing the effect of electrolyte concentration at different pH on the change of the frequency (ΔF) and dissipation (ΔD) for cationic cellulose nanofibril films. The zoom of the frequency (ΔF) data emphases the effect of the electrolyte concentration on the water content in the films.

Surprisingly, the water uptake was found to be insensitive to changes in electrolyte concentration at pH 8.0. An increase in NaCl concentration introduces a decrease in Δf comparable to the bulk effect. The energy dissipation curves show an increase in the dissipation for cationic NFC films at pH 8 when the buffer was added. This can be explained by the loosening of the NFC network upon addition of a buffer. However, a further increase in electrolyte concentration does not affect the dissipation values. At pH 4.5, however, the film was sensitive to changes in electrolyte concentration as expected from Donna effect. An addition of 0.1 mM NaCl does not significantly affect the swelling of the film. However the addition of 1 mM NaCl caused a small de-swelling of the NFC film, since the frequency increased 5 Hz and the dissipation decreased 3×10^{-6}. Further additions of 10 mM and 100 mM NaCl caused an additional de-swelling of the NFC film (in Fig. 26 right).

An increased electrolyte concentration is expected to decrease swelling, but the extent of electrostatic crosslinking (between cationic and anionic groups in cat. NFC) is expected to be decreased with an increased ionic strength, so apparently the two effects cancel out at pH 8 each other. Previously Ahola et al. (2008b) studied the effect of electrolyte addition on the frequency and dissipation changed for unmodified and anionically modified NFC. They observed similar de-swelling upon salt addition for highly charge anionic NFC, as presented in this thesis data for cationic NFC at lower pH. The effect of electrolyte concentration on swelling and surface interactions of both cationic NFC at pH 4.5 and studied by Ahola anionic NFC at pH 8 can be explained by Donnan effects. For anionic NFC charge is highest at pH 8 due to deprotonation of carboxyl groups

The high charge promotes swelling, and the effect is reduced by addition of salt. For cationic NFC studied in **Paper I**, the degree of crosslinking is lower, and the charge effect is higher at pH 4.5 than that at pH 8. Hence, the swelling is more pronounced at those conditions, and with increased electrolyte concentration deswelling is observed.

4.2 Interactions on nanosized cellulose particles: All cellulose multilayers

An understanding of the interplay between the long cationic nanofibrils andshort rod-like anionic CNCs is crucial. It is important not only from a fundamental point of view, but also the knowledge gained regarding the mutual interaction between these two colloidal cellulosic objects could be beneficial in utilizing them in high-end new applications such as smart coatings and composite materials.

4.2.1 Effect of initial layer on LbL build-up of cationic NFC and anionic CNCs

The interactions between cationic NFC and anionic CNCs were studied by applying the QCM-D technique and colloidal probe microscopy. The build-up of LbL layers from those two colloidal cellulosic objects was studied in situ with QCM-D (**Paper II**). The amphoteric nature of cationic NFC affected the build-up of all cellulose multilayers based on cationic NFC and anionic CNC. A significantly lower adsorption of the first cationic NFC layer onto bare SiO_2 crystal at pH 4.5 compared to pH 8.3 was detected. (Fig. 27)

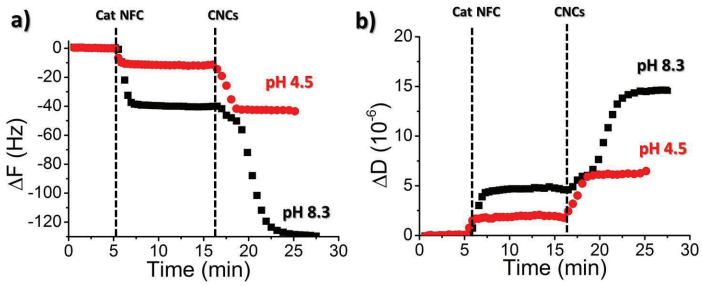

Figure 27. Frequency change (a) and dissipation (b) upon LbL build-up of all cellulose structures by sequential adsorption of cationic NFC and anionic CNC at pH 4.5 (red) and pH 8.3 (black).

For the in situ adsorption of cationic NFC, a decrease in frequency signal (-10 Hz) and (-40 Hz) for pH 4.5 and pH 8.3 was detected, respectively (Fig 27a). Corresponding to these changes the sensed adsorbed mass was calculated to be 0.6 mg/m^2 for fibrils deposited at pH 4.5 and 1.6 mg/m^2 at pH 8.3. The formation of first cationic NFC layer also affected the adsorption of anionic CNCs. A lower amount of CNCs was adsorbed at

lower pH with frequency changed around -30 Hz (1.6 mg/m^2) while for higher pH, - 60 Hz (6.1 mg/m^2). The charge of the CNCs is constant in both studied pH.

The dissipation values (Fig. 27b) are also lower for the layers at pH 4.5. The (adsorbed) sensed mass was calculated using Johannsmann equation (eq. 3.5). At low pH, where carboxyl groups are protonated and cat NFC possesses higher overall positive charge, the adsorbed fibrils form a flat and rigid layer according to the ΔD values. For more details reader is referred to the Experimental part, and **Paper II**.

For successful multilayer build-up it is essential that the first layer possesses sufficient coverage (Decher 1997). As presented in Fig. 27 the insufficient formation of first cationic NFC layer in situ QCM chamber at pH 4.5 affected the build-up of the following layers. Thus, we decided to spin coat the first layer of cationic NFC on the QCM sensor from a neutral aqueous dispersion and start the LbL deposition of CNCs on these substrates (Fig. 28). In this case successful LbL deposition was possible at both pHs. From these similarly constructed substrates, a higher initial adsorption of CNCs was observed at pH 4.5 compared to pH 8.3 (Fig 28a, b).

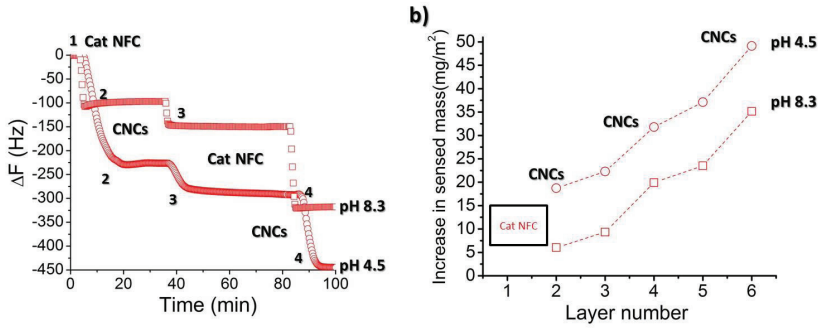

Figure 28. Frequency change (a), and total sensed mass (b) upon LbL build-up of all cellulosic structures by sequential adsorption of cationic NFC and anionic CNCs at pH 4.5 (spheres) and pH 8.3 (squares). In a) the first layer of cationic NFC was spin coated where upon the layer build-up continued as in Fig. 27a. For simplicity only first 4 layers are presented. After each adsorption step rinsing with the appropriate buffer was conducted; because no significant change in frequency or dissipation was observed, this step is omitted here. In b) the overall increase in sensed mass calculated using the Johannsmann estimation (3.4) as a function of layer number is shown. pH 4.5 (spheres) and pH 8.3 (squares).

Fig. 29a presents the change in dissipation as a function of frequency response for LbL deposition on spin coated cationic NFC at low and high pH. Interestingly, upon adsorption of first layer of CNCs on the swollen cationic NFC film at pH 4.5 the slope is negative which we interpret as water removal from the cationic film. As was previously stated the cationic NFC layer is more swollen at low pH due to its higher positive charge. The following adsorptions of both cationic NFC and anionic CNCs gradually increase the dissipation value. At pH

8.3 the slope in Fig. 29b shows a continuous increase in ΔD as a function of Δf suggesting that both NFC and CNC layers are swollen with water.

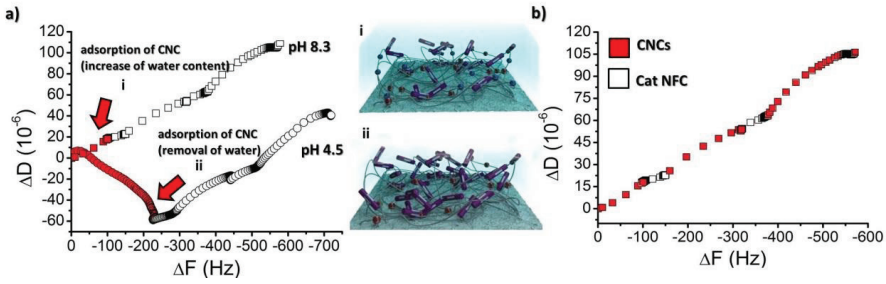

Figure 29. a) *f*-D plot for in situ LbL deposition of cationic NFC and anionic CNCs at pH 8.3 (squares) and pH 4.5 (spheres) on the spin coated cat NFC layer. The red arrows indicate the change in Δ*f* and ΔD after initial adsorption of CNCs. The schematic representations of the addition of CNCs at pH 8.3 (i) and pH 4.5 (ii) are also presented. In b) the difference between layer viscoelastic properties for cat NFC (open symbols) and anionic CNCs (closed symbols) for adsorption at pH 8.3 is presented.

4.2.2 Effect of the underlying layer on surface forces in a multilayer system

The surface force interactions between a multilayer system constructed from sequential adsorption of cationic NFC and anionic CNCs were also studied in **Paper II**. Colloidal probe microscopy (CPM) with attached colloidal cellulose sphere was applied. Figure 30 presents the forces, normalized by the probe radius, as the function of apparent separation.

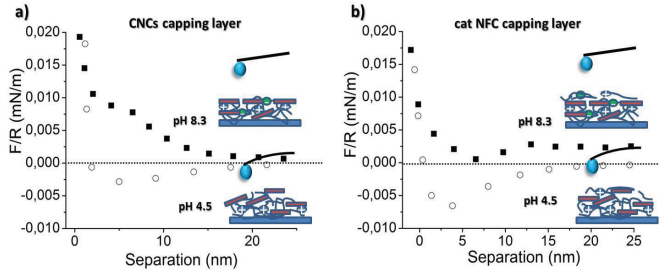

Figure 30. Effect of capping layer and amphoteric nature of NFC fibrils on normalized forces vs. separation on approach between cellulose sphere, and $(NFC/CNC)_6$ multilayer system with CNC (a) and NFC (b) capping layer at pH 8 (closed symbols) and pH 4.5 (open symbols). The electrolyte concentration was 1 mM of respective buffers. The schematic representation of multilayer formation and interaction with cellulose sphere is presented for each system.

The ultrathin films were spin assembled on mica as described in **Paper II**. Regardless of the capping layer used, the forces between LbL layers and the negatively charged cellulose colloidal sphere were purely attractive on approach at pH 4.5 (unfilled symbols Fig. 30) although the attraction was stronger when cationic NFC was used as a capping layer (Fig. 30b). As mentioned above, cationic NFC (which possesses both anionic and cationic charge) is more cationic at lower pH which leads to higher positive charge in the multilayer system.

Also the cationic layer extension at pH 4.5 in the system where CNC was used as capping layer could be a reason for the observed attraction (Fig. 30a). The more swollen and more flexible cationic NFC fibrils could, in such conditions migrate through the CNCs layer and interact with the negatively charged cellulose sphere, causing more attraction on approach. A similar effect was found for PAH in CNCs/PAH multilayer studied by Cranston (2010).

Figure 31 includes a fit to the DLVO theory (Derjaguin 1941, Verwey, Overbeek 1948) for the multilayer system at both pHs. The lines show the best fit to DLVO theory based on the algorithm for the boundary condition of constant surface potential (dotted lines) and for constant surface charge (solid lines) (Devereux, de Bruyn 1963).

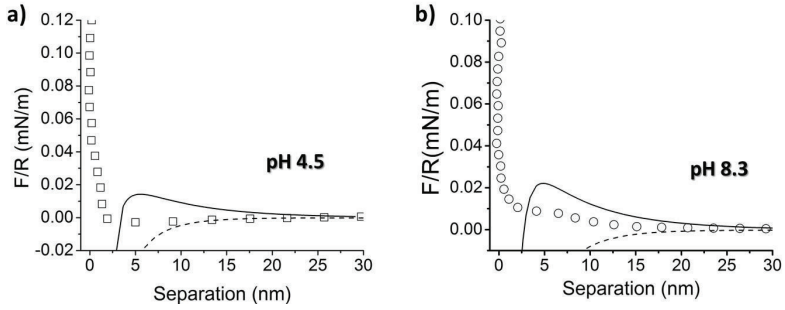

Figure 31. Normalized forces as the function of apparent separation between cellulose sphere and cationic NFC/CNCs (6 multilayers system) with a capping CNCs layer (a) pH 4.5, (b) pH 8.3, and a fit to DLVO-theory for multilayer system. The buffer concentration in all cases was 1 mM. The best fit was achieved with surface potentials of -12 mV and -3 mV for amorphous cellulose sphere and multilayer cat NFC/CNCs respectively at pH 4.5. For pH 8.3 the best fit was achieved with surface potential -15 mV, -5mV for cellulose sphere and multilayer cat NFC/CNCs. A Hamaker constant of 8.0 x10-21 J for cellulose in water, previously determined from ellipsometry measurements (Bergström et al. 1999) was used and the decay length was calculated based on the known electrolyte concentration.

The best fit was achieved when a surface potential of -12 mV and -15 mV for cellulose sphere at pH 4.5 and pH 8.3, respectively, was used. It has been previously shown that the surface potential of similar regenerated cellulose substrates is pH dependent (Rutland et al. 1997, Österberg, Claesson 2000). Formerly, a surface

potential around -20 mV in neutral media has been used for similar spheres (Bergström et al. 1999, Eronen et al. 2012) but also lower surface potentials have been reported (Attard et al. 1998, Salmi et al. 2007a, Ahola et al. 2008b, Elazzouzi-Hafraoui et al. 2008). The best corresponding fit to estimate the surface potential of the multilayer system with the CNCs capping layer were -2 mV and -5 mV for pH 4.5 and pH 8.3, respectively. The estimated value for multilayer system was fitted to the conditions; when the multilayer film was expected to have higher positive charge (pH 4.5) a less negative surface potential was used.

4.3 Interactions between nanofibrils and polymers

Simple mixing of hydrophilic NFC with hydrophobic polymers is difficult and often leads to phase separation. Laborious grafting reactions or modification of NFC with a soft component by covalent interaction can be ways to introduce the hydrophobic molecules to cellulose fibrils. However, those reactions might still be difficult to be performed in aqueous conditions, and that would further require solvent exchange procedures or modification of NFC to work in non-aqueous solvents. Both of those pretreatments can alter the H-bonding structure within the fibrils, which in consequence can lead to distortion in NFC performance. In order to avoid problems with mixing of soft polymeric components with hydrophilic NFC and to create sufficient mutual interactions between those soft and hard domains in future composite materials a more versatile approach is needed. Such an approach could be based on simple self-assembly, where the soft domains can be introduced to the NFC fibrils via non-covalent interactions. Two different routes that were studied in this thesis utilize such a concept, and are presented in upcoming sections

4.3.1 Two routes to self-assemble NFC with soft polymers

In **Paper III** and **IV** two platform concepts for preparation of biomimetic NFC based nanocomposites based on self-assembly were introduced. These two routes are based on ionic interactions (**Paper III**) and non-ionic interactions (**Paper IV**). In **Paper III** anionic nanofibrillated cellulose was combined with cationic block copolymers via ionic interactions. The concept is illustrated in Scheme 2. Upon combining the cationic PB-b-PDMAEMAq block copolymer micelles and anionically charged NFC nanofibrils (carboxymethylated), a colloidal complex is formed where the cationic polyelectrolyte served as an anchor for the hydrophobic polybutadiene phase inside the micelles. The complexation between the colloidal nanofibrils and colloidal micellar spheres prevents macroscopic phase separation. The simple mixing of polybutadiene and NFC would lead to macroscopic phase separation, poor interfacial bonding and little interaction between both components.

Scheme 2. Concept of complexation of quarternized poly (1,2-butadiene)-bloc-poly(dimethylaminethyl methacrylate) micelles with anionic nanofibrillated cellulose NFC and their subsequent packing into biomimetic hard/soft composites due to ionic complexation of the fibrillar and spherical colloidal objects.

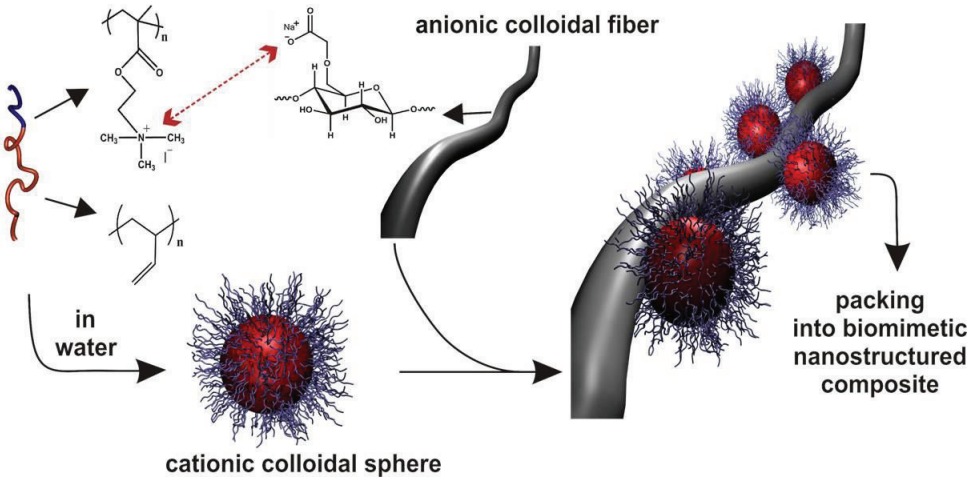

Fig. 32 summarizes the characterization of an amphiphilic block copolymer, which self-assembles in polar solvent to form colloidal nanoparticles (micelles), where the hydrophobic segments collapse into the core, surrounded by a stabilizing corona of hydrophilic chains. The PB-b-PDMAEMAq form micelles during the dialysis from DMF into water. The shape and the size of the micelles were assessed by combining the scattering and imaging techniques. The *z*-average hydrodynamic diameter of the PB-b-PDMAEMAq was determined using dynamic light scattering (DLS) to be 65 nm (Fig. 32a) with low a polydisperisty index of 1.07. The spherical shape of micelles was further confirmed by imaging the adsorbed 0.2 mg/L solution of micelles on mica and imaged in water with AFM (Fig. 32b, c). The measured diameters of the micelles was 80-100 nm and the height was around 11 – 14 nm (Fig. 32c). The adsorbed micelles after drying flatten on the NFC film surface, thus the height observed via AFM imaging is smaller compare to diameter. Also the diameter of the micelles detected via imaging is overestimated due to the dimensions and geometry of the AFM tip (Wang, Chen 2007). The AFM imaging was applied here as a tool to visualize the preserved form of the micelles on the NFC film after drying, not for strict characterization of the micelles.

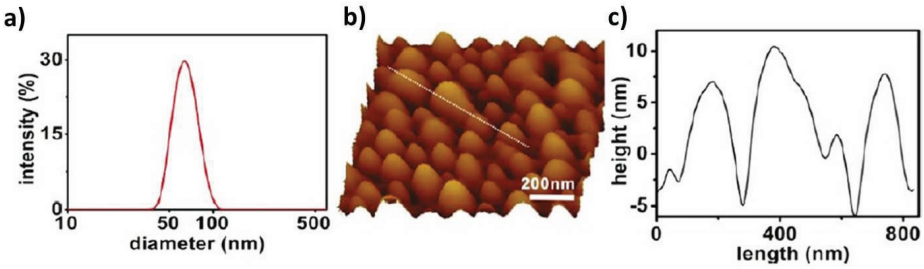

Figure 32. a) Distribution of the hydrodynamic diameter of PB-*b*-PDMAEMAq micelles in water obtained by DLS. b) AFM height images of PB-*b*-PDMAEMAq micelles adsorbed onto mica imaged in water. The concentration of block copolymer was 0.2 mg/L. The *z*-range is 15 nm. c) Height profile corresponding to the line shown in (b).

The second route introduced in **Paper IV** is based on the similarity in the backbone between cellulose and a water soluble polysaccharide (CMC). As discussed already in *Chapter 2.3.2*, the main interactions between cellulose and polysaccharides have been suggested to be hydrogen bonding of unsubstituted chains region, van der Waals (Ishimaru, Lindström 1984, Sjöström 1993) attractions and also, as recently suggested by Lindman *et al.* (Lindman et al. 2010) hydrophobic interactions. By utilizing non-ionic interactions between nanofibrillated cellulose and CMC it was possible to self-assemble those two colloidal structures by simple physical adsorption. The concept is illustrated in Scheme 3. Prior to adsorption, CMC was first modified with OMe-PEG-amine in the presence of EDC and NHS, as presented in Figure 33. More detailed information regarding the chemical modification procedure can be found in **Paper IV**.

Scheme 3. Concept of the complexation of carboxymethyl cellulose grafted with poly ethylene glycol (CMC-*g*-PEG) with unmodified nanofibrillated cellulose, and their subsequent packing into biomimetic hard/soft composites due to non-ionic complexation between CMC and NFC.

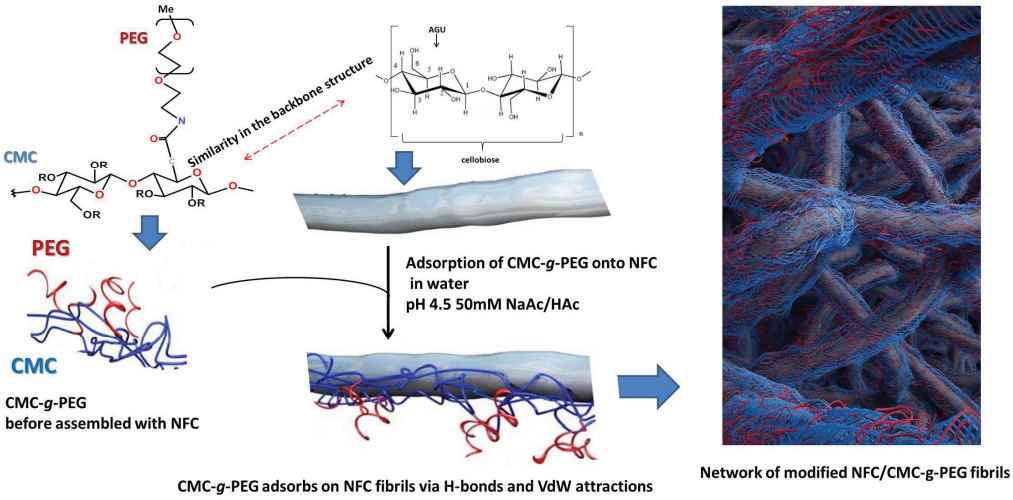

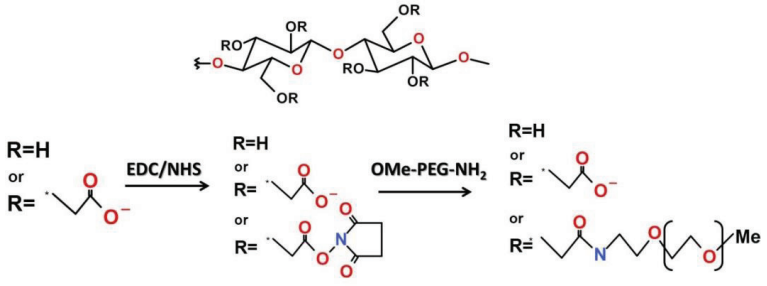

Figure 33. Grafting of OMe-PEG-NH_2 on carboxymethyl cellulose using water soluble carbodiimide and esterification agent.

The amine/carboxyl ratio used in the modification was 0.4 mmol g^{-1} / 3.6 mmol g^{-1} which gives an 11% decrease in carboxyl content if all OMe-PEG amine is grafted to CMC. The distance between carboxymethyl groups in CMC with a DS of 0.7 has been determined to be approximately 0.7 nm (Hoogendam et al. 1998). That would mean that if 11% of carboxyls have reacted with OMe-PEG amine the distance between PEG chains on CMC would be approximately 6 nm if they are evenly distributed along the CMC backbone. The Mw of CMC was 250kDa which gives the length value of 752 nm when considering the cellobiose length to be 1.03 nm. The length of the PEG chains with the Mw of 2000 was calculated to be 12.6 nm, where the length of the EG monomer is 2.75Å (Harder et al. 1998). In order to calculate the conformation of the chains, the Flory radius of

the free PEG chains $R_F = aN^{2/3}$ can be calculated with a = 0.275 nm (monomer length), and N = 45, the number of EG units per chain. The calculated R_F value for (PEG 2kDa) is about 2.69 nm. In the deGennes formalism (deGennes 1987), the brush regime exists for $D < R_F$ and the mushroom regime for $D > R_F$, where D is the grafting distance between the PEG chains. In our case D was around 6 nm. That would suggest that the PEG chains are in mushroom conformation in aqueous solution.

4.3.2 Adsorption of PB-b-PDMAEMAq on NFC

In order to understand in more detail the binding between soft and hard components in biomimetic composites, the QCM-D technique was applied. In **Paper III** cationic PB-*b*-PDMAEMAq micelles and the anionic NFC nanofibrils were studied. The two colloidal object exhibit opposite charges, and thus we expect a tight binding via ionic complexation, similar to inter-polyelectrolyte complexes at the molecular length scale. The main driving force for the complexation is the entropic gain due to the counterion release. Since anionic NFC is a weak polyelectrolyte with a pH-dependent ionization of the carboxylic acid groups, an increase of pH favors complexation. Figure 34 shows a decrease in frequency (-50Hz) (black) and increase in dissipation (17×10^{-6}) (blue) for in situ adsorption of anionic NFC on PEI (that was used as anchoring polyelectrolyte for NFC) at pH 8. The increase in dissipation value indicates that NFC film is highly swollen and contains a substantial amount of water.

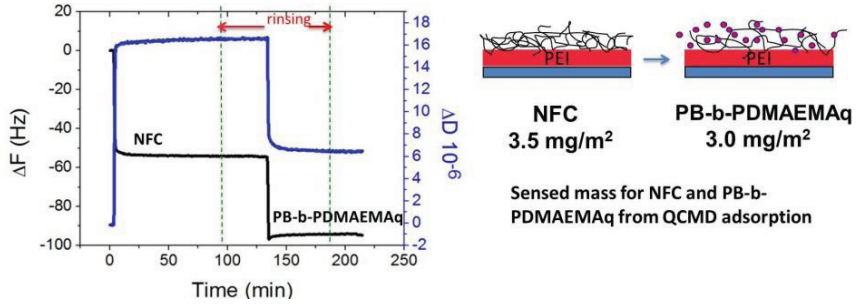

Figure 34. QCMD data (3rd overtone) showing the changed in frequency (black) and dissipation (blue) upon first adding aqueous NFC dispersion (t = 0 min) and then aqueous PB-b-PDMAEMAq micelles (t = 134 min).

The addition of PB-b-PDMAEMAq micelles causes a further decrease in frequency signal (- 41 Hz), due to adsorption of block copolymer onto the NFC layer. The dissipation value decreases upon addition of PB-b-PDMAEMAq (7×10^{-6}), suggesting that water is removed from the NFC network during the adsorption, and the film becomes more rigid. The schematic representation of the adsorbed films is presented in Fig. 34 with the calculated sensed mass for both NFC (3.5 mg/m^2) and PB-b-PDMAEMAq (3.0 mg/m^2) obtained by applying the Johannsmann's equation (Eq. 3.5).

After adsorption the film was dried and imaged by AFM in air. Fig. 35 shows roughly globular structures on the NFC, where the diameter is in the range of 80 – 150 nm and height in the range of 8 – 14 nm. Such structures indicate that the block copolymer has indeed adsorbed on the NFC network and stays in micellar form even after the water removal. Although the glass transition of PB is low (-15°C) and micelles have a soft core, there was no indication towards the opening of the micelles or subsequent film formation on the surface.

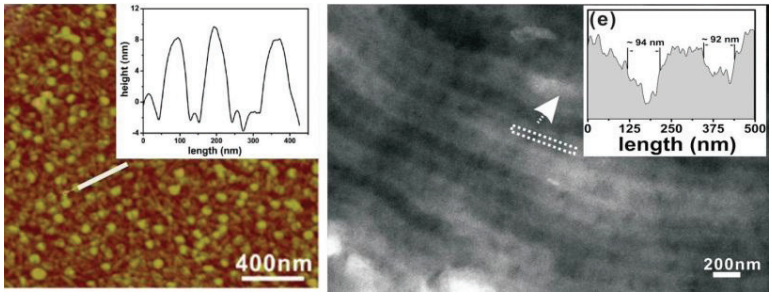

Figure 35. AFM height image of adsorbed PB-b-PDMAEMAq micelles on the NFC film imaged in air (z-range 15nm) the inset shows a height profile of the section analysis indicated by the line in image (a). Cross section TEM image of the composite NFC/PB-b-PDMAEMAq with the weight fraction 2.5/1 (b).

Nanocomposites were made of the NFC/PB-b-PDMAEMAq block copolymers, and were examined by TEM. It can be seen from the TEM micrograph in Fig. 35b that the NFC/PB-b-PDMAEMAq block copolymer nanocomposite has periodic structure with alternating NFC and PB-b-PDMAEMAq domains with a periodicity of around 160 – 200 nm. This indicates that the micellar structure is preserved after the composite formation. More information of the mechanical properties of the NFC/PB-b-PDMAEMAq composite material is given in *Chapter 4.5*.

4.3.3 Adsorption of CMC-*g*-PEG on NFC

The second system we studied (**Paper IV**) was based on non-ionic interactions between modified CMC and unmodified NFC. In order to better understand the supramolecular assembly of those two colloidal objects, in situ adsorption experiments were performed with (QCM-D). Figure 36 summarizes the adsorption of both un-modified and PEG-modified CMC (CMC-*g*-PEG) on a spin coated NFC layer. Since both CMC and NFC are negatively charged, the double layer repulsion will have to be overcome for sufficient adsorption. The effect of electrostatic repulsion can be suppressed by decreasing the pH (Eronen et al. 2011b, Laine et al. 2000) or increasing the electrolyte concentration (Orelma et al. 2011, Liu et al. 2011, Filpponen et al. 2012).

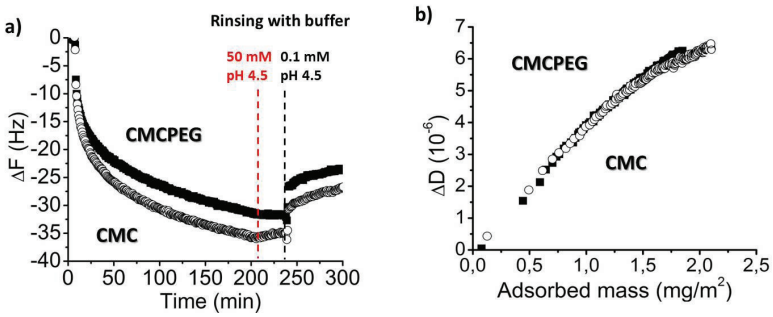

Figure 36. In situ QCM-D adsorption of CMC (open symbols) and CMC-g-PEG closed symbols) on NFC ultrathin films. a) presents change in frequency as a function of time with the rinsing step, b) change in dissipation as a function of adsorbed mass. The mass was calculated using Sauerbrey equation (3.3).

In Fig. 36a the change in frequency as a function of time, and in Fig. 36b the change in dissipation vs. adsorbed mass is presented. The adsorption of both CMC and CMC-g-PEG on NFC is irreversible and there is only a small increase in frequency upon rinsing, due to removal of loosely attached polymer (Fig. 36a red dotted line). Adsorption of unmodified CMC, which was used as a reference, is slightly higher (2.3 mg/m^2) compared to CMC-*g*-PEG (1.75 mg/m^2). Nevertheless, the adsorption kinetics (Fig 36a, b) as well as the change in dissipation is very similar for both samples, indicating that the affinity between the backbones of the polysaccharides is governing the adsorption (Mishima et al. 1998). The slightly lower adsorbed mass sensed for CMC-*g*-PEG could be explained by increased steric hindrance between the PEG grafted chains and NFC, which suppresses complex formation. Hence, the modification does not significantly affect the adsorption of CMC on cellulose. For both systems the final change in dissipation was around 6×10^{-6}. The increase in dissipation suggests that the formed layer is well hydrated, soft and viscous. After adsorption the films were dried and imaged in AFM (Fig. 37). The adsorbed polymers are not visible and do not change the roughness of the film.

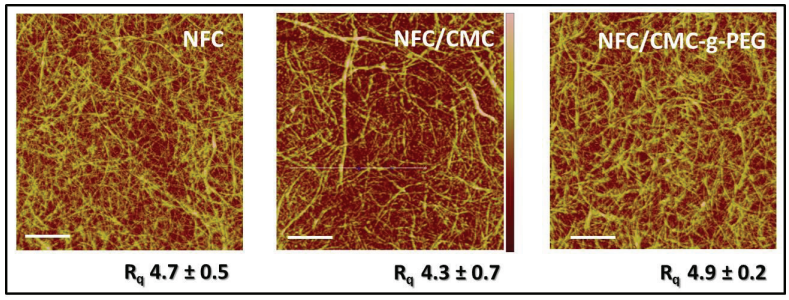

Figure 37. AFM height image of NFC films and after CMC and CMC-g-PEG adsorption from 100 mg/L pH 4.5 buffer solution (all images in air). The fibrils are around 5-20 nm from all samples. The scale size for all AFM images is 25μm^2.

4.3.4 pH effect on conformation of adsorbed CMC layer

Since both CMC and NFC are weak polyacids, the interactions between them will be strongly pH dependent. First, we decided to study the interfacial forces between a negatively charged cellulose sphere and NFC at two different pHs (4.5 and 7.3). At lower pH the carboxyl groups present on cellulose sphere and on NFC are partly protonated, while at higher pH they are mainly dissociated. The influence of pH on the DLVO forces is presented in Fig. 38. It can be seen that longer range repulsion occurs at pH 7.3 than that at pH 4.5, indicating an increased electrostatic repulsion due to the increased charge on purely anionic NFC and cellulose sphere. The forces were compared to best fits to DLVO theory. The closest fit was obtained assuming a surface potential of -25 mV at pH 7.3 and -12 mV for pH 4.5. Although that was just a rough estimation, we noticed that they are in the same range as previously reported potentials for various cellulose surfaces (Attard et al. 1998, Bergström et al. 1999, Salmi et al. 2007a, Ahola et al. 2008b, Eronen et al. 2012)

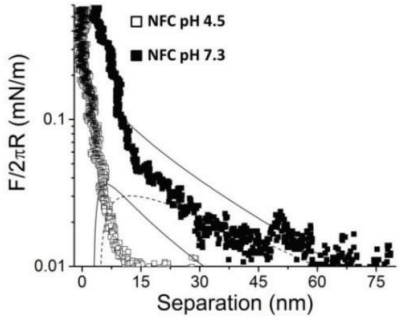

Figure 38. Normalized force profiles on approach as a function of relative separation between cellulose sphere against an NFC film at pH 4.5 (open symbols) and pH 7.3 (closed symbols). The buffer concentration in both cases is 0.1mM. The lines are best fit to DLVO theory at 0.1 mM electrolyte solution which corresponds to the Debye length of 30nm (calculated value, not a fitting parameter) and Hamaker constant of 8×10^{-21}J. The two solid line represents the forces assuming constant surface charge boundary condition and the broken line the corresponding calculated force assuming constant suface potential.

Before the more complicated system with CMC-g-PEG was studied we decided to check the interaction between the cellulose sphere and NFC film in presence of CMC at both pH conditions. Already the adsorption of CMC dramatically changes the forces between NFC and the colloidal cellulose sphere. After adsorption of CMC (Fig. 39 spheres), a longer ranged force component was observed. The normalized force for unmodified NFC at pH 7.3 is shown for comparison.

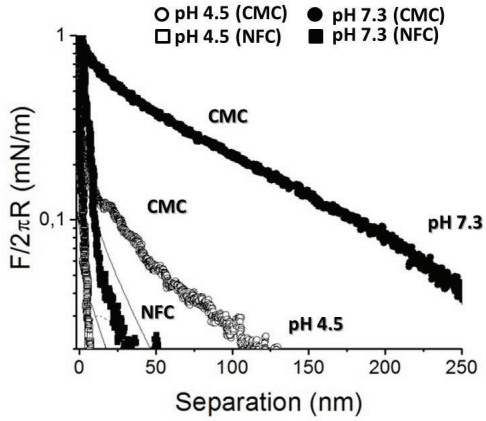

Figure 39. Normalized force profiles on approach as a function of relative separation between cellulose sphere against NFC film (squares) and after CMC adsorption (spheres) at pH 4.5 (open symbols) and pH 7.3 (closed symbols). The buffer concentration in both cases is 0.1 mM.

The long range repulsion cannot be described by DLVO theory since the decay length is much longer than the calculated Debye length of 30 nm for the system. This is characteristic for an (electro) steric force (Schneider et al. 2008). More charges due to de-protonation of carboxylic groups at higher pH leads not only to stronger double layer force due to the overlapping of counter-ion clouds but, more importantly, to more extended conformation of the adsorbed CMC, and consequently, a strong steric repulsion. Hence, stronger repulsion is observed for CMC at higher pH. The conformational changes of adsorbed CMC layers upon changes in pH were also observed with help of QCM-D (Fig. 40). CMC was adsorbed at pH 4.5 on the NFC film with 50 mM NaCl, to sufficiently protonate the carboxyl groups, suppress the electrostatic repulsion and improve the adsorption. Thereafter, the surface was rinsed with a combination of buffer solution and 0.1 mM NaCl. The first dotted line donotes the change from pH 4.5 to pH 7.3. Upon increasing the pH the CMC layers and underlying NFC layer swell which is observed as a decrease in Δf (-43 Hz) and increase in ΔD ($+8\times10^{-6}$) (Fig. 40). It is important to note that these changes are due to the pH response of both NFC and CMC, although the response of CMC, having a higher charge, is probably dominanting.

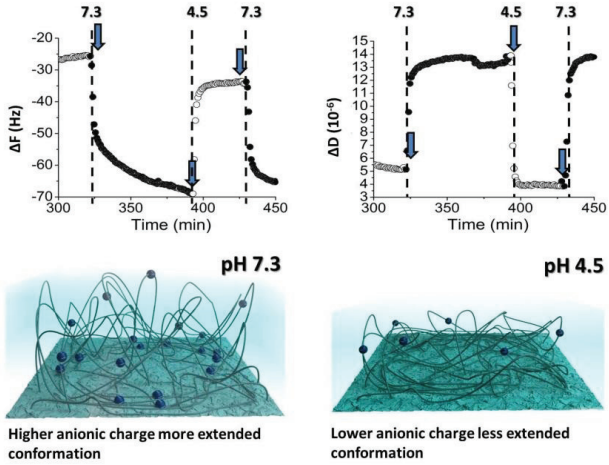

Figure 40. QCM-D data (3rd overtone) showing the effect of pH on the change in frequency and dissipation for CMC adsorbed onto spin coated NFC film. The arrows indicate the changes in pH. pH 4.5 0.1 mM NaAc/HAc (open symbols), and pH 7.3 KH_2PO_4/NaH_2PO_4 (closed symbol) buffer solutions. The corresponding schematic drawing illustrates the CMC chains behavior in the two buffer solutions. The blue spheres represent deprotonated carboxylic groups.

We note that a very similar response is observed for adsorbed CMC-*g*-PEG (see **Paper IV,** Supporting Information). When the pH is changed back to 4.5, most of the water is removed from the film (second dotted line). We speculate that upon decreasing the pH back to pH 4.5, some water is trapped in the layer, observed as a smaller decrease in frequency (-10 Hz). The cycle was repeated and the film repeatedly reacts to changes in pHs. These effects were, hence, also seen in surface force measurements Fig. 39.

4.4 Friction forces and lubrication of NFC systems

The study of friction, wear, and lubrication has long been of enormous practical importance, since the functioning of many mechanical, electromechanical and biological systems depends on the appropriate friction and wear values. At the moment only a few studies have dealt with the nanotribiology of cellulose. The friction forces of different cellulose model surfaces interacting with an amorphous cellulose sphere (Stiernstedt et al. 2006a), or when two cellulose sphere were modified by adsorption of polysaccharides; xyloglucan (Stiernstedt et al. 2006b) and chitosan (Nordgren et al. 2009a) have been reported before. So far there are no reports related to the frictional behavior of nanocellulose surfaces. Adhesive and lubricating properties of polysaccharides have been recently investigated (Gourdon et al. 2008, Stokes et al. 2011). Also the effect of polysaccharides adsorption on cellulose with respect to friction and normal forces have been outlined by few research groups before (Holmberg et al. 1997a, Stiernstedt et al. 2006b, Nordgren et al. 2009a).

In this thesis work we decided to test the lubricating properties of modified carboxymethyl cellulose attached on the NFC surface. The lubricating properties of a CMC-g-PEG layer on NFC fibrils were studied both in liquid (**Paper IV**) and in air (**Paper V**). We suggest that by studying the frictional behavior between reinforcing NFC segments and soft domains, which account for the composite structure, an understanding of the mechanical properties of composites can be developed.

4.4.1 Aqueous lubrication of NFC induce by polysaccharide adsorption

Because polyethylene glycol (PEG) has been rated as an effective aqueous lubricant we decided to graft it to CMC chains and self-assemble it with colloidal NFC to study its effect on the friction forces between cellulose fibrils. It is known that when two surfaces bearing brush-like polymer chains slide past each other under compression in good solvent, the inter-chain repulsion arising from increased osmotic pressure, together with the formation of cushion-like layer at the interface, leads to a substantial reduction in frictional force (Klein et al. 1994, Plunkett et al. 2003, Lee et al. 2007). We believe that such behavior could be beneficial for dispersibility of fibrils in aqueous solution which further would affect the formation of the dry composite film. Interactions between a cellulose sphere and NFC before and after adsorption of CMC-g-PEG were studied in terms of friction force and a schematic representation of those two approaches is presented in Scheme 4.

Scheme 4. Two systems where forces are measured between cellulose sphere and NFC before a) and after b) CMC-g-PEG in situ AFM liquid cell adsorption.

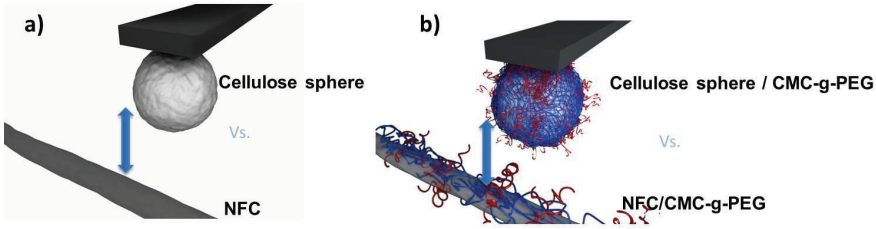

Only a few studies have dealt with the nanotribological response of cellulose, and so far there are no reports of using NFC films as substrates. We decided to extend the understanding of frictional phenomena in cellulose research by adding information on NFC films behavior under lateral force. Figure 41a collects the lateral friction data as a function of applied load for a cellulose sphere sliding against spin coated NFC film, immersed in 0.1 mM buffer solution at both pH 4.5 and pH 7.3, in the presence and absence of 100 mg/L CMC-*g*-PEG solution.

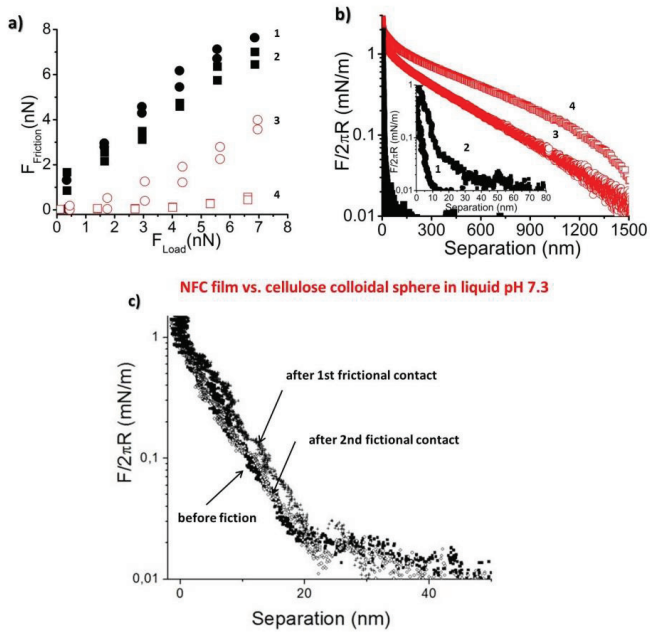

Figure 41. a) Lateral friction as a function of load between NFC film and cellulose sphere before (1, 2) and after adsorption of CMC-g-PEG (3, 4). Measurements were conducted in aqueous 0.1 mM electrolyte solution at pH 4.5 (circles) and at pH 7.3 (squares) b) The corresponding force normalized with the radius of the cellulose sphere on approach on a semilogarithmic scale. The inset shows the normal forces between the NFC film and the cellulose sphere at pH 4.5 (1) and pH 7.3 (2), c) Normal forces between NFC film and cellulose sphere before and after frictional contacts (the same spot was measured).

When the cellulose probe is moved into contact with the NFC film (Fig. 41a, curves 1 and 2), as soon as contact is reached, adhesive contact is made and the friction force jumps to a certain level. Thereafter, the friction increases almost linearly with increasing load. The effect seems even more pronounced at pH 7.3 (Fig. 41 line (2)). Only a slight change in friction coefficient is observed for NFC at different pHs; μ=1.00 ± 0.05 and μ= 0.84±0.08 were measured at pH 4.5 and pH 7.3, respectively. The slightly lower value at pH 7.3 reflects the increased lubrication by increased electrosteric repulsion. Fig. 41c presents the normal forces between NFC film and cellulose sphere detected before and after frictional contact. As it can be seen the force curve profiles are similar indicating that the substrate even though soft and swollen in studied condition remains stable. However it is important to point out that more than two frictional sliding on the same spot were not recorded, so the data about fatigue wear of the NFC surface are not available.

Water-based lubricants perform well in systems where the charged hydrophilic surfaces provide an electrostatic “double layer” repulsion, and the protruding layer of either the hydrophilic surface or the swollen

lubricant film provide additionally "steric" repulsion, all leading to low friction. Additionally, in hydrophilic systems the tightly bound water molecules add an extension to the hydrated layer increasing repulsions which are beneficial in lowering the friction forces. Such behavior is observed between the cellulose sphere and NFC film after adsorption of CMC-g-PEG. The lubricating effect of CMC-*g*-PEG is strongly pH dependent. A drastically reduced friction is observed at pH 7.3 (Figure 41a open squares) but only moderate friction mediation is noted at the lower pH (Fig. 41a open spheres). The corresponding normal forces are presented in Fig. 41b and the inset shows the approach force for unmodified NFC at different pHs since it is virtually invisible on the scale of 41b. The addition of CMC-*g*-PEG drastically increases the repulsion under both pH conditions. This vastly increased, and much longer ranged, steric interaction is almost certainly the main reason for the significant reduction of the frictional forces in the presence of adsorbed polymer. When CMC is in extended conformation with higher water content associated with the layers the PEG molecules contain more water, which in addition can improve lubrication.

Interestingly two different friction regimes for CMC-g-PEG adsorbed on NFC are observed at pH 7.3 (Fig. 42).

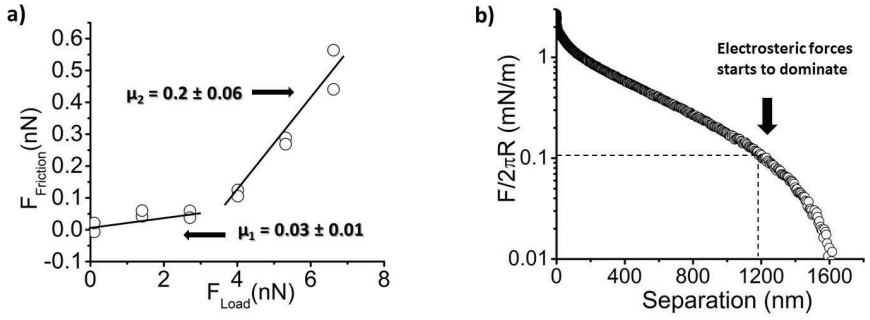

Figure 42. Friction force as a function of load between NFC film and cellulose sphere after adsorption of CMC-g-PEG at pH 7.3. The slope of the solid lines represents the friction coefficients. b) Corresponding normalized force vs. separation showing the correlation between the loads and forces.

Both of these regimes nonetheless display dramatically lower friction than the bare cellulose surfaces. At low load (below approximately 3 nN), a very low friction coefficient μ_1=0.03 ± 0.01 is observed, while at higher load the friction coefficient is slightly higher, μ_2=0.2 ± 0.06. This is characteristic for a situation where the main energy dissipating mechanism changes with the load. The transition between regimes corresponds to the trend observed in the normal force curve profile at a relative separation of around 1200 nm (Fig. 42b). The value 4 nN corresponds to about 0.1mN/m normalized force on approach (Fig. 42b) and it becomes clear that at large separations/low loads (under 4nN) the load is carried by electrostatic double layer repulsion and/or a long-ranged steric repulsion (possibly from dilute, hydrated CMC-g-PEG chains which overlap at maximum chain

extension). This interaction provides a highly hydrated cushioning effect, yielding good interfacial lubrication. At higher load (above 4nN) /shorter separations the load is supported by the electrosteric force seen in figures 42b and 41b. In the first case the surfaces will slide on a liquid layer between the surfaces and the friction will be low compared to friction between surfaces in mechanical contact. The more than 2-fold increase of the friction coefficient in the higher friction regime arises from the increased density of chains, the commensurately lower water content and the increased probability of the physical contact, of chain – chain interactions.

For comparison we also studied the frictional response of an unmodified CMC layer adsorbed on an NFC film at both pH values. The total reduction in friction for the system where CMC was adsorbed was 13% and 22% when pH 4.5 and pH 7.3 were used, compared to CMC-g-PEG system where the reduction was much higher, 65% and 88% for the respective pHs. It is possible that by modifying CMC with higher Mw PEG chains, the lubricating effect could be even stronger.

4.4.2 Lubrication of NFC via polysaccharide adsorption, studied in air

So far the measurements have been concerned with interactions in liquid. However, the interactions can also be measured between a nanocellulose film and a colloidal sphere with and without CMC-g-PEG, in air, with a view to understanding the role of adhesion and its effect on the friction force and lubrication.

The friction force as a function of load for a cellulose sphere against a NFC film at 35% relative humidity (RH) is shown in Fig. 43a and the corresponding normal forces in Fig. 43b.

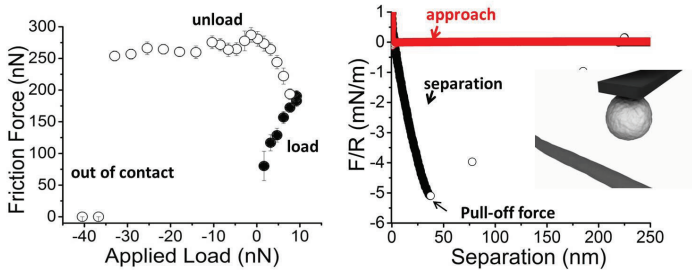

Figure 43. a) Friction force as a function of load for an amorphous cellulose sphere on NFC film and on b) Normal forces on approach (red) and separation (black) for the system with a cellulose sphere interacting with the NFC film.

When the surfaces are brought into contact, the surfaces jump to the contact due to attractive force. After contact, the friction force increases approximately linearly with increasing applied load as predicted by Amontons' law. At an external applied load of 10 nN the loading cycle is reversed and the friction force is measured as the load is stepwise reduced (open symbols). A significant hysteresis is observed. A similar type of

hysteresis has previously been observed in cellulosic systems and explained as an increase in true contact area (Chen et al. 1991, Bogdanovic et al. 2001) or capillary condensation (Feiler et al. 2007). It has been reported that the effect of capillary condensation on the adhesion and friction hysteresis between cellulose surfaces is especially pronounced at RH above 60% (Feiler et al. 2007)). In this work force and friction measurements were carried out at 35% RH, well below the indicated threshold of 60% for the formation of capillary condensates, which discards capillary condensation as the main cause of the friction hysteresis in our system. A very interesting feature in Fig. 43a is the remarkable increase of the friction force when the applied load started to be reduced from the maximum value of about 10 nN. Considering the high adhesion observed between the cellulose sphere and the NFC film (Fig. 43b), probably some NFC fibrils were partly pulled out when the separation of the surfaces was initiated by gradually decreasing the applied load. The partly pulled out NFC fibrils would alter the roughness and the contact area at the contact spot between cellulose sphere and NFC film, explaining the initial increase of the friction force in the unload curve and the subsequent hysteresis. Additionally, since the fibrils during the lateral experiment can be pulled-out from the surface they remained attached to the colloidal probe (indicated as 250nN friction forces present on unload cyckle even though the surfaces are not in contact -30nm separation). This is quite typical behavior observed in the system with high adhesion when the strong attractive bridging between the surfaces is possible and it has been previously reported for cellulose systems (Feiler et al. 2007).

Figures 44b-d show the friction curves between a cellulose colloid probe and a NFC film when CMC-g-PEG is adsorbed in one or both surfaces (Fig. 44a is attached for comparison). In general, CMC-g-PEG has a lubrication effect since lower friction values were observed after polymer adsorption. For instance, the friction force of 165 nN between cellulose sphere and NFC film at an applied load of 10 nN was reduced to 65 nN, 7.5 nN or 15 nN when CMC-g-PEG was adsorbed on the cellulose sphere, on the NFC film or on both surfaces, respectively. The friction hysteresis observed between uncoated cellulose surfaces vanished after CMC-g-PEG adsorption on NFC film (Figs. 44b, d). Although of lower magnitude, a friction hysteresis was still present between NFC fibrils and CMC-g-PEG coated cellulose sphere (Fig. 44c). These results suggest that the uncoated NFC films are responsible for the friction hysteresis, supporting the hypothesis that pulling out of NFC fibrils is the underlying mechanism of that phenomenon. The friction data correlates well with the strength of adhesion between the surfaces, quantified from the pull-off forces in the separation force curves (Fig. 43b).

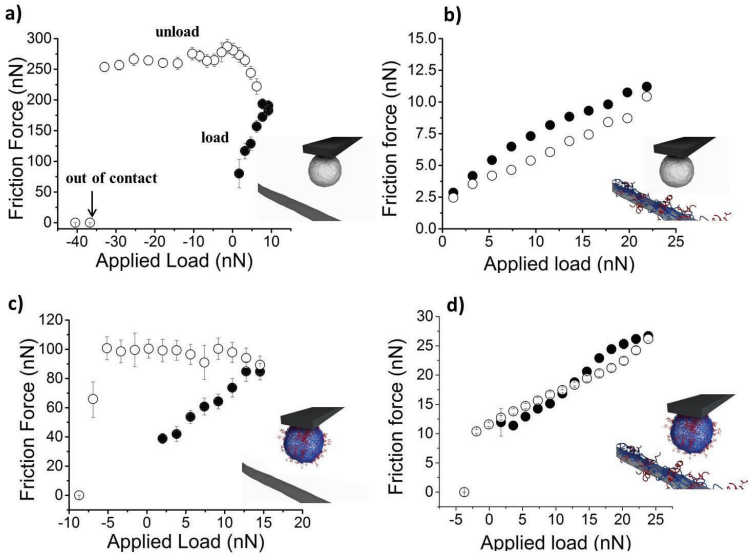

Figure 44. a) Friction force between a cellulose colloid probe and a NFC film as a function of applied load. c-d) Friction force between a cellulose colloid probe and a NFC film as a function of applied load after adsorption of CMC-g-PEG on: b) only NFC film; c) only cellulose colloid probe; and d) both on NFC film and cellulose colloid probe. Closed symbols in correspond to load curves, whereas open symbols represent unload curves. All measurements were performed at 35% RH.

Table 3 presents the average values of pull-off forces for the different cellulose systems studied in this work. The pull-off force for cellulose sphere vs. NFC is high -6.3 ± 1.4 mN/m and indicates strong adhesion. However, when NFC is modified with CMC-g-PEG the pull-off force is considerably lower with a value -0.8 ± 0.3 mN/m.

Table 3. Pull-off forces and friction coefficients between different cellulose surfaces. Mean values of at least 6 (pull-off forces) and 3 (friction coefficients) measurements are presented together with their standard deviations.

System	Pull-off forces (mN/m)	μ Friction coefficient
cellulose sphere vs. NFC film	-6.3 ± 1.4	8.44 ± 2.58
cellulose sphere vs. NFC / CMC-g-PEG	-0.8 ± 0.3	0.57 ± 0.07
cellulose sphere / CMC-g-PEG vs. NFC film	-2.8 ± 0.8	3.97 ± 0.23
cellulose sphere / CMC-g-PEG vs. NFC / CMC-g-PEG	-2.4 ± 1.1	0.83 ± 0.20

The pull-off forces were also measured when the cellulose sphere is also modified with CMC-g-PEG. When such a modified colloidal sphere interacted either with NFC or with NFC/CMC-g-PEG films the pull-off force values were very similar; -2.8 ± 0.08 and -2.4 ± 1.1 respectively (Table 3). We speculate that the reason could be NFC ultrathin uncoated substrate, which increased the adhesion via pullout of the fibers from the surfaces on separation. When NFC is coated with CMC-g-PEG the effect is demised and thus the pull-off force is very low (0.8 mN/m).

The corresponding friction coefficients were calculated for all studied system and the values are collected in Table 3. The lubrication effect of CMC-g-PEG is reflected on the lower values of friction coefficient obtained when the polymer was adsorbed on one or both cellulose surfaces. The friction coefficient between cellulose sphere and NFC film decreased one order of magnitude (from 8.44 ± 2.58 to 0.57 ± 0.07) after the adsorption of CMC-g-PEG on NFC. This is related to the dramatic decrease of adhesion observed after coating the NFC with CMC-g-PEG, and the consequent effect on the partial pulling out of NFC fibrils pointed out before. The intermediate value of 3.97 ± 0.23 for the friction coefficient between NFC film and cellulose sphere modified with CMC-g-PEG correlates with the intermediate adhesion and the presence of friction hysteresis in that system. A low friction coefficient of 0.83 ± 0.20 was obtained when the polymer was adsorbed on both surfaces, which confirms that the coating of NFC films with CMC-g-PEG significantly reduces the adhesion and the friction coefficient between the cellulose surfaces. Nevertheless, the friction coefficient when both surfaces were coated by CMC-g-PEG is slightly higher than in the case where the polymer was only adsorbed on NFC (0.83 ± 0.20 vs. 0.57 ± 0.07), which could be probably due to the entanglement of PEG chains from both surfaces.

4.4.3 Adhesion in NFC systems

The friction coefficient and friction forces reported in air are considerably higher compared to the values reported earlier in the aqueous environment (**Paper IV**). Measurements on molecularly smooth surfaces and single asperity contacts have shown that the friction force is dependent on the contact area and also on adhesion. The adhesion contribution is especially more pronounced in air than in liquid. The adhesion adds to the effective load leading to increase the friction force.

Figure 45a shows an attractive force pulling the probe into contact with the surface upon approach.

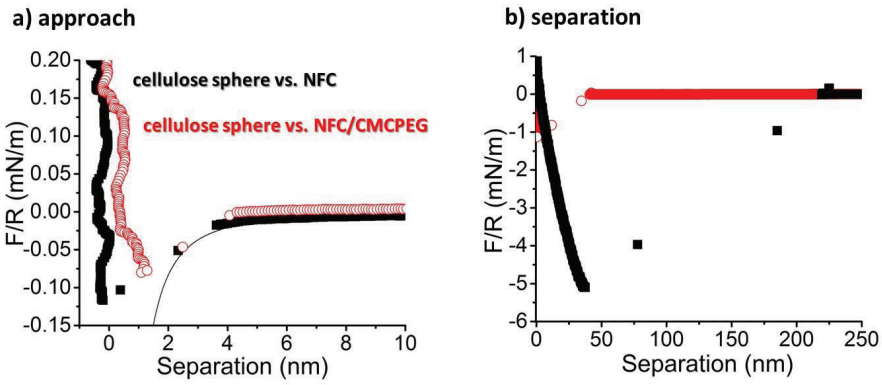

Figure 45. Normal forces on a) approach and b) separation for the systems where cellulose sphere interact with NFC without (black closed symbols) and with (red open symbols) CMC-g-PEG modification. The solid line represents the fit to van der Waals attraction with Hamaker constant 0.2×10^{-20} J.

The distance of the jump-in for the system where the cellulose sphere interacts with the NFC film with and without CMC-g-PEG are both around 4-7 nm. The jump contact takes place when the gradient of the attractive force exceeds the spring constant of the cantilever used. Considering the conditions chosen to carry out the force experiments (in air, RH 35%), the attraction observed at short distances must be due to van der Waals forces. Using a Hamaker constant of 0.2×10^{-20} J, equation (Eq 2.1 *Chapter 2.3.1*) could fit the experimental data very well (solid line in Fig. 45a).

The Hamaker constant of 0.2×10^{-20} J used in this study for cellulose surfaces interacting in air is about 30 times lower than the value of 5.8×10^{-20} J previously reported by Bergström *et al.* (Bergström et al. 1999). However, the spectroscopic ellipsometry experiments conducted by Bergström were performed on very smooth TMSC films which RMS roughness in the range between 0.16 - 0.24 nm. In presented studies the NFC films were rougher with the values between 4 – 5 nm (Fig. 37). Van der Waals forces are affected by surface roughness, decreasing as the roughness increases (Mazur, Maradudin 1981). In studied system here for more rough surfaces the lower van der Waals force contribution and lower the apparent Hamaker constant were observed.

As can be clearly seen from the pull-off forces (Table 3), adhesion is reduced from -6.3 ± 1.4 mN/m to -0.8 ±0.3 mN/m after adsorption of CMC-g-PEG onto NFC film (Fig. 45b). We speculate that when the cellulose spheres interact with unmodified NFC film, hydrogen bond formation (between both donor and acceptors side form cellulose) is possible during the short contact time. This is seen in the higher pull-off force when the surfaces are separated. When the NFC is modified by adsorption of CMC-g-PEG the H-bond formation is lower

since PEG chains can contribute with only an acceptor for H-bond formation (Deng et al. 1996), so the adhesion between surfaces measured on the retrace curve after contact is lower.

In this chapter the lateral forces in NFC with and without CMC-g-PEG modification in both aqueous media and dry conditions have been presented. The experiments were performed to assess the prominence of the interactions between composites components when the composite is formed. The aqueous lubrication of NFC fibrils with modified polysaccharide was studied in **Paper IV**. The good dispersion of well hydrated and lubricated fibrils is beneficial for the formation of even, non-aggregated films upon water removal. The connection between the lubrication and mechanical performance of free standing film in air was studied in **Paper V**. When the NFC surface is modified with CMC-g-PEG, a significant friction reduction was displayer with preserving high adhesion between the fibrils. We foresee that such a reduction in friction in dry state with high adhesion preserved between the reinforcing fibers could have a beneficial effect on interfacial sliding in biomimetic composites. The first steps to prove the importance of the lubrication between the NFC segments in composite materials were undertaken during this thesis. The mechanical properties of the composite film with the composition NFC/CMC-g-PEG 99/1 w/w is discussed in more detail in *Chapter 4.5.2,* and it shows synergic performance which is beyond the simple rule of mixture. It is suggested that the lower friction between the fibrils when CMC-g-PEG is present could be one of the reasons for the excellent performance.

4.5 NFC reinforced composite materials

The challenge in constructing nanocellulose based composite materials is to maintain the stiffness and strength of NFC, while increasing the strain-to-failure. By applying two different approaches we put an effort into understanding the importance of the mixing ratio of a composite material as well as the mutual interactions between two components from which the nanocomposites are made (**Paper III** and **V**)**.** In previous chapters we emphasized the importance of good bonding between the soft and hard domains. Herein, in upcoming chapter we present the mechanical properties of free-standing composite films, which were produced upon water removal using simple vacuum filtration (**Paper III**), or by applying pressurized filtration follow by hot press treatment **(Paper V**).

4.5.1 Mechanical properties of NFC/PB-b-PDAMEAq

Our interest was focused on biomimetic composites with a large fraction of reinforcing NFC domains, with only a small weight fraction of soft block copolymers. The PB-b-PDAMEAq function was devoted to energy dissipation mechanism. It is meant to slow the propagation of cracks and bring the plasticizing effect to the composites mechanical behavior. Because we wanted to assess how the ratio between the soft and hard domains

influences the mechanical performance, we have chosen different compositions where the dominant weight fraction always belongs to NFC.

The attractive ionic bonding between the oppositely charged nanofibrillar and spherical colloids prevented macroscopic phase separation. Scanning electron microscopy shows the nanofibrillar network structure (Figure 46 a) and a layered internal structure on the mesoscale for NFC: PB-b-PDAMEAq 2.5:1(Figure 46b).

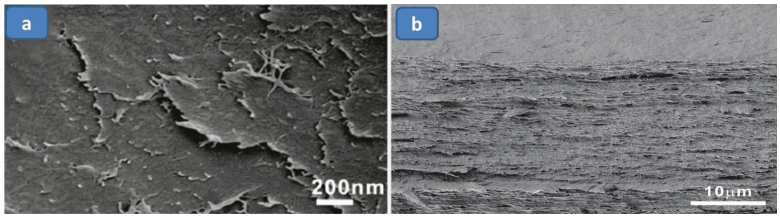

Figure 46. SEM image of the top surface (a) and fracture surface (b) of nanocomposites for the NFC/PB-b-PDMAEMAq sample with the weight fraction 2.5/1 w/w.

The NFC/PB-b-PDMAEMAq colloidal complexes are randomly oriented in planes to form a web-like fibrous network along the substrate during vacuum filatration. The fracture surface (Figure 46b) displays some vertical holes and protrusion between the various nanocellulose layers, indicating that the intralaminar NFC interaction is stronger than the interlaminar one. The composite might have a certain limited void content which is a consequence of the random in-plane orientation distribution of the NFC. The mesostructure of the composite was already presented in *Chapter 4.3.2* Figure 35b, where the TEM micrograph for a NFC/PB-b-PDMAEMAq was presented reviling preserved micellar arrangement of block copolymer aligned in pearl necklace fashion on NFC strands. The micelles are retained after drying of the composites despite the low glass transition temperature of the BP part that could allow disintegration of the micelles. The PB-b-PDAEMAq micelles are well separated and do not form a continuous film.

The stress-strain curves, work of fracture, Young's modulus and strain-to break for the series of composites are indicated in Figure 47 and summarized in Table 4. For pure NFC paper the Young's modulus can reach 12.5 GPa which is was reported before for similar nanocellulose paper (Svagan et al. 2007).

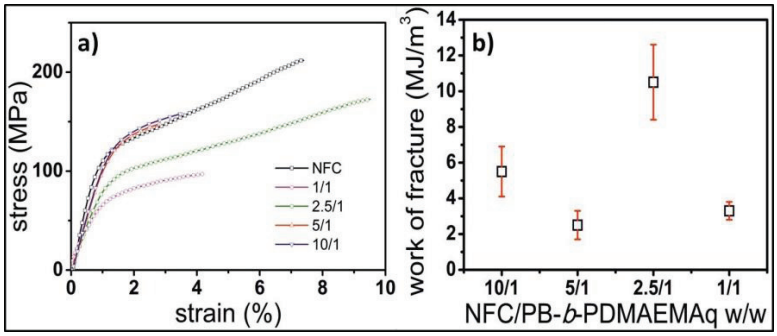

Figure 47. Stress-strain curves for NFC/PB-b-PDMAEMAq composites (a). Mass ratios of NFC and PB-b-ODMAEMAq are indicated in the legend. (b) Work of fracture as a function of the composition.

A small addition of the block copolymer (compositions 10/1, and 5/1) leads to a slightly decreasing in the moduli to values of 10.4 and 11.1 GPa (Table 4). Their stress-strain curves look very similar, indicating only minor influence of PB-b-PDMAEMAq (Figure 47a). Even though there was no big difference between the two compositions those both curves are remarkably different than the pure NFC, pointing at different interactions between the nanofibrils in the presence of the block copolymer. The increase of the weight fraction of PB-b-PDMAEMAq to the ratio 1/1 w/w leads to the further decrease of the modulus to 6.2 GPa. Nonlinearities were found where looking at the toughness as a function of the composition (Figure 47b). Toughness, which could be defined as the work of fracture is estimated from the area under the stress-strain curve, for the composition 2.5/1 was 2-3 times higher than for other composite ratios. Even compared to pure NFC there was still more than a 20% higher strain-to-failure, Fig 47a, Table 4.

Table 4. Mechanical Properties of the NFC/PB-b-PDMAEMAq Composites where the fraction of rubbery block copolymer increases toward the bottom.

Sample	Young's modulus (GPa)	Tensile strength (MPa)	Strain-to-failure (%)	Work of fracture (MJ/m^3)
NFC	12.5 (1.0)	202 (21.0)	6.8 (1.4)	9.8 (3.0)
10/1	10.4 (1.2)	166 (13.7)	4.5 (0.9)	5.5 (1.4)
5/1	11 (1.2)	144.8 (16.2)	2.4 (0.5)	2.5 (0.8)
2.5/1	7.3 (1.0)	165.2 (21.8)	9.1 (0.7)	10.5 (2.1)
1/1	6.2 (0.2)	95.8 (1.2)	4.6 (0.5)	3.3 (0.5)

We suggest that the PB soft domain in our composites serves two purposes. First, it enables more effective crack deflection at the hard/soft. Additionally, the lubrication of the nanoscale fibers by a synthetic block copolymer with low T_g can favor fiber pullout versus fiber fracture and hence, contribute to toughening. We examined the lubrication effect between the hard and soft domains in **Paper IV** and **V,** where we studied the frictional response of NFC films with and without CMC-*g*-PEG addition in liquid and in air.

4.5.2 Mechanical properties of CMC-*g*-PEG composites

It is known that the NFC tends to agglomerate due to strong inter particle van der Waals forces and hydrogen bonding. This aggregation impairs stress-transfer (by lowering the particle area / volume ratio) and weakens the composite since the agglomerated nanoparticles often behave as micro or even macroscopic defects. At the same time it is very crucial that the nature and the strength of the NFC-polymer interface are well controlled. One approach to improve the interfacial stress transfer efficiency is through the covalent attachment of functional groups to the surface of NFC, which could first improve the bonding between the NFC and polymer matrix and second, contribute to better dispersion of the NFC in the polymeric matrix. In the previous section we discussed the situation where the soft domains were introduced to NFC fibrils via ionic complexation. Such an approach already showed some improvement in the toughness. However the addition of a cationic block copolymer to the anionic NFC led to removal of water (see Fig 33 in *Chapter 4.3.2*). We believe that such dewatering of fibrils could cause aggregation of the fibrils which could, in consequence, lead to worse dispersion and finally deteriorate the composite films performance.

The second approach we presented in *Chapter 4.3.1* is based on NFC modification by introducing polysaccharides which interact with nanocellulose via H-bonding or van der Waals forces. In opposite to ionic complexation such interactions do not remove water at the NFC/polysaccharide interface. Moreover, as it has been already shown in *Chapter 4.3.4* the addition of CMC can also improve the stability of the complex by introducing more steric repulsion, which prevents aggregation.

Introducing CMC-g-PEG to NFC fibrils, as it was discussed in the previous *Chapter 4.4*, improved the aqueous lubrication and it is likely that this will provide beneficial dispersion properties for the even dried free-standing films. Figure 48 presents a photograph of composite made of 99/1 w/w NFC/CMC-g-PEG composition. More even film is produced in the presence of PEG compared to unmodified NFC film.

In **Paper V** oppositely to **Paper III** we focused on demonstrating the correlation between adhesion and lubrication on mechanical performance, not on finding optimal rations between components. Thus, only one ratio of components was studied.

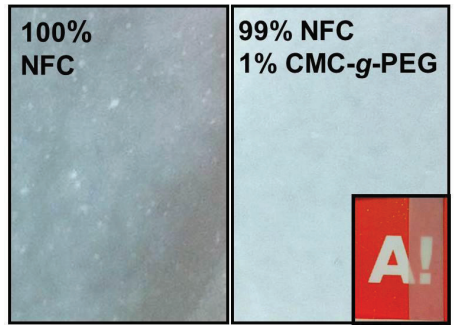

Figure 48. Photograph of free-standing film made from a), 100% NFC vacuum filtrated from water dispersion, and b) of composite having NFC/CMC-g-PEG 99/1 w/w. The inset shows the translucence of the composites.

Although there is some removal of fibrils during film formation (Österberg et al. 2013), the low concentration of CMC-g-PEG (1 w/w %) ensures that all added polymer is adsorbed to the fibrils and the ratio will be unaffected by the filtration. About 2 w-% of CMC can irreversible adsorbed to cellulose fibers depending on the polymer charge (Laine et al. 2000) but the adsorption on NFC could be higher due to larger accessible surface area. The stress-strain curve, Young's modulus, and strain-to-break, of 100% NFC film is compared with the NFC/CMC-g-PEG film with the ration 99/1 w/w in Fig. 49 and Table 5.

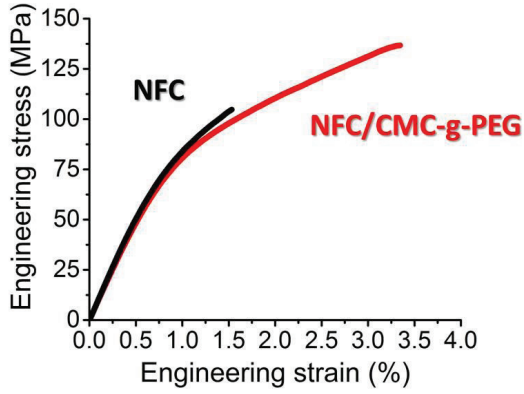

Figure 49. Stress-strain curves for NFC/CMC-g-PEG composite (red) and NFC reference (black)

Table 5. Mechanical Properties of the NFC/CMC-g-PEG Composite compared with 100% NFC film.

Sample	Young's Modulus (GPa)	engineering stress (MPa)	strain-to-failure (%)	work-of-fracture (MJ/m^3)
NFC (100%)	10.39 ± 0.14	107.11 ± 1.64	1.5 ± 0.09	1.04
NFC/CMC-g-PEG (99/1 %)	9.49 ± 0.48	124.42 ± 7.60	2.7 ± 0.56	3.09

For pure NFC paper the Young's modulus can reach 10.4 GPa, a value that was also reported for a similar nanocellulose paper (Österberg et al. 2013). Upon a small addition of CMC-g-PEG (1% w/w) the moduli only slightly decreases to the value 9.5 GPa. However, the stress-strain curves are different, indicating different interactions between the components than those which are between nanofibrils without modification. After addition of a small amount of CMC-g-PEG more plastic deformation is observed. The work-of-fracture, estimated by the area under the stress-strain curve (Henriksson et al. 2008), was almost three times higher for the nanocomposite than for unmodified NFC paper. The work-of-fracture is a measure of material toughness, and the increased toughness also allows reaching higher engineering strength, as observed in Fig 49. We speculate that the observed synergy is related to the surface forces between the components and the role of the soft polysaccharide layer in the complex.

Evans *et al.*(Wang et al. 2001, Evans et al. 2001) suggested that the lubricating effect of the soft domains in nacre leads to shearing and stretching of the organic phase within the slipping reinforcing domains, and provides resistance to deformation. We suggest that the CMC-g-PEG phase works in a similar way in the NFC/CMC-g-PEG nanocomposite, as shown by the low friction coefficient in the presence of CMC-g-PEG. Furthermore, the strong adhesion present both at NFC vs. CMC-g-PEG interface, and when both cellulose surfaces are modified with CMC-g-PEG, (see Table 3) ensures good bonding. Additionally, hydrogen bond formation and their rupture (Scheme 5a) during the sliding when load is applied could further contribute to toughening.

Scheme 5. a) Possible kinds of H-bonds formation between NFC and CMC-g-PEG interfaces, (1) between PEG from and CMC, (2) between CMC and NFC, and (3) between CMC from one chain with CMC from other chain, b) CMC-g-PEG induced lubrication between NFC fibrils

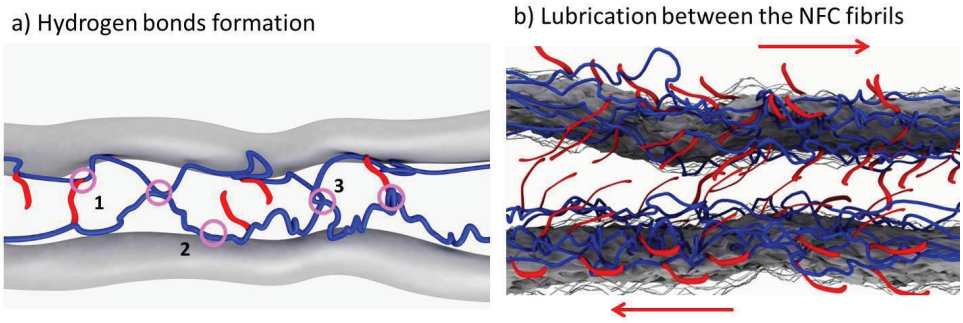

Moreover the lubricating effect of CMC-g-PEG layer allows friction reduction between the reinforcing NFC fibrils when the composite is under stress (Scheme 5b). Additionally the soft PEG layer could enable more effective crack deflection at the hard/soft (NFC/CMC-g-PEG) interface and henceforth contribute a second attractive benefit for toughening. However, we acknowledge that we can only speculate on this at the moment and more careful examination of fraction region and the crack dissipation mechanism would be needed. Finally the lubrication in the liquid state (**Paper IV**) and strong repulsion observed between the NFC fibrils after CMC-g-PEG modification could contribute to the formation of more even and better dispersed film in the dry state. The more uniform structure of the composite would exhibit improved mechanical properties.

4. CONCLUDING REMARKS

The general approach of this thesis is focused on determining the fundamental interactions in nanocellulose systems and their importance in constructing novel and advanced cellulose-based materials. More specifically two major aims were investigated. The first contained in **Papers I** and **II,** concentrated on the introduction of a new nanocellulose material (namely cationic NFC) and its fundamental behaviors with relation to charge, solvent and interaction with other nanocellulose particles. Cationic NFC, at the time when we published the first article was not well known and the extensive characterization included in **Paper I** became a very important contribution. This understanding of fundamental behavior of NFC allows utilizing that new grade of nanofirbillated cellulose in other applications, like multilayers formation of all cellulose films (**Paper II**).

The second aim was more specific, concentrating on the interfacial interaction between NFC and polymers in order to assess importance of their mutual interplay and the effect that this would have on the mechanical performance of the composite films based on nanocellulose. In **Paper III** the versatile and simple concept to self-assemble cellulose particle with an oppositely charged block-copolymer was introduced. This procedure allows biomimetic approach on nanocomposites that contain a large fraction of NFC reinforcements separated by rubbery domains. The complexation between the colloidal nanofibrils and the colloidal micellar spheres prevented macroscopic phase separation and gave rise to composites with an alternating nanoscale hard /soft architecture. Due to the nanoscopic control over fracture energy dissipation, significantly larger strain and toughness could be achieved. Interfibrillar lubrication, which was one of the explanations of the improved mechanical performance of the composites, was further studied in **Papers IV** and **V**. There a different approach to conjugate the nanocellulose with soft domains was implemented. Instead of attractive ionic complexation in, **Paper IV** the nature-driven adsorption of a polysaccharide with a similar backbone as cellulose was explored. The strong affinity of carboxymethyl cellulose for NFC fibrils was utilized as a bonding agent to introduce the soft (low T_g) polymer which would act to improve energy dissipation mechanism upon crack formation. To assess the importance of the lubrication between NFC segments we applied colloidal probe microscopy to study the lateral response between acting particles. The adsorption of CMC-g-PEG markedly increased the lubrication by reduction of the friction coefficient by 88% compared to the bare NFC film. In **Paper V** we continued with the same system, but now the friction force was studied in air. Such an approach is more relevant for the estimation of the extent of importance which lubrication has on mechanical performance of composite materials. Here again modified NFC film with CMC-g-PEG shows a significant reduction in friction compared to two sliding cellulose surfaces, even with the adhesion effect taken into account. The attractive vdW contributions to force and adhesion were deeply discussed in this paper. Furthermore, we evaluated the reduction in friction force in composite materials by studying the mechanical performance of the films composed of NFC/CMC-g-PEG. The synergetic performance, which is beyond the simple rule of mixing was, achieved. By introducing modified

polysaccharide as a lubricating and boning agent in NFC based nanocomposite, we presented a simple and versatile platform concept where the strength and stiffness of the reinforcing segments is preserved and the strain and the toughness of the composite is significantly improved.

5. REFERENCES

Abe, K., Iwamoto, S. & Yano, H. 2007, "Obtaining cellulose nanofibres with a uniform width of 15nm from wood", *Biomacromolecules,* vol. 8, no. 10, pp. 3276-3278.

Agoda-Tandjawa, G., Durand, S., Berot, S., Blassel, C., Gaillard, C., Garnier, C. & Doublier, J.-. 2010, "Rheological characterization of microfibrillated cellulose suspensions after freezing", *Carbohydrate Polymers,* vol. 80, no. 3, pp. 677-686.

Ahola, S., Myllytie, P., Österberg, M., Teerinen, T. & Laine, J. 2008a, "Effect of Polymer Adsorption on Cellulose Nanofibril Water Binding Capacity and Aggregation", *BioResources,* vol. 3, no. 4, pp. 1315-1328.

Ahola, S., Salmi, J., Johansson, L.S., Laine, J. & Österberg, M. 2008b, "Model Films from Native Cellulose Nanofibrils. Preparation, Swelling, and Surface Interactions", *Biomacromolecules,* vol. 9, no. 4, pp. 1273-1282.

Ahola, S., Salmi, J., Johansson, L., Laine, J. & Österberg, M. 2008c, "Model films from native cellulose nanofibrils. Preparation, swelling and surface interactions", *Biomacromolecules,* vol. 9, no. 4, pp. 1273–1282.

Akerholm, M. & Salmen, L. 2001, "Interaction between wood polymers studied by dynamic FT-IR spectroscopy.", *Polymer,* vol. 42, no 3, pp. 963- 969.

Almog, Y. & Klein, J. 1985, "Interactions between mica surfaces in a polystyrene-cyclopentane solution near the θ-temperature", *Journal of Colloid and Interface Science,* vol. 106, no. 1, pp. 33-44.

Altaner, C., Apperley, D.C. & Jarvis, M.C. 2006, "Spatial relationships between polymers in Sitka spruce: Proton spin-diffusion studies.", *Holzforschung,* vol. 60, pp. 665-673.

Andersson, S.R., Serimaa, R., Paakkari, T., Saranpaa, P. & Pesonen, E. 2003, "Crystallinity of wood and the size of cellulose crystallites in Norway spruce*(Picea abies)*.", *Journal of Wood Science,* vol. 49, pp. 531-537.

Andresen, M., Johansson, L., Tanem, B.S. & Stenius, P. 2006, "Properties and characterization of hydrophobized microfibrillated cellulose", *Cellulose,* vol. 13, no. 6, pp. 665-677.

Andresen, M., Stenstad, P., Moretro, T., Langsrud, S., Syverud, K., Johansson L-S & Stenius, P. 2007, "Nonleaching antimicrobial films prepared from surface-modified microfibrillated cellulose", *Biomacromolecules,* vol. 8, no. 7, pp. 2149-2155.

Angles, M.N. & Dufresne, A. 2001, "Plasticized Starch/Tunicin Whiskers Nanocomposite Materials. 2. Mechanical Behavior", *Macromolecules,* vol. 34, pp. 2921-2931.

Araki, J., Wada, M., Kuga, S. & Okano, T. 1998, "Flow properties of microcrystalline cellulose suspension prepared by acid treatment of native cellulose", *Colloids and Surfaces A: Physicochemical and Engineering Aspects,* vol. 142, pp. 75-82.

Araki, J., Wada, M., Kuga, S. & Okano, T. 1999, "Influence of surface charge on viscosity behavior of cellulose microcrystal suspension.", *Journal of Wood Science,* vol. 45, pp. 258-261.

Araki, J., Wafa, M., Kuga, S. & Okano, T. 2000, "Birefringent Glassy Phase of a Cellulose Microcrystal Suspension", *Langmuir,* vol. 16, pp. 2413-2415.

Araki, J. & Kuga, S. 2001, "Effect of Trace Electrolyte on Liquid Crystal Type of Cellulose Microcrystals", *Langmuir,* vol. 17, pp. 4493-4496.

Argyris, D., Ashby, P.D. & Striolo, A. 2011, "Structure and orientation of interfacial water determine atomic force microscopy results: insights from molecular dynamics simulations", *ACS Nano,* vol. 5, no. 3, pp. 2215-2223.

Ashby, M.F. & Jones, D.R.H. 1989, *Engineering materials 1: an introduction to their properties and applications.* Pergamon Press, Oxford.

Atalla, R.H. & Vanderhart, D.L. 1984, "Native Cellulose: A Composite of Two Distinct Crystalline Forms", *Science,* vol. 223, no. 4633, pp. 283-285.

Attard, P., Schulz, J.C. & Rutland, M.W. 1998, "Dynamic surface force measurement. I. van der Waals collisions.", vol. 69, pp. 3852-3866.

Atalla, R.H. & Vanderhart, D.L. 1999, "The role of solid state C-13 NMR spectroscopy in studies of the nature of native cellulose", *Solid State Nuclear Magnetic Resonance,* vol. 15, pp. 1-19.

Aulin, C., Ahola, S., Josefsson, P., Nishino, T., Hirose, Y., Österberg, M. & Wågberg, L. 2009, "Nanoscale Cellulose Films with different Crystallinities and Mesostructures-Their Surface Properties and Interaction with Water", *Langmuir,* vol. 25, no. 13, pp. 7675-7685.

Aulin, C., Johansson, E., Wågberg, L. & Lindström, T. 2010, "Self-organized Films from Cellulose I Nanofibrils Using the Layer-by-Layer Technique", *Biomacromolecules,* vol. 11, no. 4, pp. 872-882.

Azizi Samir, M.A.S., Alloin, F., Paillet, M. & Dufresne, A. 2004, "Tangling effect in fibrillated cellulose reinforced nanocomposites", *Macromolecules,* vol. 37, pp. 4313-4316.

Azizi Samir, M.A.S., Alloin, F. & Dufresne, A. 2005, "Review of Recent Research into Cellulosic Whiskers, Their Properties and Their Application in Nanocomposite Field", *Biomacromolecules,* vol. 6, no. 2, pp. 612-626.

Bardage, S., Donaldson, L., Tokoh, C. & Daniel, G. 2004, "Ultrastructure of the cell wall of unbeaten Norway spruce pulp fiber surfaces.", *Nordic Pulp & Paper Research Journal,* vol. 19, pp. 448-452.

Battista, O.A. 1950, "Hydroslysis and Crystallization of Cellulose", *Industrial and Engineering Chemistry,* vol. 42, pp. 502-507.

Battista, O.A., Coopick, S., Howsmo, J.A., Moreead, F.F. & Sisson, W.A. 1956, "Level-Off Degree of Polymerization: relation to polyphase structure of cellulose fibers.", *Industrial and Engineering Chemistry,* vol. 48, pp. 333-335.

Beamson, G. & Briggs, D. 1992, "High Resolution XPS of organic polymers." in *The Scienta ESCA300 Databse*, Wiley edn, Chichester .

Beck-Candanedo, S., Roman, M. & Gray, D.G. 2005, "Effect of Reaction Conditions on the Properties and Behavior of Wood Cellulose Nanocrystal Suspensions", *Biomacromolecules,* vol. 6, no. 2, pp. 1048-1054.

Bergström, L., Stemme, S., Dahlfors, T., Arwin, H. & Ödberg, L. 1999, "Spectroscopic Ellipsometry Characterisation and Estimation of the Hamaker Constant of Cellulose", *Cellulose,* vol. 6, no. 1, pp. 1-13.

Bertrand, P., Jonas, A., Laschewsky, A. & Legras, R. 2000, "Ultrathin Polymer-Coatings by Coplexation of Polyelectrolytes at Interaces - Suitable Materials, Structure and Properites", *Macromolecules Rapid Communication,* vol. 21, pp. 319-348.

Bhushan, B., Israelachvili, J.N. & Landman, U. 1995, "Nanotribiology: friction, wear and lubrication at atomic scale", *Nature,* vol. 374, pp. 607-616.

Biggs, S. 1995, "Steric and bridging forces between surfaces bearing adsorbed polymer: an atomic force microscopy study", *Langmuir,* vol. 11, no. 1, pp. 156-162.

Binnig, G., Quate, C.F. & Gerber, C. 1986, "Atomic Force Microscope", *Physical Review Letters,* vol. 56, no. 9, pp. 930-934.

Blomberg, E., Poptoshev, E., Claesson, P.M. & Caruso, F. 2004, "Surface Interactions during Polyelectrolyte Multilayer Buildup. 1. Interactions and Layer Structure in Dilute Electrolyte Solutions", *Langmuir,* vol. 20, pp. 5432-5438.

Blomberg, E., Poptoshev, E. & Caruso, F. 2006, "Surface Interactions during Polyelectrolyte Multilayer Build-Up. 2. The Effect of Ionic Strength on the Structure of Preformed Multilayers", *Langmuir,* vol. 22, pp. 4153-4157.

Boddohi, S. & Kipper, M.J. 2010, "Engineering Nanoassemblies of Polysaccharides", *Advanced Materials,* vol. 22, no. 28, pp. 2998-3016.

Bogdanovic, G., Tiberg, F. & Rutland, M.W. 2001, "Sliding Friction between Cellulose and Silica Surfaces", *Langumir,* vol. 17, pp. 5911-5916.

Bonderer, L.J., Studart, A.R. & Gaucker, L.J. 2008, "Bioinspired Design and Assembly of Platelet Reinforced Polymer Films", *Science,* vol. 319, pp. 1069-1073.

Bondeson, D., Kvien, I. & Oksman, K. 2006, "In cellulose Nanocomposites: Processing, Characterization , and Properties; Oksmanm K.; Sainm M.; ACS, Symposium Series 938", , ed. S.S.9. ACS, American Chemical Society, Washington, DC.

Bowden, F.P. & Tabor, D. 1950, *"The Friction and Lubrication of Solids. Part I",* Oxford edn, Oxford University Press.

Brown, R.M. 1996, "The biosynthesis of cellulose", *Journal of Macromolecular Science: Pure and Applied Chemistry,* vol. A33, pp. 1345-1373.

Brown, E.E. & Laborie, M.G. 2007, "Bioengineering Bacterial Cellulose/Poly(ethylene oxide) Nanocomposites", *Biomacromolecules,* vol. 8, no. 10, pp. 3074-3081.

Bulota, M., Jääskeläinen, A., Paltakari, J. & Hughes, M. 2011, "Properties of biocomposites: influence of preparation method testing environment and a comparison with theoretical medels", *Journal of Materials Science,* vol. 46, pp. 3387-3398.

Bulota, M., Kreitsmann, K., Hughes, M. & Paltakari, J. 2012, "Acetylated microfibrillated cellulose as a toughening agent in poly(lactic acid)", *Journal of Applied Polymer Science,* vol. 126, no. S1, pp. E449-E458.

Butt, H.J. 1991, "Measuring electrostatic, van der Waals, and hydration forces in electrolyte solutions with an atomic force microscope", *Biophys.J.,* vol. 60, no. 6, pp. 1438-1444.

Butt, H.J., Cappella, B. & Kappl, M. 2005, "Force measurements with the atomic force microscope: technique, interpretation and applications", *Surface Science Reports,* vol. 59, no. 1-6, pp. 1-152.

Butt, H.J., Berger, R., Bonaccurso, E., Chen, Y. & Wang, J. 2007, "Impact of atomic force microscopy on interface and colloid science", *Advances in Colloid and Interface Science,* vol. 133, no. 2, pp. 91-104.

Capadona, J., Shanmuganathan, K., Trittschuh, S., Seidel, S., Rowan, S.J. & Weder, C. 2009, "Polymer Nanocomposites with Nanowhiskers Isolated from Microcrystalline Cellulose", *Biomacromolecules,* vol. 10, pp. 712-716.

Carambassis, A. & Rutland, M.W. 1999, "Interactions of cellulose surfaces: effect of electrolyte.", *Langmuir,* vol. 15, no. 17, pp. 5584-5590.

Chan, D.Y.C. & Horn, R.G. 1985, "The drainage of thin liquid films between solid surfaces", *Journal of Colloid and Interface Science,* vol. 83, no. 10, pp. 5311-5324.

Charreau, H., Forest, M. & Vazguez, A. 2013, "Nanocellulsoe Patents Trends: A Comprehensive Review on Patents on Cellulose Nanocrystals, Microfibrillated and Bacteria Cellulose", *Recent Patents on Nanotechnology,* vol. 7, pp. 56-80.

Chen, Y.L., Helm, C.A. & Israelachvili, J.N. 1991, "Molecular Mechanisms Associated with Adhesion and Contact Angle Hysteresis of Monolayer Surfaces", *Journal of Physical Chemistry B,* vol. 95, pp. 10736-10747.

Claesson, P.M., Blomberg, E. & Poptoshev, E. 2001, "Surface forces and emulsion stability in" in *Encyclopedic handbook of Emulsion Technology*, ed. Sjöblom J, Marcel Dekker Inc.,New York, pp. 305-326.

Claesson, P.M., Poptoshev, E., Blomberg, E. & Dedinaite, A. 2005, "Polyelectrolyte-mediated surface interactions", *Advances in Colloid and Interface Science,* vol. 114-115, no. 30, pp. 173-187.

Cranston, E.D. & Gray, D.G. 2006, "Morphological and Optical Characterization of Polyelectrolyte Multilayers Incorporating Nanocrystalline Cellulose", *Biomacromolecules,* vol. 7, no. 9, pp. 2522-2530.

Cranston, E.D. & Gray, D.G. 2008, "Birefringence in spin-coated films containing cellulose nanocrystals", *Colloids and Surfaces A: Physicochemical and Engineering Aspects,* vol. 325, no. 1-2, pp. 44-51.

Cranston, E.D., Gray, D.G. & Rutland, M.W. 2010, "Direct Surface Force Measurements of Polyelectrolyte Multilayer Films Containing Nanocrystalline Cellulose", *Langmuir,* vol. 26, no. 22, pp. 17190–17197-17190–17197.

Decher, G. 1997, "Fuzzy nanoassemblies: Toward layered polymeric multicomposites", *Science,* vol. 277, no. 5330, pp. 1232-1237.

Decher, G., Hong, J.D. & Schmitt, J. 1992, "Buildup of Ultrathin Multilayer Films by a Self-Assembly Process.3. Consecutively Alternating Adsorption of Anionic and Cationic Polyelectrolytes on Charged Surfaces.", *Thin Solid Films,* vol. 210, no. 1-2, pp. 831-835.

Decher, G. & Schlenoff, J.B. (eds) 2003, *Multilayer Thin Films. Sequential Assembly of Nanocomposite Materials*, Wiley-Vch.

deGennes, P.G. 1987, "Polymers at an interface: a simplified view.", *Advanced in Colloid Interface Science,* vol. 27, pp. 189-209.

Deng, L., Mrksich, M. & Whitesides, G.M. 1996, "Self-assembled monolayers of alkanethiolates presenting tri(propylene sulfoxide) groups resist the adsorption of protein.", *Journal of American Chemical Society,* vol. 18, no. 21, pp. 5136-5137.

Derjaguin, B.V.a.L.L. 1941, *Acta Phys. Chim. USSR,* vol. 14, pp. 633-662.

Devereux, O.F. & de Bruyn, P.L. 1963, "Interaction of Plane-Parallel Double Layers", Massachusetts Institute of Technolog Press; Cambridge, MA

Ding, S. & Himmel, M.E. 2006, "The maize primary cell wall microfibril:A new model derived from direct visualization", *Journal of Agricultural and Food Chemistry,* vol. 54, no. 3, pp. 597-606.

Donaldson, L. 2007, "Cellulose microfibril aggregates and their size variation with cell wall type", *Wood Science and Technology,* vol. 41, pp. 443-460.

Dong, X.M., Kimura, T., Revol, J.F. & Gray, D.G. 1996, "Effects of Ionic Strength on the Isotropic-Chiral Nematic Phase Transition of Suspensions of Cellulose Crystallites", *Langmuir,* vol. 12, pp. 2076-2082.

Dong, X., Revol, J.F. & Gray, D.G. 1998, "Effect of microcrystallite preparation conditions on the formation of colloid crystals of cellulose", *Cellulose,* vol. 5, pp. 19-32.

Duchesne, I., Hult, E., Molin, U., Daniel, G., Iversen, T. & Lennholm, H. 2001, "The influence of hemicellulose on fibril aggregation of kraft pulp fibers as revealed by FE-SEM and CP/MAS 13C-NMR.", *Cellulose,* vol. 8, pp. 103-111.

Ducker W A,Senden T.J.and Pashley R.M. 1991, "Direct measurement of colloidal forces using an atomic force microscope", *Nature,* vol. 353, no. 6341, pp. 239-241.

Dufresene, W.A., Cavaille, J.Y. & Vignon, M.R. 1997, "Mechanical behaviour of sheets prepared from sugar beet cellulose microfibrils.", *Journal of Applied Polymer Science,* vol. 64, pp. 1185-1194.

Duran, N., Lemes, A.P. & Seabra, A.B. 2012, "Review of cellulose nanocrystals paptents: preparation, composites and general applications", *Recent Patents on Nanotechnology,* vol. 6, pp. 16-28.

Edgar, C.D. & Gray, D.G. 2003, "Smooth model cellulose I surfaces from nanocrystal suspensions", *Cellulose,* vol. 10, no. 4, pp. 299-306.

Eichhorn, S.J. & Davies, G.R. 2006, "Modelling the crystalline deformation of native and regenerated cellulose", *Cellulose,* vol. 13, no. 3, pp. 291-307.

Eichhorn, S., Dufresne, A., Aranguren, M., Marcovich, N., Capadona, J., Rowan, S., Weder, C., Thielemans, W., Roman, M., Renneckar, S., Gindl, W., Veigel, S., Keckes, J., Yano, H., Abe, K., Nogi, M., Nakagaito, A., Mangalam, A., Simonsen, J., Benight, A., Bismarck, A., Berglund, L. & Peijs, T. 2010, "Review: current international research into cellulose nanofibres and nanocomposites", *Journal of Materials Science,* vol. 45, no. 1, pp. 1-33.

Elazzouzi-Hafraoui, S., Nishiyama, Y., Putaux, J., Heux, L., Dubreuil, F. & Rochas, C. 2008, "The Shape and Distribution of Crystalline Nanoparticles Prepared by Acid Hydrolysis of Native Cellulose.", *Biomacromolecules,* vol. 9, no. 1, pp. 57-65.

Endler, A. & Persson, S. 2011, "Cellulose synthases and synthesis in Arabidopsis.", *Molecular Plant,* vol. 4, pp. 199-211.

Eriksson, M., Torgnysdotter, A. & Wågberg, L. 2006, "Surface Modification of Wood Fibers Using the Polyelectrolyte Multilayer Technique:Effects on Fiber Joint and Paper Strength Properties", *Industrial & Engineering Chemistry Research,* vol. 45, no. 15, pp. 5279-5286.

Eronen, P., Österberg, M., Heikkinen, S., Tenkanen, M. & Laine, J. 2011a, "Interactions of structurally different hemicelluloses with nanofibrillar cellulose", *Carbohydrate Polymers,* vol. 86, pp. 1281-1290.

Eronen, P., Junka, K., Laine, J. & Österberg, M. 2011b, "Interaction Between Water Soluble Polysaccharides and Native Nanofibrillar Cellulose Thin Films", *BioResources,* vol. 6, no. 4, pp. 4200-4217.

Eronen, P., Laine, J., Ruokolainen, J. & Österberg, M. 2012, "Comparison of Multilayer Formation Between Different Cellulose Nanofibrils and Cationic Polymers", *Journal of colloid and interface science,* vol. 373, no. 1, pp. 84-93.

Evans, A.G., Suo, Z., Wang, R.Z., Aksay, I.A., He, M.Y. & Hutchinson, J.W. 2001, "Model for the robust mechanical behaviour of nacre", *Journal of Material Research,* vol. 16, no. 9, pp. 2475-2484.

Eyeholzer, C., Bordeanu, N., Lopez-Suevos, F., Rentsch, D., Zimmermann, T. & Oksman, K. 2010, "Preparation and characterization of water-redispersible nanofibrillated cellulose in powder form.", *Cellulose,* vol. 17, pp. 19-30.

Fält, S., Wågberg, L. & Vesterlind, E. 2003, "Swelling of Model Films of Cellulose Having Different Charge Densities and Comparison to the Swelling Behavior of Corresponding Fibers", *Langmuir,* vol. 19, no. 19, pp. 7895-7903.

Feiler, A., Larson, I., Jenkins, P. & Attard, P. 2000, "A quantative study of interaction forces and friction in aqueous colloidal systems", *Langmuir,* vol. 16, pp. 10269-10277.

Feiler, A., Jenkins, P. & Rutland, M.W. 2005, "Effect of relative humidity on adhesion and frictional properties of micro- and nano-scopic contacts", *Journal of Adhesion Science and Technology,* vol. 19, pp. 165-179.

Feiler, A., Stiernstedt, J., Theander, K., Jenkins, P. & Rutland, M.W. 2007, "Effect of Capillary Condensation on Friction Force and Adhesion", *Langmuir,* vol. 23, pp. 517-522.

Fengel, D. 1970, "Ultrastructural behavior of cell wall polysaccharides", *Tappi Journal,* vol. 53, pp. 497-503.

Fengel, D. & Wegener, G. (eds) 1989, *Wood - Chemistry, Ultrastructure, reakctions.*, Walter de Gruyter edn, Walter de Gruyter, Berlin.

Fernandes, A.N., Thomas, L.H., Altaner, C.M., Callow, P., Forsyth, V.T., Apperley, D.C., Kennedy, C.J. & Jarvis, M.C. 2011, "Nanostructure of cellulose microfibrils in spruce wood.", *Proceedings of the National Academy of Sciences,* vol. 108, pp. E1195-E1203.

Fevier, V., Canova, G.R., Cavaille, J.Y., Chanzy, H., Dufresne, A. & Gauthier, C. 1995a, "Nanocomposite materials from latex and cellulose whiskers", *Polymers for Advanced Technologies,* vol. 6, pp. 351-355.

Fevier, V., Chanzy, H. & Cavaille, J.Y. 1995b, "Polymer Nanocomposites Reinforced by Cellulose Whiskers", *Macromolecules,* vol. 28, pp. 6365-6367.

Filpponen, I. 2009, *PhD. Thesis,* North Carolina State university, Raleigh, NC.

Filpponen, I., Kontturi, E., Nummelin, S., Rosilo, H., Kolehmainen, E., Ikkala, O. & Laine, J. 2012, "Generic Method for Modular Surface Modification of Cellulosic Materials in Aquous Medium by Swquential "Clic" reaction and Adsorption", *Biomacromolecules,* vol. 13, no. 3, pp. 736-742.

Fleer, G.J., Cohen Stuart, M.A., Scheutjens, J.M.H.M., Cosgrove, T. & Vincent, B. 1993, *Polymers at interface,* Chapman& Hall, University Press, Cambridge.

Fratzl, P. & Weinkamer, R. 2007, "Nature's hierarchical materials", *Progress in Materials Science,* vol. 52, pp. 1263-1334.

Frey-Wyssling, A. 1954, "The fine structure of cellulose microfibrils", *Science,* vol. 119, pp. 80-82.

Gandini, A. 2011, "The irruption of polymers from renewable resources on the scene of macromolecular science and technology", *Green Chemistry,* vol. 13, no. 5, pp. 1061-1083.

Gao, J.P., Luedtke, W.D., Gourdon, D., Ruths, M., Israelachivili, J.N. & Landman, U. 2004, "Frictional forces and Amontons' law: From the molecular to the macroscopic scale.", *Journal of Physical Chemistry B,* vol. 108, pp. 3410-3425.

Garcia de Rodriguez, N. L., Thielemans, W. & Dufresne, A. 2006, "Sisal cellulose whiskers reinforced polyvinyl acetate nanocomposites", *Cellulose,* vol. 13, pp. 261-270.

Glasser, W.G., Atalla, R.H., Blackwell, J., Brown Jr., M.R., Burchard, W., French, A.D., Klemm, D. & Nishiyama, Y. 2012, "About the structure of cellulose: debating the Lindman hypothesis", *Cellulose,* , no. 19, pp. 589-598.

Gourdon, D., Lin, Q., Oroudjev, E., Hansma, H., Golan, Y., Arad, S. & Israelachivili, J. 2008, "Adhesion and Stable Low Friction Provided by a Subnanometer-Thick Monolayer of a Natural Polysaccharide", *Langmuir,* vol. 24, pp. 1534-1540.

Grunnert, M. & Winter, W.T. 2002, "Nanocomposites of Cellulose Acetate Butyrate Reinforced with Cellulose Nanocrystals", *Journal of Polymers and the Environment,* vol. 10, pp. 27-30.

Guhados, G., Wan, W. & Hutter, J.L. 2005, "Measurement of the Elastic Modulus of Single Bacterial Cellulose Fibers Using Atomic Force Microscopy", *Langmuir,* vol. 21, pp. 6642-6646.

Gustafsson, J., Ciovica, L. & Peltonen, J. 2002, "The ultrastructure of spruce kraft pulps studied by atomic force microscopy (AFM) and X-ray photoelectron spectroscopy (XPS).", *Polymer,* vol. 44, no. 3, pp. 661-670.

Habibi, Y., Goffin, A., Schiltz, N., Duquesne, E., Dubois, P. & Dufresne, A. 2008, "Bionanocomposites based on poly(3-caprolactone)-grafted cellulose nanocrystals by ring-opening polymerization", *Journal of Materials Chemistry,* vol. 18, pp. 5002-5010.

Habibi, Y., Lucia, L.A. & Rojas, O.J. 2010, "Cellulose Nanocrystals; Chemistry, Self-Assembly, and Applications", *Chem. Rev.,* vol. 110, pp. 3479-3500.

Hamaker, H.C. 1937, "The London-van der Waals attraction between spherical particles", *Physica,* vol. 4, pp. 1058-1072.

Hansma, H.G., Kim, K.J., Laney, D.E., Garcia, R.A., Argaman, M., Allen, M.J. & Parsons, S.M. 1997, "Properties of biomolecules measured from atomic force microscope images: A review", *Journal of Structural Biology,* vol. 1197, pp. 99-108.

Harder, P., Grunze, M., Dahint, R., Whitesdies, G.M. & Laibinis, P.E. 1998, "Molecular Conformation in Oligo(ethylene glycol)-Terminated Self-Assembled Monolayers on Gold and Silver Surfaces Determines Their Ability To Resist Protein Adsorption", *Jorunal of Physcial Chemistry B,* vol. 102, pp. 426-436.

Hartley, P.G. 1999, "Measurement of colloidal interactions using atomic force microscope" in *Colloid-Polymer Interactions From Fundamentals to Practive*, ed. Fainato, R.S and Dublin P.L, John Wiley & Son Inc.; edn, pp. 253-286.

Haworth, W.N. 1932, "Die Konstitution einiger Kohlenhydrate", *Berichte der deutschen chemischen Gesellschaf (A),* vol. 65, no. 4, pp. 43-65.

Heim, L.O., Blum, J., Preuss, M. & Butt, H.J. 1999, "Adhesion and friction forces between spherical micrometer-sized particles.", *Physiacal Review Letters,* vol. 83, pp. 3328-3331.

Heimenz, P.C. & Rajagopalan, R. (eds) 1997, *Principles of Colloid and Surface Chemistry*, 3rd Ed., Marcel Dekker, Inc. edn, pp. 485-490.

Henriksson, M. & Berglund, L.A. 2007, "Structure and properties of cellulose nanocomposite films containing melamine formaldehyde", *Journal of Applied Polymer Science,* vol. 106, no. 4, pp. 2817-2824.

Henriksson, M., Berglund, L.A., Isaksson, P., Lindström, T. & Nishino, T. 2008, "Cellulose nanopaper structures of high toughness", *Biomacromolecules,* vol. 9, no. 6, pp. 1579-1585.

Hermans, P.H. & Weidinger, A. 1949, "X-ray studies on the crystallinity of cellulose", *Journal of Polymer Science,* vol. 4, pp. 135-144.

Herth, W. 1983, "Arrays of plasma-membrane rosettes involved in cellulose microfibril formation of*Spirogyra*.", *Planta,* vol. 159, pp. 347-356.

Hirai, A., Inui, O., Horii, F. & Tsuji, M. 2009, "Phase Separation Behavior in Aqueous Suspensions of Bacterial Cellulose Nanocrystals Prepared by Sulfuric Acid Treatment", *Langmuir,* vol. 25, pp. 497-502.

Ho, T.T.T., Zimmermann, R., Hauert, R. & Caseri, W. 2011, "Preparation and characterization of cationic nanofibrillated cellulose from etherification and high-shear disintegration processes", *Cellulose,* vol. 18, pp. 1391-1406.

Hodges, C.S. 2002, "Measuring forces with the AFM: polymeric surfaces in liquids", *Advances in Colloid and Interface Science,* vol. 99, no. 1, pp. 13-75.

Holmberg, M., Berg, J., Stemme, S., Ödberg, L., Rasmusson, J. & Claesson, P. 1997a, "Surface Force Studies of Langmuir-Blodgett Cellulose Films", *Journal of colloid and interface science,* vol. 186, no. 2, pp. 369-381.

Holmberg, M., Wigren, R., Erlandsson, R. & Claesson, P.M. 1997b, "Interactions between cellulose and colloidal silica in the presence of polyelectrolytes", *Colloids and Surfaces A: Physicochemical and Engineering Aspects,* vol. 129-130, pp. 175.

Hon, D.N.-. 1994, "Cellulose : a random walk along its hitorical path", *Cellulose,* vol. 1, no. 1, pp. 1-25.

Hoogendam, C.W., de Keizer, A., Cohen Stuart, M.A., Bijsterbosch, B.H., Smit, J.A.M., van Dijk, J.A.A.P., van der Horst, P.M. & Batelaan, J.G. 1998, "Persistence Length of Carboxymethyl Cellulose As Evaluated from Size Exclusion Chromatography and Potentiometric Titrations", *Macromolecules,* vol. 31, pp. 6297-6309.

Höök, F., Rodahl, M., Brzezinski, P. & Kasemo, B. 1998, "Energy Dissipation Kinetics for Protein and Antibody Antigen-Adsorption under Shear Oscillation on a Quartz Crystal Microbalance", *Langmuir,* vol. 14, no. 4, pp. 729-734.

Horvath, E. & Lindström, T. 2007, "The influence of colloidal interactions on fiber network strength", *Journal of Colloid and Interface Science,* vol. 309, pp. 511-517.

Hult, E.L., Larsson, P.T. & Iversen, T. 2000, "A comparative CP/MAS C-13-NMR study of cellulose structure in sprice wood and kraft pulp", *Cellulose,* vol. 7, pp. 35-55.

Hult, E.L., Larsson, P.T. & Iversen, T. 2001, "Cellulose fibril aggregation - an inherent property of kraft pulps.", *Polymer,* vol. 42, pp. 3309-3314.

Hult, E.L., Iversen, T. & Sugiyama, J. 2003, "Characterization of the supermolecular structure of cellulose in wood pulp fibers.", *Cellulose,* vol. 10, pp. 103-110.

Hutter, J.L. & Bechhoefer, J. 1993, "Calibration of atomic force microscope tips", *Review of Scientific Instruments,* vol. 64, no. 7, pp. 1868-1873.

Iler, R.K. 1966, "Multilayers of colloidal particles", *Journal of colloid and interface science,* vol. 21, no. 6, pp. 569-594.

Iotti, M., Gregersen, Ø, Moe, S. & Lenes, M. 2011, *Rheological Studies of Microfibrillar Cellulose Water Dispersions*, Springer Netherlands.

Ishimaru, Y. & Lindström, T. 1984, "Adsorption of water-soluble, nonionic polymers onto cellulosic fibers", *Journal of Applied Polymer Science,* vol. 29, no. 5, pp. 1675-1691.

Israelachvili, J.N. & Pashley, R.M. 1984, "Measurments of the hydrophobic interaction between two hydrophobic surfaces in aqueous electrolyte solutions", *Journal of Colloid and Interface Science,* vol. 98, no. 2, pp. 500-514.

Israelachvili, J.N. 1991," *Intermolecular and Surface Forces,"*2nd ed. American Press, San Diego.

Israelachvili, J. & Wennerström, H. 1996, "Role of hydration and water structure in biological and colloidal interactions", *Nature,* vol. 379, pp. 219-225.

Iwamoto, S., Nakagaito, A., Yano, H. & Nogi, M. 2005, "Optically transparent composites reinforced with plant fiber-based nanofibers.", *Applied Physics A: Materials Science & Processing,* vol. 89, pp. 461-466.

Iwamoto, S. 2008, "The effect of hemicelluloses on wood pulp nanofibrillation and nanofiber network characteristics", *Biomacromolecules,* vol. 9, no. 3, pp. 1022-1026.

Iwamoto, S., Kai, W., Isogai, A. & Iwata, T. 2009, "Elastic Modulus of Single Cellulose Microfibrils from Tunicate Measured by Atomic Force Microscopy", *Biomacromolecules,* vol. 10, no. 9, pp. 2571.

Jakob, H.F., Fengel, D., Tschegg, S.E. & Fratzl, P. 1995, "The elementary cellulose fibril in Picea abies: Comparison of transmission electron microscopy, small-angle X-ray scattering and wide-angle X-ray scattering results", *Macromolecules,* vol. 28, pp. 8782-8787.

Jean, B., Dubreuil, F., Heux, L. & Cousin, F. 2008a, "Structural Details of Cellulose Nanocrystals/Polyelectrolytes Multilayers Probed by Neutron Reflectivity and AFM", *Langmuir,* vol. 24, no. 7, pp. 3452-3458.

Jean, B., Heux, L., Dubreuil, F., Chambat, G. & Cousin, F. 2008b, "Non-Electrostatic Building of Biomimetic Cellulose-Xyloglucan Multilayers", *Langmuir,* vol. 25, no. 7, pp. 3920-3923.

Jean, B., Heux, L., Dubreuil, F., Chambat, G. & Cousin, F. 2009, "Non-Electrostatic Building of Biomimetic Cellulose-Xyloglucan Multilayers", *Langmuir,* vol. 25, no. 7, pp. 3920-3933.

Ji, H., Hone, D., Pincus, P.A. & rossi, G. 1991, "Polymer bridging between two parallel plates", *Macromolecules,* vol. 23, no. 3, pp. 698-707.

Johannsmann, D., Mathauer, K., Wegner, G. & Knoll, W. 1992, "Viscoelastic properties of thin films probed with a quarz-crystal resonator", *Phys Rew B,* vol. 46, no. 12, pp. 7808-7815.

Johansson, L., Tammelin, T., Campbell, J.M., Setala, H. & Osterberg, M. 2011, "Experimental evidence on medium driven cellulose surface adaptation demonstrated using nanofibrillated cellulose", *Soft Matter,* , no. 22, pp. 10917-10924.

Kanika, C., Lee, S., Lee, B.P., Dalsin, J.L., Messersmith, P.B. & Spencer, N.D. 2009, "A novel low-friction surface for biomedical applications: Modification of poly(dimethylsiloxane) (PDMS) with polyethylene glycol(PEG)-DOPA-lysine", *Journal of Biomedical Materials Research Part A,* vol. 90A, pp. 742-749.

Karppinen, A., Vesterinen, A., Saarinen, T., Pietikäinen, P. & Seppälä, J. 2011, "Effect of cationic polymethacrylates on the rheology and flocculation of microfibrillated cellulose", *Cellulose,* vol. 18, no. 6, pp. 1381-1390.

Klein, J., Kumacheva, E., Mahalu, D., Perahia, D. & Fetters, L.J. 1994, "Reduction of frictional force between solid surfaces bearing polymer brushes", *Nature,* , no. 370, pp. 634-636.

Klemm, D., Philipp, B., Heinze, T., Heinze, U. & Wagenknecht, W. (eds) 1998, *Comprehensive Cellulose Chemistry, Volume 1, Fundamentals and Analytical Methods*, Wiley-VCH, Weinheim.

Klemm, D. 2001, "Bacterial synthesized cellulose - artificial blood vessels for microsurgery", *Progress in Polymer Science,* vol. 26, no. 9, pp. 1561-1603.

Klemm, D., Heublein, B., Fink, H. & Bohn, A. 2005, "Cellulose: Fascinating Biopolymer and Sustainable Raw Material", *Angewandte Chemie International Edition,* vol. 44, no. 22, pp. 3358-3393.

Klemm, D., Kramer, F., Moritz, S., Lindström, T., Ankerfors, M., Gray, D. & Dorris, A. 2011, "Nanocelluloses: A New Family of Nature-Based Materials", *Angewandte Chemie International Edition,* vol. 50, no. 24, pp. 5438-5466.

Koljonen, K., Österberg, M., Johansson, L. & Stenius, P. 2003, "Surface chemistry and morphology of different mechanical pulps determined by ESCA and AFM", *Colloids and Surfaces A: Physicochemical and Engineering Aspects,* vol. 228, pp. 143-158.

Kong, K., Wilding, M.A., Ibbett, R.N. & Eichhorn, S.J. 2008, "Molecular and crystal deformation of cellulose: uniform strain or unifrom stress?", *Faraday Discuss,* vol. 139, pp. 283-298.

Kontturi, E., Thüne, P.C. & Niemantsverdriet, J.W. 2003, "Novel method for preparing cellulose model surfaces by spin coating", *Polymer,* vol. 44, no. 13, pp. 3621-3625.

Kontturi, E., Tammelin, T. & Österberg, M. 2006, "Cellulose-model films and the fundamental approach", *Chemical Society Reviews,* vol. 35, no. 12, pp. 1287-1304.

Kopta, S. & Salmeron, M. 2000, "The atomic scale origin of wear on mica and its contribution to friction.", *Journal of Chemical Physics,* vol. 113, pp. 8249-8252.

Korayem, M.H., Ebrahimi, N. & Korayem, A.H. 2011, "Modeling and Simulation of Tapping-mode Atomic Force Microscopy in Liquid.", *Nanoscience and Nanotechnology,* vol. 1, pp. 14-21.

Krässig, H. (ed) 1996, *Cellulose, Polymer Monographs*, Gordon and Breach Science Publishers, Amsterdam.

La Mer, V.K. & Healy, T.W. 1963, "Adsorption-flocculation reactions of macromolecules at the solid-liquid interface", *Rev. Pure Appl. Chem,* vol. 13, pp. 112-133.

Lachman, N. & Daniel Wagner, H. 2010, "Correlation between interfacial molecular structure and mechanics in CNT/epoxy nano-composites", *Composites Part A: Applied Science and Manufacturing,* vol. 41, no. 9, pp. 1093-1098.

Lachman, N., Wiesel, E., Guzman de Villoria, R., Wardle, B.L. & Wagner, H.D. 2012, "Interfacial load transfer in carbon nanotube/ceramic microfiber hybrid polymer composites", *Composites Science and Technology,* vol. 72, no. 12, pp. 1416-1422.

Lahiji, R.R., Xu, X., Reifenberger, A.R., Rudie, A. & Moon, R.J. 2010, "Atomic Force Microscopy Chracterization of Cellulose Nanocrystals", *Langmuir,* vol. 26, no. 6, pp. 4480-4488.

Laine, J., Lindstrom, T., Glad Nordmark, G. & Risinger, G. 2000, "Studies on topochemical modification of cellulose fibres Part 1. Chemical conditions for the attachment of carboxymethyl cellulose onto fibres", *Nord.Pulp Pap.Res.J.,* vol. 15, no. 5, pp. 520-526, Paper and coating chemistry symposium, Stockholm, Sweden, 6-8 June 2000 (C, K, P, S).

Larsson, P.T., Wickholm, K. & Iversen, T. 1997, "A CP/MAS 13C NMR investigation of molecular ordering in cellulose.", *Carbohydrate Polymers,* vol. 302, no. 1-2, pp. 19-25.

Lee, S., Mueller, M., Heeb, R., Zurucher, S., Tosatti, S., Henirich, M., Amstad, F., Pechmann, S. & Spencer, N.D. 2006, "Self-healing behaviour of a polyelectrolyte-based lubricant additive for aqueous lubrication of oxide materials.", *Tirbology Letters,* vol. 24, no. 3, pp. 217-223.

Lee, S., Spencer, N.D., Erdemir, A. & Marin, J.,-M. 2007, "In Superlubricity" in , eds. S. Lee, N.D. Spencer, A. Erdemir & J. Marin -M., Elsevier edn,Amsterdam, pp. 365.

Li, X.D., Chang, W.C., Chao, Y.J., Wang, R.Z. & Chang, M. 2004, "Nanoscale structure and mechanical characterization of a natural nanocomposite material: shell of red abalone", *Nano Letters,* vol. 4, pp. 613-617.

Lifshitz, E.M. 1956, "The theory of molecular attractive forces between solids", *Soviet Physics - JETP,* vol. 2, pp. 73-83.

Lin, N., Huang, J., Chang, P.R., Feng, J. & Yu, J. 2011, "Surface acetylation of cellulose nanocrystal and its reinforcing function in poly(lactic acid)", *Carbohydrate Polymers,* vol. 83, no. 4, pp. 1834-1842.

Lindman, B., Karlström, G. & Stigsso, L. 2010, "On the mechanism of dissolution of cellulose", *Journal of Molecular Liquids,* , no. 156, pp. 76-81.

Lindström, T., Ankerfors, M. & Henriksson, G. 2007, *Method for treating chemical pulp for manufacturing microfibrillated cellulose*, PCT Int Appl. 2007SE-82; 2006-272:14 edn, Sweden.

Liu, Z., Choi, H., Gatenholm, P. & R. Esker, A.R. 2011, "Quartz Crystal Microbalance with Dissipation Monitoring and Surface Plasmon Resonance Studies of Carboxymethyl Cellulose Adsorption onto Regenerated Cellulose Surfaces", *Langmuir,* , no. 14, pp. 8718-8728.

Lvov, Y.M. & Decher, G. 1994, "Assembly of Multilayer Ordered Films by Alternating Adsorption of Oppositely Charged Marcomolecules", *Crystallography Reports,* vol. 39, pp. 628-647.

Magonov, S.N., Elings, V. & Whangbo, M.H. 1997, "Phase imaging and stiffness in tapping-mode atomic force microscopy", *Surface Science,* vol. 375, pp. L385-L391.

Magonov, S.N. 2000, *Atomic force microscopy in analysis of polymers,* John Wiley & Sons Ltd., Chichester.

Manias, E. 2007, "Stiffer by design", *Nature Materials,* vol. 6, pp. 9-11.

Martin, Y., Williams, C.C. & Wickramasinghe, H.K. 1987, "Atomic force microscope-force mapping and profmng on a sub 100 A scale", *J. Appl. Phys,* vol. 61, no. 10, pp. 4723-4729.

Matsuo, M., Sawatari, C., Iwai, Y. & Ozaki, F. 1990, "Effect of Orientation Distribution and Crystallinity on the Measurement by X-ray Diffraction of the Crystal Lattice Moduli of Cellulose I and I1", *Macromolecules,* vol. 23, pp. 3266-3274.

Mazur, P. & Maradudin, A.A. 1981, "Effects of surface roughness on the vad der Waals force between macroscopic bodies. II. Two rough surfaces", *Physical Review B,* vol. 23, no. 2, pp. 695-705.

Medronho, B., Ramano, Q., Graca Miquel, M.A., Stigsso, L. & Lindman, B. 2012, "Rationalizing cellulose (in)solubility: reviewing basic physicochemical aspects and role of hydrophobic interactions", *Cellulose,* vol. 19, pp. 581-587.

Menig, R., Mayers, M.H., Mayers, M.A. & Vecchio, K.S. 2000, "Quasi-static and dynamic mechanical response of*Haliotis rufescens*(abalone) shells.", *Acta Materialia,* vol. 48, pp. 2383-2398.

Meyer, K.H. & Lotmar, W. 1936, "Sur l'élasticité de la cellulose.(Sur la constitution de la partie cristallisée de la cellulose IV)", *Helvetica Chimica Acta,* vol. 19, pp. 68-86.

Millon, L.E. & Wan, W.K. 2006, "The polyvinyl alcohol–bacterial cellulose system as a new nanocomposite for biomedical applications", *Journal of Biomedical Materials Research Part B: Applied Biomaterials,* vol. 79B, pp. 245-253.

Mishima, T., Hisamatsu, M., York, W.S., Teranishi, K. & Yamada, T. 1998, "Adhesion of beta-glucans to cellulose", *Carbohydrate Research,* vol. 308, no. 3-4, pp. 389-395.

Momeni, K. & Yassar, R.S. 2009, "Analytical formulation of stress distribution in cellulose nanocomposites.", *Journal of Computational and Theoretical Nanoscience,* vol. 6, pp. 1511-1518.

Moon, R.J., Martini, A., Nairn, J., Simonsen, J. & Youngblood, J. 2011, "Cellulose nanomaterials review: structure, properties and nanocomposites", *Chem.Soc.Rev.,* vol. 40, pp. 3941-3994.

Mueller, M., Czihak, C., Vogl, G., Fratzl, P., Schober, H. & Riekel, C. 1998, "Direct observation of microfibril arrangement in a single native cellulose fiber by microbeam small-angle X-ray scattering.", *Macromolecules,* vol. 31, pp. 3953-3957.

Mueller, S.C. & Brown, R.M. 1980, "Evidence for an intramembrane component associated with a cellulose microfibril-synthesizing complex in higher plants.", *The Journal of Cell Biology,* vol. 84, pp. 315-326.

Munch, E., Launey, M.E., Alsem, D.H., Saiz, E., Tomsia, A.P. & Ritchie, R.O. 2008, "Tough, Bio-Inspired Hybrid Materials", *Science,* vol. 322, pp. 1516-1520.

Mwaikambo, L.Y. & Ansell, M.P. 1996, "The determination of porosity and cellulose content of plant fibers by density methods.", *Journal of Materials Science Letter,* vol. 20, pp. 2095-2096.

Naderi, A. & Claesson, P.M. 2006, "Adsorption Properties of Polyelectrolyte-Surfactant Complexes on Hydrophobic Surfaces Studied by QCM-D", *Langmuir,* vol. 22, no. 18, pp. 7639-7645.

Nakagaito, A.N. & Yano, H. 2004, "The effect of morphological changes from pulp fiber towards nano-scale fibrillated cellulose on the mechanical properties of high-strength plant fiber based composites", *Applied Physics A: Materials Science & Processing,* vol. 78, no. 4, pp. 547-552.

Nakagaito, A.N., Iwamoto, S. & Yano, H. 2005a, "Bacterial cellulose: ultimate nano-scalar cellulose morphology for production of high-strength composites.", *Applied Physics A: Materials Science & Processing,* vol. 80, pp. 93-97.

Nakagaito, A.N. & Yano, H. 2005b, "Novel high-strength biocomposites based on microfibrillated cellulose having nano-ordered-unit web-like network structure", *Applied Physics A: Materials Science & Processing,* vol. 80, pp. 155-159.

Nakagaito, A.N. & Yano, H. 2008a, "The effect of fiber content on the mechanical and thermal expansion properties of biocomposites based on microfibrillated cellulose", *Cellulose,* vol. 15, pp. 555-559.

Nakagaito, A.N. & Yano, H. 2008b, "Toughness enhancement of cellulose nanocomposites by alkali treatment of the reinforcing cellulose nanofibrers", *Cellulose,* vol. 15, pp. 323-331.

Nehls, I., Wagenknecht, W., Philipp, B. & Stscherbina, D. 1994, "Characterization of cellulose and cellulose derivatives in solution by high resolution 13C-NMR spectroscopy"", *Progress in Polymer Science,* vol. 19, no. 1, pp. 29-78.

Neuman, R.D., Berg, J.M. & Claesson, P. 1993, "Direct measurement of surface forces in papermaking and paper coating systems", *Nordic Pulp & Paper Research Journal,* vol. 8, pp. 96-104.

Newman, R.H. 1999, "Estimation of the lateral dimensions of cellulose crystallites using C-13 NMF signal strengths", *Solid State Nuclear Magnetic Resonance,* vol. 15, pp. 21-29.

Newman, R.H. 2004, "Homogeneity in cellulose crystallinity between samples of*Pinus radiata*wood.", *Holzforschung,* vol. 58, pp. 91-96.

Niimura, H., Yokoyama, T., Kimura, S., Matsumoto, Y. & Kuga, S. 2010, "AFM observation of iltrathin microfibrils in fruit tissues.", *Cellulose,* vol. 17, pp. 13-18.

Ninham, B.W. & Parsegian, V.A. 1971, "Electrostatic potential between surfaces bearing ionizable groups in ionic equilibrium with physiologic saline solution", *Journal of Theoretical Biology,* vol. 31, no. 3, pp. 405-428.

Nishino, T., Takano, K. & Nakamae, K. 1995, "Elastic modulus of the crystalline regions of cellulose polymorphs", *Journal of Polymer Science, Part B: Polymer Physics,* vol. 33, no. 11, pp. 1647-1651.

Nishiyama, Y., Langan, P. & Chanzy, H. 2002, "Crystal structure and hydrogen-bonding system in cellulose 1 beta from synchrotron X-ray and neutron fiber diffraction.", *Journal of American Chemical Society,* vol. 124, pp. 9074-9082.

Nishiyama, Y., Kim, U.J., Kim, D.Y., Katsumata, K.S., May, R.P. & Langan, P. 2003, "Periodic disorder along ramie cellulose microfibrils.", *Biomacromolecules,* vol. 4, pp. 1013-1017.

Nordgren, N., Eronen, P., Österberg, M., Laine, J. & Rutland, M.W. 2009a, "Mediation of the Nanotribological Properties of Cellulose by Chitosan Adsorption", *Biomacromolecules,* vol. 10, no. 3, pp. 645-650.

Nordgren, N., Eronen, P., OÌˆsterberg, M., Laine, J. & Rutland, M.W. 2009b, "Mediation of the Nanotribological Properties of Cellulose by Chitosan Adsorption", *Biomacromolecules,* vol. 10, no. 3, pp. 645.

Notley, S.M., Biggs, S., Craig, V.S.J. & Wågberg, L. 2004a, "Adsorbed layer structure of a weak polyelectrolyte studied by colloidal probe microscopy and QCM-D as a function of pH and ionic strength", *Physical Chemistry Chemical Physics,* vol. 6, pp. 2379-2386.

Notley, S.M., Pettersson, T. & Wågberg, L. 2004b, "Direct Measurement of Attractive van der Waals' Forces between Regenerated Cellulose Surfaces in an Aqueous Environment", *Journal of the American Chemical Society,* , no. 43, pp. 13930-13931.

Notley, S.M., Eriksson, M. & Wågberg, L. 2005, "Visco-elastic and adhesive properties of adsorbed polyelectrolyte multilayers determined in situ with QCM-D and AFM measurements", *J.Colloid Interface Sci.,* vol. 292, no. 1, pp. 29-37.

Notley, S.M., Eriksson, M., Wågberg, L., Beck, S. & Gray, D.G. 2006, "Surface Forces Measurements of Spin-Coated Cellulose Thin Films with Different Crystallinity", *Langmuir,* vol. 22, no. 7, pp. 3154-3160.

Notley, S.M. 2008, "Effect of introduced charge in cellulose gels on surface interactions and the adsorption of highly charged cationic polyelectrolytes", *Physical Chemistry Chemical Physics,* vol. 10, no. 13, pp. 1819-1825.

Okano, T., Kuga, S., Wafa, M., Araki, J. & Ikuina, J. 1999, *(Nisshin Oil Mills Ltd. Japan)*, JP 98/151052, Japan.

Okubo, K., Fujii, T. & Thostenson, E.T. 2009, "Multi-scale hybrid biocomposite: Processing and mechanical characterization of bamboo fiber reinforced PLA with microfibrillated cellulose", *Composites Part A: Applied Science and Manufacturing,* vol. 40, pp. 469-475.

Ono, H., Matsui, T. & Miyamato, I. 1999, *(Asahi Kasei Kogyo Kabushiki Kaisha, japam)*, WO 98/JP5462, Japan.

Orelma, H., Filpponen, I., Johansson, L., Laine, J. & Rojas, O.J. 2011, "Modification of Cellulose Films by adsorption of CMC and Chitosan for Controlled Attachment of Biomolecules", *Biomacromolecules,* vol. 12, pp. 4311-4318.

Österberg, M. & Claesson, P. 2000, "Interactions between cellulose surfaces: effect of solution pH", *Journal of Adhesion Science and Technology,* vol. 14, no. 5, pp. 603-618.

Österberg, M., Laine, J., Stenius, P., Kumpulainen, A. & Claesson, P.M. 2001, "Forces between Xylan-Coated Surfaces: Effect of Polymer Charge Density and Background Electrolyte", *Journal of colloid and interface science,* vol. 242, no. 1, pp. 59-66.

Österberg, M., Vartiainen, J., Lucenius, J., Hippi, U., Seppälä, K., Serimaa, R. & Laine, J. 2013, "A Fast Method to Produce Strong NFC Films as a Platform for Barrier and Functional Materials", *Acs Applied Materials & Interfaces,* , pp. 4640-4647.

O'Sullivan, A. 1997, "Cellulose: the structure slowly unravels.", *Cellulose,* vol. 4, no. 3, pp. 173-207.

Pääkkö, M., Ankerfors, M., Kosonen, H., Nykänen, A., Ahola, S., Österberg, M., Ruokolainen, J., Laine, J., Larsson, P.T., Ikkala, O. & Lindström, T. 2007, "Enzymatic hydrolysis combined with mechanical shearing and high-pressure homogenisation for nanoscale cellulose fibrils and strong gels", *Biomacromolecules,* vol. 8, no. 6, pp. 1934-1941.

Pääkkö, M., Vapaavuori, J., Silvennoinen, R., Kosonen, H., Ankerfors, M., Lindström, T., Berglund, L.A. & Ikkala, O. 2008, "Long and entangled native cellulose I nanofibers allow flexible aerogels and hierarchically porous templates for functionalities", *Soft Matter,* vol. 4, no. 12, pp. 2492.

Paananen, A., Österberg, M., Rutland, M.W., Tammelin, T., Saarinen, T., Tappura, K. & Stenius, P. 2004, "Interactions between cellulose and xylan:An atomic force microscope and quartz crystal microbalance study" in *ACS Symposium Series 864 (Hemicelluloses)* American Chemical Society, , pp. 269-290.

Pei, A., Butchosa, N., Berglund, L.A. & Zhou, Q. 2013, "Surface quaternized cellulose nanofibrils with high water absorbency and adsorption capacity for anionic dyes", *Soft Matter,* vol. 9, pp. 2047-2055.

Perry, S.S., Somorjai, G.A., Mate, C.M. & White, R.L. 1995, "Adhesion and friction properites of hydrogenated amorphous cabon films measured by atomic force microscopy.", *Tribology Letters,* vol. 1, pp. 233-246.

Pettersson, T., Nordgren, N. & Rutland, M.W. 2007, "Comparison of different methods to calibrate torsional spring constant and photodetector for atomic force microscopy friction measurements in air and liquid RID C-8177-2011", *Review of Scientific Instruments,* vol. 78, no. 9, pp. 093702-2-093702-8.

Peura, M., Müller, M., Vainio, U., Sarén, M., Saranpää, P. & Serimaa, R. 2008, "X ray microdiffraction reveals the orientation of cellulose microfibrils and the size of cellulose crystallites in single Norway sprice tracheids", *Trees - Structure and Function,* vol. 22, pp. 49-61.

Phillips, D.L., Xing, J., Liu, H., Chong, C.K. & Corke, H. 1999, "Raman spectroscopic determination of the degree of cationic modification in waxy maize starches.", *Analytical Letters,* vol. 32, pp. 3049-3058.

Pigorsch, E. 2009, "Spectroscopic characterization of cationic quarternary ammonium starches", *Starch,* vol. 31, pp. 129-138.

Plunkett, M.A., Feiler, A. & Rutland, M.W. 2003, "Atomic force microscopy measurments of adsorbed polyelectrolyte layers. 2. Effect of composition and substrate on structure, force and friction", *Langmuir,* vol. 19, no. 10, pp. 4180-4187.

Podsiadlo, P., Choi, S., Shim, B., Lee, J., Cuddihy, M. & Kotov, N.A. 2005, "Molecularly Engineered Nanocomposites:Layer-by-Layer Assembly of Cellulose Nanocrystals", *Biomacromolecules,* vol. 6, no. 6, pp. 2914-2918.

Podsiadlo, P., Tang, Z., Shim, B.S. & Kotov, N.A. 2007, "Counterintuitive Effect of Molecular Strength and Role of Molecular Rigidity on Mechanical Properties of Layer-by-Layer Assembled Nanocomposites", *Nano Letters,* vol. 7, no. 5, pp. 1224-1231.

Pokroy, B., Vladislav, D. & Zolotouabko, E. 2009, "Nacre in mollusk shells as a multilayered structure with strain gradient", *Advanced Functional Materials,* vol. 19, pp. 1054-1059.

Poptoshev, E., Carambassis, A., Österberg, M., Claesson, P.M. & Rutland, M.W. 2000, *Prog. Colloid Polym Sci.,* vol. 116, pp. 79-83.

Poptoshev, E. & Claesson, P.M. 2002, "Weakly charged polyelectrolyte adsorption to a glass and cellulose studied by surface force technique", *Langmuir,* vol. 28, no. 4, pp. 1184-1189.

Postek, M.T., Vladar, A., Dagata, J., Farkas, N., Ming, B., Wagner, R., Raman, A., Moon, R.J., Sano, R., Wegner, T.H. & Beeche, J. 2011, "Development of the metrology and imaging of cellulose nanocrystals.
", *Measurments Science and Technology,* vol. 22, pp. 024005-025015.

Putman, C.A.J., Van der Werf, O. K., De Grooth, B.G., Van Hulst, N.F. & Greve, J. 1994, "Tapping mode atomic force microscopy in liquid", *Applied Physics Letters,* vol. 64, pp. 2454-2456.

Ralston, J., Larson, I., Rutland, M.W., Feiler, A.A. & Kleijn, M. 2005, "Atomic force microscopy and direct surface force measurements", *Pure Applied Chemistry,* vol. 77, no. 12, pp. 2149-2170.

Rambowicz, E. (ed) 1995, *Friction and wear of materials*, John Wiley and Sons edn, New York.

Ranby, B.G. & Noe, R.W. 1961, "Crystallization of cellulose and cellulose derivatives from dilute solution. I. Growth of single crystals", *Journal of Polymer Science,* vol. 51, pp. 337-347.

Rand, R.P., Fuller, N.L. & Lis, L.J. 1979, "Myelin Swelling and Measurments of Forces between Myelin Membranes", *Nature,* vol. 297, pp. 258-260.

Rankl, C., Pastushenko, V., Kienberger, F., Stroh, C.M. & Hinderdorfer, P. 2004, "Hydrodynamic damping of a magneticaly osciallatedra cantiliver close to a surface", *Ultramicroscopy,* vol. 100, pp. 201-208.

Reitsma, M. G.; Gates, R.S.; Cook, R.F., “Lateral force cantilever for precise atomic force microscope friction measurments”, 2008, Proceedings of the XIth International Congress and Exposition, Floride USA

Revol, J.F. 1982, "On the cross-sectional shape of cellulose crystallites in Valonia ventricosa", *Carbohydrate Polymers,* vol. 2, pp. 123-134.

Revol, J.F., Bradford, H., Giasson, J., Marchessault, R.H. & Gray, D.G. 1992, "Helicoidal self-ordering of cellulose microfibrils in aqueous suspension", *International Journal of Biological Macromolecules,* vol. 14, pp. 170-172.

Rodahl, M., Höök, F., Krozer, A., Brzezinski, P. & Kasemo, B. 1995, "Quartz crystal microbalance setup for frequency and Q-factor measurements in gaseous and liquid environments", *Review of Scientific Instruments,* vol. 66, no. 7, pp. 3924-3930.

Rojas, O.J., Claesson, P.M., Muller, D. & Neuman, R.D. 1998, "The Effect of Salt Concentration on Adsorption of Low-Charge-Density Polyelectrolytes and Interactions between Polyelectrolyte-Coated Surfaces", *Journal of Colloid and Interface Science,* vol. 205, pp. 77-88.

Roman, M. & Winter, W.T. 2004, "Effect of Sulfate Groups from Sulfuric Acid Hydrolysis on the Thermal Degradation Behavior of Bacterial Cellulose", *Biomacromolecules,* vol. 5, pp. 1671-1677.

Ruiz, M.M., Cavaille, J.Y., Dufresne, A., Gerard, J.F. & Fraillat, C. 2000, "Processing and characterization of new thermoset nanocomposites based on cellulose whiskers.", *Composites Interfaces,* vol. 7, pp. 117-131.

Rusli, R. & Eichhorn, S.J. 2008, "Determination of the stiffness of cellulose nanowhiskers and the fibermatrix interface in a nanocomposite using Raman spectroscopy", *Applied Physics Letters,* vol. 93, pp. 033111-033111-3.

Rutland, M.W., Carambassis, A., Willing, G.A. & Neuman, R.D. 1997, "Surface force measurements between cellulose surfaces using scanning probe microscopy", *Colloids and Surfaces A: Physicochemical and Engineering Aspects,* vol. 123-124, pp. 369-374.

Sader, J., Chon, J. & Mulvaney, P. 1999, "Calibration of rectangular atomic force microscope cantilevers", *Review of Scientific Instruments,* vol. 70, no. 10, pp. 3967-3969.

Saito, T., Nishiyama, Y., Putaux, J., Vignon, M. & Isogai, A. 2006, "Homogeneous Suspensions of Individualized Microfibrils from TEMPO-Catalyzed Oxidation of Native Cellulose", *Biomacromolecules,* vol. 7, no. 6, pp. 1687-1691.

Saito, T., Kimura, S., Nishiyama, Y. & Isogai, A. 2007, "Cellulose nanofibres prepared by TEMPO-mediated oxidation of native cellulose", *Biomacromolecules,* vol. 8, no. 8, pp. 2485-2491.

Saito, T., Hirota, M., Tamura, N., Kimura, S., Fukuzumi, H., Heux, L. & Isogai, A. 2009, "Individualization of Nano-Sized Plant Cellulose Fibrils by Direct Surface Carboxylation Using TEMPO Catalyst under Neutral Conditions", *Biomacromolecules,* vol. 10, no. 7, pp. 1992-1996.

Saito, T., Kuramae, R., Wohlert, J., Berglund, L.A. & Isogai, A. 2013, "An Ultrastrong Nanofibrillar Biomateril: The strength of Single Cellulose Nnaofirbils Revealed via Sonication-Induced Fragmentation.", *Biomacromolecules,* vol. 14, pp. 248-253.

Salmen, L. & Bergstrom, E. 2009, "Cellulose structure arrangement in relation to spectral changes in tensile loading FTIR.", *Cellulose,* vol. 16, pp. 975-982.

Salmi, J., Österberg, M., Stenius, P. & Laine, J. 2007a, "Surface forces between Cellulose Surfaces in Cationic Polyelectrolyte Solutions: The Effect of Polymer Molecular Weight and Charge Density", *Nordic Pulp and Paper Research Journal,* vol. 22, no. 2, pp. 249-257.

Salmi, J., Österberg, M. & Laine, J. 2007b, "The effect of cationic polyelectrolyte complexes on interactions between cellulose surfaces", *Colloids and Surfaces A: Physicochemical and Engineering Aspects,* vol. 297, no. 1-3, pp. 122-130.

Sassi, J.F. & Chanzy, H. 1995, "Ultrastructural aspects of the acetylation of cellulose", *Cellulose,* vol. 2, pp. 111-127.

Sauerbrey, G. 1959, "The use of quartz oscillators for weighing thin layers and for microweighing", *Z.Phys,* vol. 155, pp. 206-222.

Schneider, C., Jusufi, A., Farina, R., Li, F., Pincus, P., Tirrell, M. & Ballauff, M. 2008, "Microsurface Potential Measurements: Repulsive Forces between Polyelectrolyte Brushes in the Presence of Multivalent Counterions", *Langmuir,* , no. 19, pp. 10612-10615.

Schurz, J. & John, K. 1975, "Long periods in native and regenerated celluloses.", *Cellulose Chemistry and Technology,* vol. 9, pp. 493-501.

Sekurada, I., Nukushina, Y. & Ito, T. 1962, "Experimental determination of the elastic modulus of crystalline regions in oriented polymers", *Journal of Polymer Science,* vol. 57, pp. 651-660.

Seydibeyoglu, M.O. & Oksman, K. 2008, "Noverl nanocomposites based on polyurethane and microfibrillated cellulose", *Composites Science and Technology,* vol. 688, pp. 908-914.

Siqueira, G., Bras, J. & Dufresne, A. 2010, "Cellulosic bionanocomposites: A review of preparation, properties and applications", *Polymers,* vol. 2, no. 4, pp. 728-765.

Siró, I. & Plackett, D. 2010, "Microfibrillated cellulose and new nanocomposite materials: a review", *Cellulose,* vol. 17, no. 3, pp. 459-494.

Sjöström, E. 1993, *Wood Chemistry: fundamentals and applications,* 2nd rev. edn, Academic Press, San Diego (CA).

Smith, B.L., Schaffer, T.E., Viani, M., Thompson, J.B. & Frederick, N.A. 1999, "Molecular mechanistic orgin of the toughness of natural adhesives, fibers and composites", *Nature,* vol. 399, pp. 761-763.

Somerville, C. 2006, "Cellulose synthesis in higher plants.", *Annual Review of Cell and Developmental Biology,* vol. 22, pp. 53-78.

Song, F., Soh, A.K. & Bai, Y.L. 2003, "Structure and mechanical properties of the organic matix layers of nacre", *Biomaterials,* vol. 24, pp. 3623-3631.

Spence, K.L., Venditti, R.A., Habibi, Y., Rojas, O.J. & Pawlak, J.J. 2010, "The effect of chemical composition on microfibrillar cellulose films from wood pulps: Mechanical processing and physical properties", *Bioresource technology,* vol. 101, no. 15, pp. 5961-5968.

Stelte, W. & Sanadi, A.R. 2009, "Preparation and Characterization of Cellulose Nanofibers from Two Commercial Hardwood and Softwood Pulps", *Industrial & Engineering Chemistry Research,* vol. 48, no. 24, pp. 11211-11219.

Stiernstedt, J., Brumer, H., Zhou, Q., Teeri, T.T. & Rutland, M.W. 2006a, "Friction between Cellulose Surfaces and Effect of Xyloglucan Adsorption", *Biomacromolecules,* vol. 7, no. 7, pp. 2147-2153.

Stiernstedt, J., Nordgren, N., Wågberg, L., Brumer III, H., Gray, D.G. & Rutland, M.W. 2006b, "Friction and forces between cellulose model surfaces: A comparison", *Journal of Colloid and Interface Science,* vol. 303, no. 1, pp. 117-123.

Stokes, J.R., Macakova, L., Chojnicka-Paszun, A., de Kruif, C.G. & de Jongh, H. H. J. 2011, "Lubrication, Adsorption, and Rheology of Aqueous Polysaccharide Solutions", *Langmuir,* , no. 7, pp. 3474-3484.

Sturcova, A., Davies, G.R. & Eichhorn, S.J. 2005, "Elastic Modulus and Stress-Transfer Properties of Tunicate Cellulose Whiskers", *Biomacromolecules,* vol. 6, pp. 1055-1061.

Sugiyama, J., Vuong, R. & Chanzy, H. 1991, "Electron diffraction study on the two cellulose pahses occurring in native cellulose from an algal cell wall", *Macromolecules,* vol. 24, pp. 4168-4175.

Sun, R., Sun, X.F. & Tomkinson, J. 2004, *Hemicelluloses and their derivative,* American Chemical Society.

Svagan, A.J., Azizi Samir, M.A.S. & Berglund, L.A. 2007, "Biomimetic Polysaccharide Nanocomposites of High Cellulose Content and High Toughness", *Biomacromolecules,* vol. 8, no. 8, pp. 2556-2563.

Swatloski, R.P., Spears, S.K., Holbrey, J.D. & Rogers, R.D. 2002, "Dissolution of Cellose with Ionic Liquids", *Journal of American Chemical Society,* vol. 124, pp. 4974-4975.

Swerin, A., Ödberg, L. & Lindström, T. 1990, "Deswelling of hardwood kraft pulp fibers by cationic polymers: the effect on wet pressing and sheet properties", *Nordic Pulp and Paper Research Journal,* vol. 5, no. 4, pp. 188-196.

Syverud, K. & Stenius, P. 2009, "Strength and barrier properties of MFC films", *Cellulose,* vol. 16, no. 1, pp. 75-85.

Taipale, T., Österberg, M., Nykänen, A., Ruokolainen, J. & Laine, J. 2010, "Effect of microfibrillated cellulose and fines on the drainage of kraft pulp suspension and paper strength", *Cellulose,* vol. 17, no. 5, pp. 1005-1020.

Taniguchi, T. & Okamura, K. 1998, "New films produced from microfibrillated natural fibres.", *Polymer International,* vol. 47, pp. 291-294.

Tashiro, K. & Kobayashi, M. 1991, "Theoretical evaluation of three-dimensional elastic constants of native and regenerated celluloses: role of hydrogen bonds", *Polymer,* vol. 32, pp. 1516-1526.

Terech, P., Chazeau, L. & Cavaille, J.Y. 1999, "A Small-Angle Scattering Study of Cellulose Whiskers in Aqueous Suspensions", *Macromolecules,* vol. 32, pp. 1872-1875.

Theander, K., Pugh, R.J. & Rutland, M.W. 2005, "Friction force measurements relevant to de-inking by means of atomic force microscope", *Journal of colloid and interface science,* vol. 291, no. 2, pp. 361-368.

Turbak, A.F., Snyder, F.W. & Sandberg, K.R. 1983, "Microfibrillated cellulose, a new cellulose product:properties, uses, and commercial potential", *Journal of Applied Polymer Science, Applied Polymer Symposium,* vol. 37, pp. 815-827.

Verwey, E.J.W. & Overbeek, J.T.G. 1948, "Theory of Stability of Lyophobic Colloids" in *Theory of the Stability of Lyophobic Colloids*, ed. E.J.W. Verwey, Elsevier Publishing Co. edn,New York, pp. 261.

Vietor, R.J., Newman, R.H., Ha, M.A., Apperley, D.C. & Jarvis, M.C. 2002, "Conformational features of crystal-surface cellulose from higher plants", *The Plant Journal,* vol. 30, pp. 721-731.

Wågberg, L., Decher, G., Norgren, M., Lindström, T., Ankerfors, M. & Axnäs, K. 2008, "The build-up of polyelectrolyte multilayers of microfibrillated cellulose and cationic polyelectrolytes", *Langmuir,* vol. 24, no. 3, pp. 784-795.

Walecka, J.A. 1956, "An investigation of low degree of substitution carboxymethylcelluloses.", *Tappi,* vol. 39, no. 7, pp. 458-463.

Walther, A., Bjurhager, I., Malho, J.-., Pere, J., Ruokolainen, J., Berglund, L.A. & Ikkala, O. 2010, "Large-Area, Lightweight and Thick Biomimetic Composites with Superior Material Properties via Fast, Economic, and Green Pathways", *Nano Letters,* vol. 10, pp. 2742-2748.

Wanasekara, N.D. & Korley, L.T.J. 2013, "Toward Tunable and Adaptable Polymer Nanocomposites", *Journal of Polymer Science, Part B: Polymer Physics,* vol. 51, no. 7, pp. 463-467.

Wang, H., Gurau, G. & Rogers, R.D. 2012, "Ionic liquid processing of cellulose", *Chemical Society Reviews,* vol. 41, pp. 1519-1537.

Wang, R.Z., Suo, Z., Evans, A.G., Yao, N. & Aksay, I.A. 2001, "Deformation mechanisms in nacre", *Journal of Material Research,* vol. 16, pp. 2485-2493.

Wang, Y. & Chen, H.Y. 2007, "Carbon nanotubes: a promising standard for quantitative evaluation of AFM tip apex geometry.", *Ultramicroscopy,* vol. 107, pp. 293-298.

Wickholm, K., Larsson, P.T. & Iversen, T. 1998, "Assignment of non-crystalline forms in cellulose I by CP/MAS C-13 NMR spectroscopy", *Carbohydrate Research,* vol. 302, pp. 123-129.

Wu, Q., Henriksson, M., Liu, X. & Berglund, L.A. 2007, "A High Strength Nanocomposite Based on Microcrystalline Cellulose and Polyurethane", *Biomacromolecules,* vol. 8, no. 12, pp. 3687-3692.

Xhanari, K., Syverud, K., Chinga-Carrasco, G., Paso, K. & Stenius, P. 2011, "Reduction of water wettability of nanofibrillated cellulose by adsorption of cationic surfactants", *Cellulose,* vol. 18, no. 2, pp. 257-270.

Xu, P. & Liu, H. 2004, "Model of microfibril elastic modulus parallel to the cell axis.", *Wood Science and Technology,* vol. 38, pp. 363-374.

Xu, P., Donaldson, L.A., Gergely, Z.R. & Staehelin, L.A. 2007, "Dual-axis electron tomography: a new approach for investigating the spatial organization of wood cellulose microfibrils", *Wood Science and Technology,* vol. 41, pp. 101-116.

Yachi, T., Hayashi, J., Takai, M. & Shimizu, Y. 1983, "Supermolecular structure of cellulose: stepwise decrease in LODP and particle size of cellulose hydrolyzed after chemical treatment.", *Journal of applied polymer science. Applied polymer symposium,* vol. 37, pp. 325-343.

Yano, H. & Nakahara, S. 2004, "Bio-composites produced from plant microfiber bundles with a nanometer unit web-like network.", *Journal of Materials Science,* vol. 39, pp. 1635-1638.

Yao, N., Epstein, A.K., Liu, W.W., Sauer, F. & Yang, N. 2009, "Organic inorganic interfaces and spiral frowth in nacre", *Journal of the Royal Society Interface,* vol. 6, pp. 367-376.

Yoon, R.H. & Ravishankar, S. 1996, "Long-range hydrophobic forces between mica surface in dodecylammonium chloride solutions in the presence of dodecanol.", *J. Colloid Interface Science,* vol. 182, pp. 363-370.

Zabler, S., Paris, O., Burgert, I. & Fratzl, P. 2010, "Moisture changes in the plant cell wall force cellulose crystallites to deform.", *Journal of Structural Biology,* vol. 171, pp. 133-141.

Zauscher, S. & Klingenberg, D.J. 2000a, "Friction between cellulose surfaces measured with colloidal probe microscopy", *Colloids and Surfaces A: Physicochemical and Engineering Aspects,* vol. 178, pp. 213-229.

Zauscher, S. & Klingenberg, D.J. 2000b, "Normal Forces between Cellulose Surfaces Measured with Colloidal Probe Microscopy", *Journal of Colloid and Interface Science,* vol. 229, no. 2, pp. 497-510.

Zauscher, S. & Klingenberg, D.J. 2000c, "Surface and friction forces between cellulose surfaces measured with colloidal probe microscopy.", *Nordic Pulp & Paper Research Journal,* vol. 15, no. 5, pp. 459-468.

Zhai, L., Nolte, A.J., Cohen, R.C. & Rubner, M.F. 2004, "pH-Gated Porosity Transitions of Polyelectrolyte Multilayers in Confined Geometries and Their Application as Tunable Bragg Reflectors", -*Macromolecules,* , no. 16, pp. 6113-6123.

Zhang, H.R. & Tong, M.W. 2007, "Influence of hemicellulose on the strucutre and properties of lyocell fibers", *Polymer Eng Sci,* vol. 47, pp. 702-706.

Zhang, H.R., Zhang, H.H., Tong, M.W., Shao, H.L. & Hu, X.C. 2008, "Comparison of the structures and properties of lyocell fibers from high hemicellulose pulp and high alpha-cellulose pulp", *Journal of Applied Polymer Science,* vol. 107, pp. 636-641.

Zhong, Q., Inniss, D., Kjoller, K. & Elins, V.B. 1993, "Fractured polymer/silica fiber surface sudied by tapping mofe atomic force microscopy.", *Surface Science,* vol. 290, pp. L688-L692.

Zhou, Q., Malm, E., Nilsson, H., Larsson, P.T., Iversen, T., Berglund, L.A. & Bulone, V. 2009, "Nanostructured biocomposites based on bacterial cellulosic nanofibers compartmentalized by a soft hydroxyethylcellulose matrix coating", *Soft Matter,* vol. 5, no. 21, pp. 4124-4130.

Zimmermann, T., Pöhler, E. & Geiger, T. 2004, "Cellulose Fibrils for Polymer Reinforcement", *Advanced Engineering Materials,* vol. 6, no. 9, pp. 754-761.

Zimmermann, T., Bordeanu, N. & Strub, E. 2010, "Properties of nanofibrillated cellulose from different raw materials and its reinforcement potential", *Carbohydrate Polymers,* vol. 79, no. 4, pp. 1086-1093.

Zuluaga, R., Putaux, J., Restrepo, A., Mondragon, I. & Ganan, P. 2007, "Cellulose microfibrils from banana farming residues: isolation and characterization.", *Cellulose,* vol. 15, pp. 585-592.

Aalto-DD 151/2013

ISBN 978-952-60-5352-3
ISBN 978-952-60-5353-0 (pdf)
ISSN-L 1799-4934
ISSN 1799-4934
ISSN 1799-4942 (pdf)

Aalto University
Aalto University School of Chemical Technology
Department of Forest Products Technology
www.aalto.fi

BUSINESS +
ECONOMY

ART +
DESIGN +
ARCHITECTURE

SCIENCE +
TECHNOLOGY

CROSSOVER

**DOCTORAL
DISSERTATIONS**